

Neural Mechanisms of **Placebo Anxiolysis**

**Dissertation with the aim of achieving a doctoral degree at the
Faculty of Mathematics, Informatics and Natural Sciences
Department of Biology of Universität Hamburg**

submitted by Benjamin Meyer

Hamburg, 2016

The following evaluators recommend the admission of the dissertation:

Prof. Dr. C. Lohr

Prof. Dr. R. Kalisch

Day of oral defense: 02.09.2016

Contents

1. Abstract	7
2. Introduction	9
2.1. Overview	9
2.2. Definition of fear and anxiety	9
2.3. Research on fear and anxiety in animals and humans.....	10
2.4. Introduction to fMRI and EEG.....	11
2.5. Studying human fear and anxiety with fMRI and EEG.....	13
2.6. Psychological mechanisms of placebo effects.....	16
2.7. Neurobiological mechanisms of placebo effects.....	18
3. Aim of this research project	21
4. Materials and Methods.....	23
4.1. Study participants	23
4.2. Experimental procedure.....	23
4.3. Electric stimulation.....	26
4.4. Skin conductance measurement.....	26
4.4.1. Skin conductance recordings.....	26
4.4.2. Analysis of skin conductance responses and levels	27
4.5. Pupillometry	28
4.5.1. Pupil size recordings	28
4.5.2. Analysis of pupil dilation	29
4.6. Statistical analysis of behavioral data.....	29
4.7. EEG	30
4.7.1. EEG recordings and preprocessing.....	30
4.7.2. ERP analysis	31
4.7.3. EEG frequency analysis	31
4.8. fMRI	31
4.8.1. fMRI data recordings.....	31
4.8.2. fMRI data preprocessing.....	32
4.8.3. Standard fMRI data analysis.....	32
4.8.4. Functional connectivity analyses.....	36
5. Results	38
5.1. Study 1	38

5.1.1.	Behavioral results	38
5.2.	Study 2	40
5.2.1.	EEG Pilot study	40
5.2.2.	Behavioral Results.....	41
5.2.3.	ERP results.....	42
5.2.4.	EEG oscillatory activity	45
5.3.	Study 3	49
5.3.1.	Behavioral Results.....	49
5.3.2.	fMRI analysis	50
5.3.2.1.	Cue-related BOLD responses.....	50
5.3.2.2.	Tonic cue unrelated BOLD signal changes	59
5.3.2.3.	Functional connectivity (FC) in large-scale neural networks.....	59
6.	Discussion.....	66
6.1.	Summary of results.....	66
6.2.	Verbally suggested treatment expectation induced placebo anxiolysis.....	66
6.3.	Autonomic cue reactivity and arousal were attenuated under placebo.....	67
6.4.	Externally directed attention decreased under placebo.....	68
6.5.	Internally directed attention increased under placebo	69
6.6.	SN activity was attenuated under placebo.....	70
6.7.	Placebo effects in different conditions activate common neural substrates.....	71
6.8.	DMN and SN-DMN functional connectivity increased under placebo.....	72
6.9.	A first psychobiological model of placebo anxiolysis.....	73
6.10.	Outlook	75
7.	List of abbreviations	78
8.	References.....	81
9.	Appendix.....	92

List of Figures

Figure 1: Biological basis of the EEG signal and major components of an EEG-recording system.....	12
Figure 2: Core regions of the salience network (SN)	14
Figure 3: The three major ICNs	15
Figure 4: Effect of treatment expectations in postoperative anxiety	17
Figure 5: Placebo effects in experimental pain, emotional processing and Parkinson's disease	20
Figure 6: Study design (Studies 1+2).....	25
Figure 7: fMRI study design (Study 3)	26
Figure 8: Example of a decomposed skin conductance (SC) time course.....	28
Figure 9: Pupillometry.....	29
Figure 10: Regressors of the GLM design matrix.....	33
Figure 11: Standard fMRI data analysis.....	35
Figure 12: Psychophysiological interaction (PPI)	36
Figure 13: Behavioral results (Study 1).....	39
Figure 14: Behavioral results (EEG Pilot study)	40
Figure 15: ERP definition (EEG Pilot Study)	41
Figure 16: Behavioral results (Study 2).....	42
Figure 17: Event-related potentials (ERPs) (Study 2)	43
Figure 18: Brain-behavior correlations (Study 2).....	44
Figure 19: P300 and LPP in high (HR) and low (LR) placebo responders (Study 2)	45
Figure 20: ITI power spectra (Study 2)	47
Figure 21: ITI theta (4-7 Hz) and alpha (8-12 Hz) activity (Study 2)	48
Figure 22: Behavioral results (Study 3).....	49
Figure 23: Pupillometry results (Study 3).....	50
Figure 24: fMRI main effects of threat (Study 3)	52
Figure 25: fMRI placebo effects in SN-related regions (Study 3)	53
Figure 26: Amygdala ROI analysis (Study 3).....	54
Figure 27: Time course of amygdala activation in blocks of three trials (Study 3)	54
Figure 28: rACC activation under placebo (Study 3).....	55
Figure 29: rACC activation vs. thalamus deactivation (Study 3).....	56
Figure 30: Threat-activated SN nodes and placebo-induced effects (Study 3).....	58
Figure 31: Threat-deactivated DMN nodes (Study 3).....	59
Figure 32: Placebo-dependent SN, SN-DMN and DMN FC (Study 3).....	60

Figure 33: Placebo-dependent FC in HRs vs. LRs (Study 3)	61
Figure 34: Placebo-dependent increases in inter- and intra-network FC for a single participant.....	62
Figure 35: Intermediate conjunction analysis of SN PPis.....	64
Figure 36: A psychobiological model of placebo anxiolysis.....	75
Figure A 1: EEG electrode set (Study 2).....	92
Figure A 2: Amygdala mask (Study 3)	92
Figure A 3: ACC mask (Study 3)	93

List of Tables

Table 1: Standard FWE-corrected whole brain analyses	51
Table 2: Placebo effects in SN nodes.....	57
Table 3: Intermediate conjunction analysis of SN PPis.....	65
Table A 1: Central executive network (CEN)	93
Table A 2: Salience network (SN).....	94
Table A 3: Default mode network (DMN)	94

1. Abstract

Placebo effects have been shown in a wide range of clinical conditions including pain, Parkinson's disease and depression. Several experimental studies have further revealed that placebo effects can strongly influence the efficacy of anxiolytic drugs and modulate negative emotional states. It is therefore not surprising that pronounced anxiolytic placebo effects have been reported in clinical studies on anxiety disorders and in daily clinical routine, where placebo treatments are frequently administered with the intention of calming anxious patients. Despite its far-reaching implications in clinical contexts, the underlying neural mechanisms of reducing fear and anxiety by the use of placebo treatments (placebo anxiolysis) have remained largely unknown.

In this research project, three consecutive studies (Studies 1-3) in healthy humans elucidated the mechanisms behind placebo anxiolysis on different levels of neural processing. In order to do so, a study design was developed to examine the effects of an anxiolytic placebo treatment in experimentally induced states of phasic fear and sustained anxiety. Phasic fear is the response to a well-defined threat and involves attentional focusing on the source of the threat as well as a concomitant phasic increase in autonomic arousal, whereas in sustained states of anxiety a potential and unclear danger requires vigilant scanning of the environment and elevated tonic arousal levels. Phasic fear was induced in the studies performed here over the course of 5 s through the anticipation of a previously experienced painful electrocutaneous stimulus signaled by a threat cue. Several threat and no-threat cues (where no pain was to be expected) were presented in an unpredictable order during experimental runs of 2-3 min. This constellation served to create a threatening context and to thus induce increased levels of vigilance and tonic autonomic arousal as in states of sustained anxiety. Participants received an inactive medication that was labeled and introduced as a potent anxiolytic drug in placebo runs and as an inactive control treatment in no-placebo runs. Skin conductance (Studies 1-3) and pupil size (Study 3) were recorded to examine the placebo-dependent effects on autonomic nervous system activity. Central nervous system activity was assessed by electroencephalography (EEG, Study 2) and functional magnetic resonance imaging (fMRI, Study 3).

Under the verbally induced illusion of having received an anxiolytic pharmacological treatment, subjective and autonomic (sympathetic and parasympathetic) responses to both threat and no-threat cues were unspecifically inhibited. Hence, there was no evidence of specific effects of the placebo manipulation on phasic fear (threat cue reaction). Rather these findings suggest globally reduced vigilance. Changes in tonic skin conductance throughout

the experimental runs were separable from phasic cue-related responses and indicated a placebo-dependent decrease in tonic sympathetic arousal levels. In combination with the reduced vigilance, the reduced tonic autonomic arousal indicates a down-regulation of sustained anxiety as opposed to phasic fear. In line with this interpretation, EEG analyses further revealed a pronounced placebo-dependent attenuation of electrophysiological markers of externally focused attention (P300 and late positive potential = LPP) and, in return, increased oscillatory correlates of internalized attention (alpha [8-12 Hz] and theta [4-7 Hz] power). fMRI analyses demonstrated reduced blood oxygen level dependent (BOLD) activity in a threat-responsive large-scale neural network, also known as the salience network, under placebo. Enhanced placebo-dependent BOLD responses were observed in the rostral portion of the anterior cingulate cortex, which has previously been shown in many studies to be activated in the context of analgesic and emotion regulatory placebo effects, suggesting a common mechanism across different placebo conditions. Functional connectivity analyses additionally revealed enhanced placebo-dependent intrinsic BOLD coupling in the default mode network, a well-described large-scale neural network associated with states of internally focused attention. Internally directed attention and the concomitant attenuation of vigilance and arousal can thus be considered a likely working mechanism underlying placebo anxiolysis.

2. Introduction

2.1. Overview

The term placebo (Latin for “I shall please”) has entered the medical lexicon to indicate a sham treatment applied by physicians to calm or please patients (1). When the administration of an inactive treatment leads to psychobiological changes resulting in a clinical improvement, this is referred to as a placebo effect or a placebo response (2).

Over the last decades, there has been significant progress in our understanding of the neurobiological mechanisms underlying placebo effects, in particular in the treatment of pain (3) but also of conditions such as Parkinson’s disease (4, 5) or depression (6). However, little is known about the neural bases of placebo effects in the treatment of fear and anxiety (placebo anxiolysis). This is remarkable, as placebo effects have been shown to strongly modulate the efficacy of anxiolytic drugs (7); placebo response rates are particularly high in clinical studies of mood and anxiety disorders (8, 9); and placebo treatments are frequently administered with the intention of calming anxious patients in daily clinical routine (10, 11).

The current project was designed in the framework of the transregional research unit FOR 1328 (<http://placeboforschung.de/>) promoted by the German Research Foundation (DFG). Its aim was to elucidate the neurobiological mechanisms of placebo anxiolysis in healthy humans. For this purpose, in three consecutive studies, temporary states of fear and anxiety were induced employing a classical anticipatory fear/anxiety study design and the effects of a placebo treatment (introduced as an anxiolytic drug) on autonomic and central nervous system (ANS, CNS) processing were analyzed. Skin conductance (SC) and pupil size recordings as well as subjective ratings were combined with functional magnetic resonance imaging (fMRI) and electroencephalography in order to obtain comprehensive insights into the widely known but poorly understood phenomenon of placebo anxiolysis.

2.2. Definition of fear and anxiety

Human fear and anxiety are both emotional states characterized by physiological and behavioral responses to threatening stimuli and/or situations and can be distinguished from one another by means of stimulus duration and specificity; fear occurs as a phasic response to a clear and well-defined threat in a circumscribed time window, whereas anxiety is a more sustained state in response to a distant and unclear threat (12). Accordingly, a non-

pathological state of fear can be triggered, for example, by suddenly encountering an aggressive dog, while a state of anxiety might be induced by walking through a dark and narrow street in a city district notorious for its high crime rate. Pathological states of fear and anxiety are summarized as anxiety disorders (AD), with different weight being given to both, depending on the AD-subtype. For example, specific phobias (e.g. arachnophobia) and posttraumatic stress disorder (PTSD) can be distinguished from one another based on threat specificity and symptom duration, whereby the former is characterized by a well-defined threat and phasic symptoms (as induced by fear) and the latter by diffuse threats and sustained symptoms [as induced by anxiety; (13, 14)].

2.3. Research on fear and anxiety in animals and humans

Animal models of fear are typically based on a Pavlovian conditioning procedure (fear conditioning), where an initially neutral visual or auditory cue (conditioned stimulus = CS) is associated with an aversive stimulus (unconditioned stimulus = US). For example, a tone (CS) might be repeatedly presented, followed by an electric shock (US). After several repetitions, the CS becomes a predictor of the US and the CS itself is then capable of eliciting fear responses (conditioned response = CR) including behavioral and physiological changes such as temporary states of immobility (“freezing”), tachycardia, sweat secretion and blood pressure elevation (15–17). The broad spectrum of fear responses can be traced back to areas within the brainstem and the lateral hypothalamus, which in phasic states of fear are both activated by the central nucleus of the amygdala (CN_A) (15).

In an example of rodent models of anxiety, the animal may be placed in an illuminated open area (an aversive environment for animals living in burrows and foraging at night) or a threatening environment in which aversive events have been experienced before (18, 19). Although states of fear and anxiety result in overlapping (but time-varying) behavioral and physiological changes, both are triggered by different nuclei. As indicated above, the CN_A triggers phasic fear responses by activating target areas in the brainstem and the lateral hypothalamus. In the case of sustained anxiety-like states, however, the bed nucleus of the stria terminalis (BNST), a part of what is referred to as the extended amygdala, activates these target areas (20).

The neurobiological substrates mediating fear and anxiety are assumed to be highly conserved across mammalian species (21), whereby the functional equivalence of key CNS structures in humans has mainly been supported by studies using fMRI (see 2.5 for more details). In cases of human fear/anxiety, the CNS activates the sympathetic branch of the ANS, which elicits diverse responses by way of projections to peripheral target organs, including increase in heart rate, blood pressure elevation, pupil dilation and sweat secretion.

The sympathetic branch of the ANS is complemented by the parasympathetic branch, which targets the same peripheral organs but induces opposing effects (22). In the current research project, sweat secretion (by SC recordings) and pupil dilation were recorded as measures of ANS activity. In order to gain insights into the effects of anxiolytic placebo treatments on CNS activity, fMRI and EEG data were acquired. Both techniques are introduced in the following section.

2.4. Introduction to fMRI and EEG

For ethical reasons, studying human brain organization is mainly restricted to noninvasive techniques, allowing only limited spatial (EEG) or temporal (fMRI) resolution, but offering the possibility to measure activity across the entire brain (i.e. large-scale neural networks). In studies of human fear and anxiety, fMRI is the most widely used technique due to its high spatial resolution in the range of millimeters as well as its ability to detect signals from cortical and brainstem areas. The fMRI signal is based on increased neuronal activity which in the CNS is coupled to a local dilation of blood vessels (23). This neurovascular coupling is characterized by an oversupply of oxygenated and a consequential decrease of deoxygenated hemoglobin. The change in ratio of diamagnetic oxygenated to paramagnetic deoxygenated hemoglobin causes a characteristic temporary change in the fMRI signal known as the blood-oxygen-level-dependent (BOLD) response, which peaks 3-5 s after synaptic stimulation (24). BOLD responses can thus be considered a marker of metabolic demands due to an increase of neuronal activity in a small volume of tissue. In typical fMRI studies, the percentual change of the BOLD signal amplitude in two or more experimental conditions is estimated for each voxel (single cuboidal 3D image unit) in a 3D-image of the brain. Voxels showing significant statistical differences between conditions are highlighted accordingly (see also 4.8).

A different approach to measuring large-scale neural activity in humans is provided by EEG. The EEG signal is based on synchronous synaptic activity within columnar assemblies of neurons arranged in parallel and perpendicular to the cortical surface. Such spatiotemporal organization is for instance given by the apical dendrites of pyramidal neurons which are thought to make the strongest contribution to the EEG signal. When these neurons receive excitatory synaptic input, a positive transmembrane current (due to the influx of Na^+) is generated, leading to an extracellular current sink at the site of the synapse and a distributed source along the dendrite down to the soma. Sinks and sources generate local field potentials, which in the case of synchronized activity within large cell populations form a dipole layer detectable as potential differences by scalp electrodes (25, 26). Figure 1 illustrates the biological basis of the EEG signal (Figure 1A) and the major components of an

EEG recording system (Figure 1B), including scalp electrodes, amplifier and recording device.

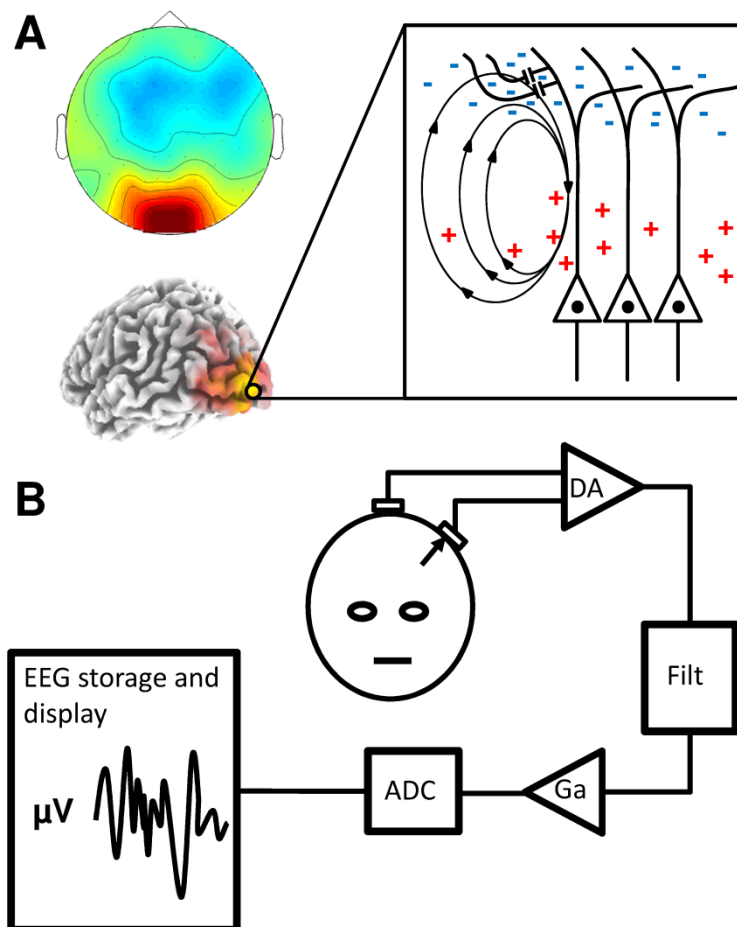


Figure 1: Biological basis of the EEG signal and major components of an EEG-recording system

(A) Cationic influx during excitatory postsynaptic potentials in cortical pyramidal cells causes local current sinks at the site of the synapse and distributed sources along the apical dendrite. Synchronized neuronal activity thereby generates extended dipole layers. (B) Dipole layers (black arrow) are measurable as potential differences in μV by scalp electrodes, connected to a signal amplifying recording system. [ADC=Analog to digital converter, DA=differential amplifier, Filt=Filter, Ga=Gain].

A common methodological approach to analyzing EEG data is to average stimulus-induced potentials (event-related potentials=ERP), which allows for the detection of differences in the time course of stimulus processing between various stimulus types and/or subjects (see also 2.5). ERPs are usually referred to by a letter followed by a number, indicating polarity (P=positive / N=negative) and latency in milliseconds relative to stimulus onset and have been used as markers for various cognitive processes in numerous EEG studies (27). For example, the P300 is a positive deflection located over parietal sites occurring ~ 300 ms after visual or auditory stimulation onsets. It has been observed in response to self-relevant external stimuli and is modulated by various factors such as stimulus probability (28, 29),

concurrent cognitive tasks (30) and the emotional value of the stimulus (31, 32). Although the exact underlying neural generators are still debated, the P300 most likely reflects the allocation of attentional resources in response to external stimuli (33).

Human electroencephalograms are characterized by rhythmic signal variations, already identifiable by visual inspection of the data. The EEG oscillations are organized in distinct frequency bands ranging from slow delta (<4 Hz) to fast gamma oscillations (>30 Hz) and reflect synchronous neural activity (34). It has been shown that characteristic frequency bands are modulated by certain cognitive tasks or behavioral states (25). For example, many studies found increased frontal theta (4-7 Hz) and alpha (8-12 Hz) oscillations during mental tasks requiring focused internally directed attention, such as working memory tasks or also meditation (35–39). Another strategy to analyze EEG data is thus to transfer the EEG signal from the time to the frequency domain to examine different oscillatory characteristics.

In contrast to fMRI, the EEG has a temporal resolution in the range of milliseconds, and thus allows for a time-exact analysis of neural activity. However, due to the distance between the electrodes and the underlying neural sources, a localization of the signal is often difficult. Future studies combining both EEG and fMRI might be able to overcome both the temporal limitations of fMRI (due to the slow BOLD response and image sample rates of $\sim 1/1$ s - $1/3$ s) as well as the spatial limitations of EEG at least to a certain extent (40).

2.5. Studying human fear and anxiety with fMRI and EEG

BOLD responses in emotion processing areas can be reliably assessed by repeatedly presenting stimuli of emotional valence (e.g. a CS), making fear conditioning well-suited for fMRI studies. In line with the animal literature, many studies have confirmed an involvement of the human amygdala in fear conditioning (41–43). Moreover, high-resolution fMRI has also revealed enhanced activity in the human BNST in states of sustained anxiety as opposed to phasic fear (44). This suggests a high degree of functional conservation in threat-responsive structures. In states of human fear and anxiety, however, these regions are accompanied by a broad network of co-activated cortical areas (45, 46), including such key structures as the dorsal anterior cingulate cortex (dACC), the dorsomedial prefrontal cortex (dmPFC) and the anterior insula (ai). As is well known from studies on fear conditioning and as shown by a meta-analysis by Mechias et al. (47), this cortical network is consistently activated during instructed fear, meaning that subjects are informed beforehand that a certain cue predicts an aversive event, thus circumventing fear learning. Seeley et al. (48) could show that the same threat-responsive cortical regions and typical threat-responsive subcortical structures are not only activated under acute stress, but furthermore exhibit intrinsic metabolic coupling at rest, as revealed by analyzing spontaneous fluctuations in BOLD signals when subjects are not

exposed to any kind of external stimulation. Together, these results suggest an intrinsically coupled neural network (ICN) that responds concertedly to threat-related stimuli. Seeley et al. referred to this network as the “salience network” (SN). Their concept of a functional neural network was further supported by a study by Hermans et al. (49), who used aversive cinematographic material to induce dynamic states of stress and found an increase in coupling within large portions of the SN. This increase could be diminished by β -adrenergic receptor blockage, suggesting that noradrenergic activity plays an important role in activating the SN. Animal studies revealed that the amygdala and the BNST both receive higher cortical projections from anterior portions of the insula (50, 51) and in Seeley et al. (2007) as well as Hermans et al. (2011) the amygdala (but not the BNST) has been confirmed as a member of the SN. However, it should be noted that due to its small size, standard fMRI procedures do not allow for a reliable detection of BOLD signals from the BNST and thus future high-resolution fMRI studies are required to further examine the interaction between the BNST and the SN. This could also help to characterize the exact role of the SN in sustained anxiety as opposed to phasic fear. Key cortical SN structures as identified by Mechias et al. (47), Seeley et al. (48) and Hermans et al. (49) are depicted in Figure 2.

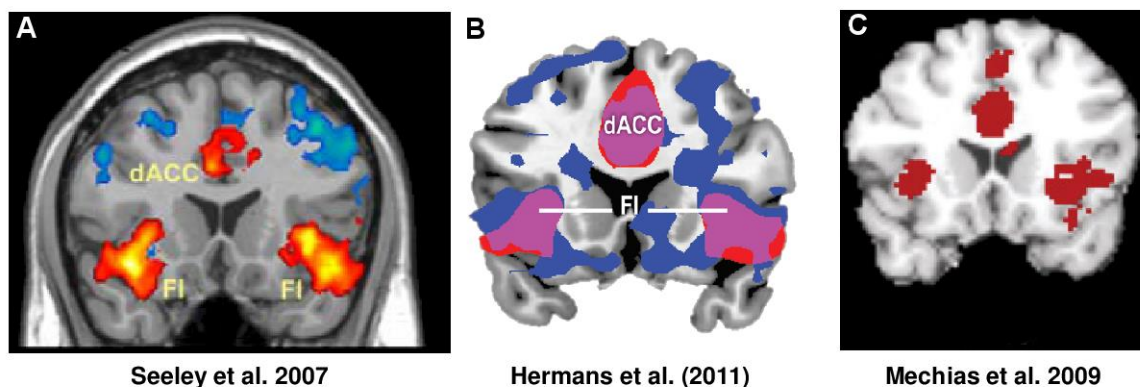


Figure 2: Core regions of the salience network (SN)

Orange areas in A indicate SN regions showing enhanced resting state coupling. The same regions exhibit enhanced coupling when aversive vs. neutral cinematographic material is presented (purple areas, B) and are also activated during instructed fear (red areas, C). FI = frontal insula, dACC = dorsal anterior cingulate cortex. [Adapted from (47–49)]

The SN belongs to a group of three major ICNs showing intrinsic interregional BOLD signal coupling (also referred to as functional connectivity = FC) at rest and consistent activation or deactivation under certain cognitive demands (52). The best characterized ICN is the default mode network (DMN), which is anchored in the ventromedial prefrontal cortex (vmPFC) and retrosplenial areas and activated during self-referential processing and consistently deactivated in stimulus driven tasks (53–55). The central executive network (CEN) is

anchored in dorsolateral prefrontal as well as parietal areas and is activated in tasks requiring maintenance and manipulation of information contents, e.g. in working memory or decision making processes (48, 56). The subdivision into distinct ICNs constitutes a fundamental principle of human brain organization, with the relationship between ICN dysfunction and psychiatric disorders currently being an active field of research (52). Figure 3 illustrates the three major ICNs.

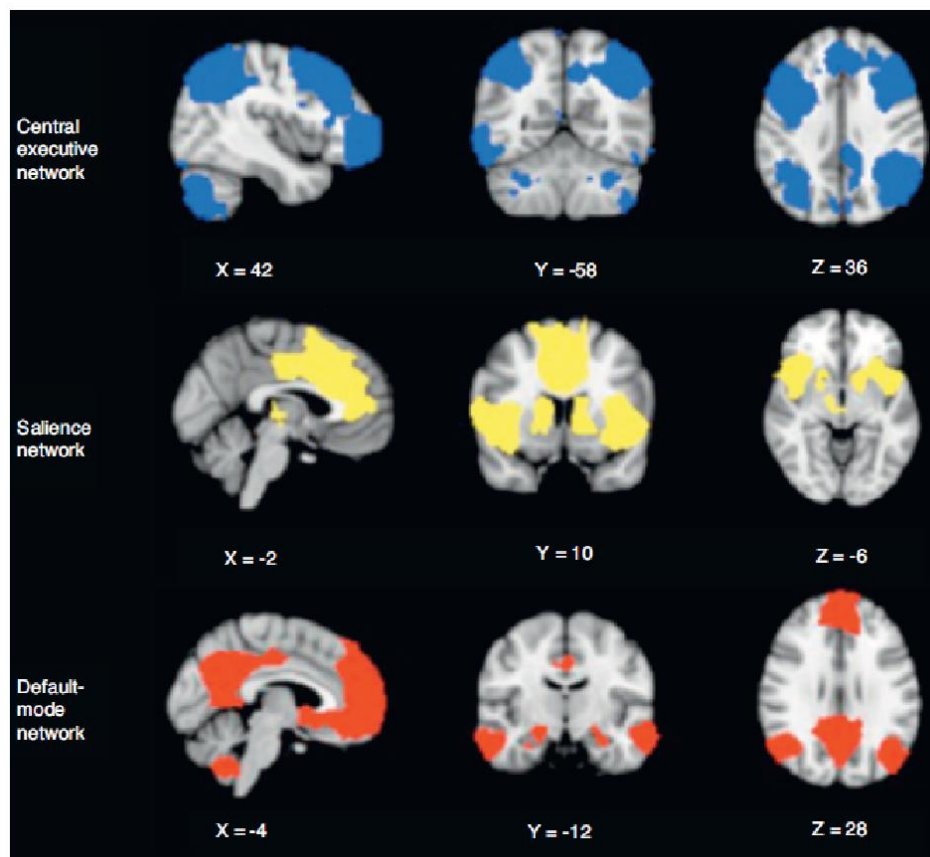


Figure 3: The three major ICNs

The central executive network (top), the salience network (middle) and the default mode network (bottom). [Adapted from (52)]

EEG is used less commonly in research on human fear and anxiety, a fact which can be explained by its limited sensitivity in detecting subcortical signals. However, one example is given by Scharmüller et al. (31), who investigated ERPs in response to pictures of spiders as well as fear-inducing, disgust-inducing and affectively neutral pictures in arachnophobics and healthy controls. Only in phobics the authors observed ERPs 340-500 and 550-770ms specifically after the presentation of pictures of spiders (referred to as P300 and late positive potential=LPP, respectively), which in agreement with the ERP literature is thought to reflect an attentional shift towards highly salient stimuli (32, 33). Interestingly, in Straube et al. (57),

arachnophobics showed enhanced BOLD responses to spider compared to control videos in the aI and dACC, suggesting the SN to be a likely generator of phobia-related ERPs.

2.6. Psychological mechanisms of placebo effects

In order to design a suitable experimental procedure for examining the neurobiological bases of placebo anxiolysis, a profound understanding of the psychological mechanisms behind placebo effects is required. Placebo effects can be induced by verbally suggesting treatment expectations and classical conditioning. Both procedures are often combined to maximize the placebo effect, but however have also been shown to work separately.

If a study participant is verbally informed about the efficacy of a treatment and is then tested without any prior treatment-related experience, the induced placebo effect is purely based on verbally suggested treatment expectation. This is not restricted to administering inert placebo treatments but can be generalized to real drugs, meaning that any drug effect might be accompanied by a placebo effect. Several studies observed relieving effects when coupling inert treatments with verbally suggested treatment expectation (58, 59). An impressive study on how mere treatment expectations can modulate the efficacy of a true anxiolytic drug was performed by Benedetti et al. (7). The authors compared the effect of open vs. hidden administration of diazepam (a potent anxiolytic and sedative drug) on postoperative anxiety in highly anxious patients after surgery and revealed a complete ineffectiveness of diazepam when the drug was administered covertly, that is unbeknownst to the patient by an infusion pump (hidden condition). In another experiment, hidden and open interruptions of diazepam administration were investigated. A significant return of anxiety was observed after 4 and 8 hours only when patients knew that drug administration had been interrupted (open condition), but not when the interruption was performed covertly (hidden condition) (Figure 4). Analogous results were shown in studies on hidden-open administrations of analgesic drugs (60).

Classical conditioning is a learning procedure and has already been described in the context of fear conditioning. However, it involves the same principle with rewarding stimuli (reward conditioning), in that the repeated presentation of an initially neutral cue followed by a rewarding stimulus can lead to a learned physiological response induced by the initially neutral cue alone (61). Reward conditioning was first introduced by Ivan P. Pavlov in his pioneering studies on dogs (62). Pavlov repeatedly combined the sound of a bell (conditioned stimulus=CS) with the presentation of food (unconditioned stimulus=US). As expected, the US but initially not the CS triggered salivatory responses (unconditioned response = UR). However, after several combined CS-US presentations, the CS alone (as a

predictor of the US) was also capable of inducing salivatory responses (conditioned response=CR).

In the case of placebo effects, the CS can be a carrier of the active drug, for example a pill or syringe, or even the medical staff applying the drug. The active drug component thus represents the US and the drug effect the UR. After repeated drug administrations (CS-US), mere CS presentation without administering any active agent (US), can induce drug-like effects (CR). Placebo effects based on classical conditioning have been elucidated in several immunological studies in animals and humans. In Goebel et al. (63), for example, study participants repeatedly received a flavored drink (CS) and the immunosuppressive drug Cyclosporin A (US) in capsule form, leading to a robust suppression of interleukin-2 (IL-2) and interferon-gamma (IFN- γ) mRNA expression (UR). In a test phase one week later, after IL-2 and IFN- γ had again reached baseline levels, the flavored drink in combination with an identical looking placebo capsule was still capable of inhibiting both IL-2 and IFN- γ (CR). In a study by Benedetti et al. (58), placebo effects based on classical conditioning were also shown to modulate the secretion of other hormones such as growth hormone (GH) or cortisol.

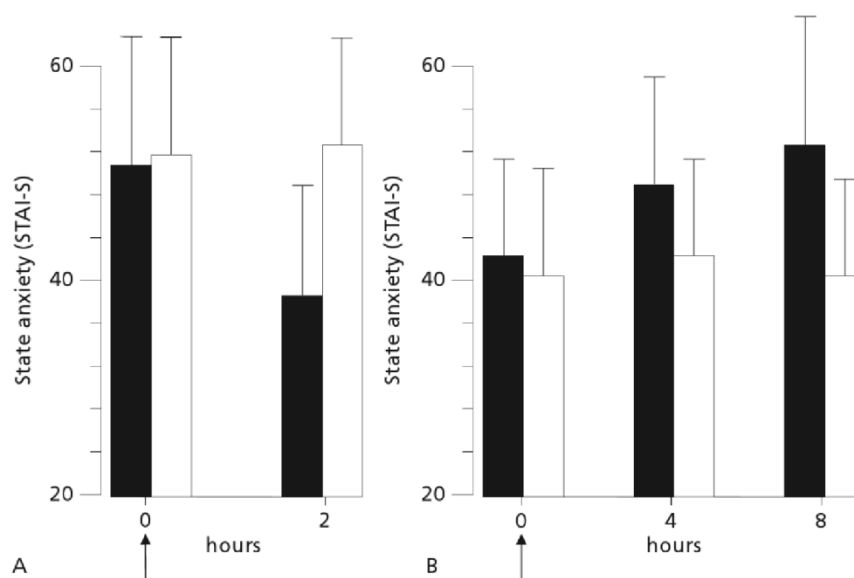


Figure 4: Effect of treatment expectations in postoperative anxiety

Open (black bars) and hidden (white bars) administration (A) and interruption (B) of diazepam in postoperative anxiety. Arrows indicate the time point of diazepam administration / interruption. State anxiety was only reduced after open treatment administration and a return of anxiety was only observed after open drug interruption. [Adapted from (7)]

It is of common practice in placebo studies to utilize a prior conditioning procedure in order to boost the participants treatment expectation, e.g. by first administering an active drug (conditioning phase), which is later replaced by a placebo in the test phase (64). In studies on placebo analgesia, the conditioning phase is often performed without an active drug by surreptitiously lowering the painful stimulation for the placebo but not for the control treatment. The placebo treatment is thus repeatedly associated with an analgesic effect in the conditioning phase, while in a later test phase, the intensity remains identical for both treatments. It has been assumed that the placebo effect in the later test phase is mainly induced by enhanced treatment expectations and does not result from classical conditioning (65). However, in a recent study, Schafer et al. (66) demonstrated persisting analgesic placebo effects after a conditioning procedure, even when study participants were made aware of receiving a placebo in the test phase. Together with studies on nonconscious activation of conditioned analgesic placebo responses (67, 68), these results suggest that pure conditioning, which is not overlaid by the effect of treatment expectation, can modulate consciously perceived states such as pain.

2.7. Neurobiological mechanisms of placebo effects

As indicated above, the psychological components mediating placebo effects are widely understood. The successful transfer of psychological concepts to neurobiological systems, however, remains a great challenge due to the multifaceted nature of placebo effects and a poor understanding on how brain processes relate to mental processes. Numerous studies have investigated placebo-dependent symptom relief in experimentally induced pain (placebo analgesia), but placebos have also been shown to modulate the symptoms of irritable bowel syndrome (69), Parkinson's disease (PD) (70) and depression (6), indicating that no single but in fact many placebo effects exist that act on different target systems (2). However, this does not exclude the existence of common regulatory sources underlying multiple placebo effects. In the following, a selection of three different target systems modulated by different placebo-dependent factors is introduced.

Placebo analgesia is by far the most intensively studied placebo effect, with current models suggesting that placebo-related positive treatment expectations induce enhanced activity in prefrontal areas, thereby initiating the release of analgesic endogenous opioids (3, 71). The first indication for a placebo-dependent modulatory effect of endogenous opioids on pain was already given by Levine in 1978 (72), who showed that the administration of Naloxone, a μ -opioid receptor blocker, prevents the manifestation of an analgesic placebo effect. This result was confirmed in several studies (73, 74) and is now well accepted in the field of placebo research. The analgesic effect of endogenous opioids results in reduced pain-related activity

in a broad network of pain-processing areas, receiving ascending nociceptive input from spinal cord neurons (75). This pain-sensitive network includes the medial thalamus, the primary and secondary somatosensory cortex (SI and SII) but also classical SN regions, such as the dACC, AI and the amygdala (76). Based on studies in animals and humans, an opioid-receptor rich system of midbrain areas has been identified, including the periaqueductal grey (PAG) and the rostroventral medulla (RVM), which is reciprocally coupled with spinal cord neurons, thereby controlling pain-related input to the pain-sensitive network (77). The PAG-RVM system itself receives afferent projections from medial prefrontal areas (78). It is the interaction between medial prefrontal areas, including the rostral portion of the anterior cingulate cortex (rACC) and the opioidergic PAG-RVM system, which is thought to mediate the analgesic placebo effect, presumably by gating the ascending nociceptive input [Figure 5A, (75, 79)]. This mechanism has been supported by numerous fMRI and PET studies, suggesting that neuroimaging techniques are highly suitable for analyzing placebo effects (74, 79, 80).

In addition to pain, other negative emotions and their associated neural substrates have been successfully modulated by placebo treatments. In Petrovic et al. (64), participants who believed they were receiving an anxiolytic and sedative drug reacted less aversively to unpleasant pictures and showed reduced picture-related neural activation in the amygdala. Interestingly, Petrovic et al. further reported a placebo-dependent activation in the rACC (Figure 5B), thus indicating some potential functional commonalities between the placebo-dependent modulation of pain and emotion-regulatory placebo effects. This latter study provides some of the motivations for the current research project.

De la Fuente-Fernández et al. (70) investigated placebo effects by injecting saline in PD patients who had been told it was an active anti-Parkinson drug. The treatment led to a release of endogenous dopamine in striatal target areas of the dopaminergic pathway (which is impaired in PD patients) as assessed by positron emission tomography (PET) using the radio-labeled D2 dopamine receptor antagonist [^{11}C]raclopride (RAC). Patients characterized by a high placebo-induced release of endogenous dopamine also showed clinical improvements. In Figure 5C, reduced color intensity after placebo administration results from a decreased binding of RAC due to elevated endogenous dopamine levels in striatal regions. The authors considered the placebo-induced release of endogenous dopamine to be a consequence of reward expectation (here the expected beneficial treatment effect), which is known to activate dopaminergic pathways in animals as well as humans (81, 82).

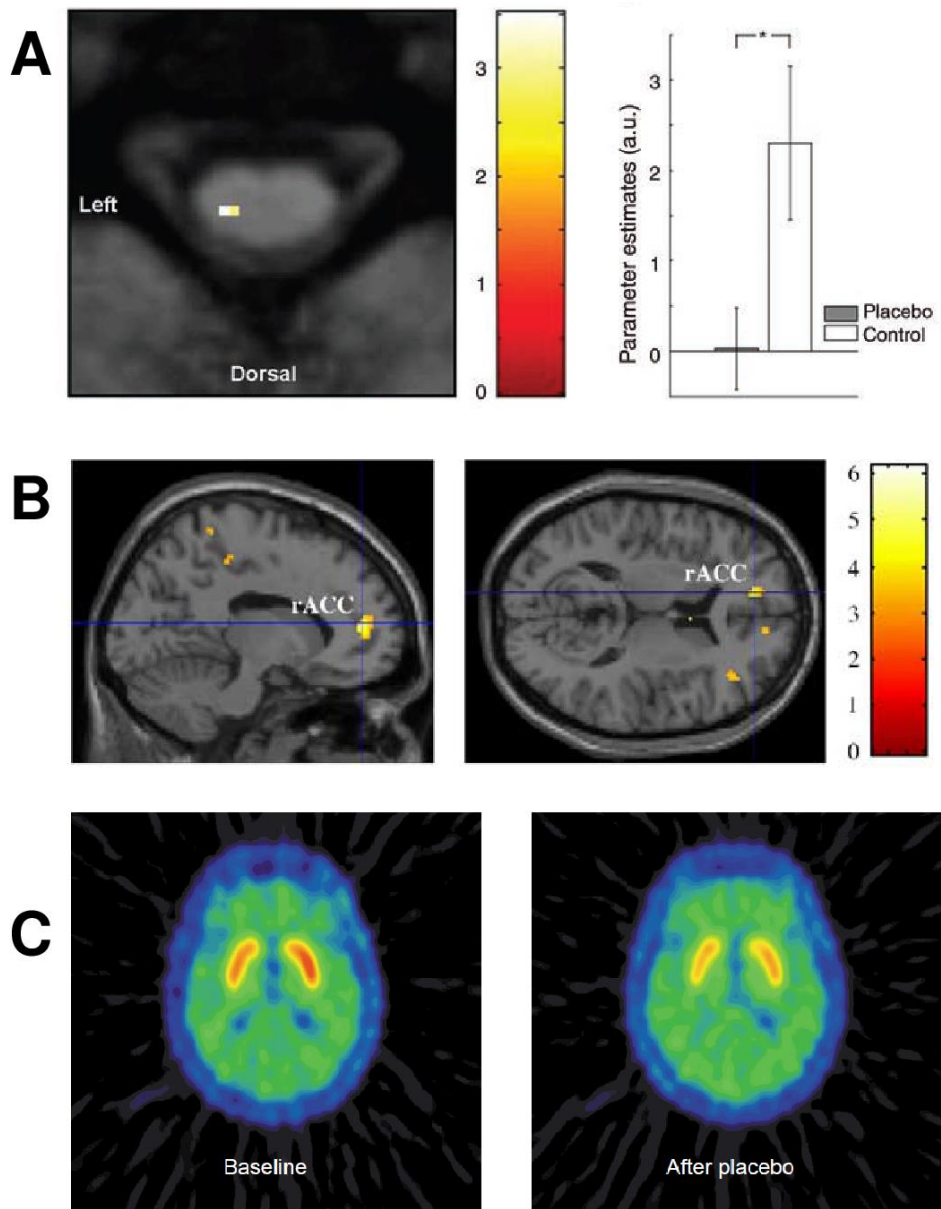


Figure 5: Placebo effects in experimental pain, emotional processing and Parkinson's disease

(A) Placebo-dependent deactivation: Decreased pain-related BOLD responses in the dorsal part of the spinal cord at the earliest stage of pain-processing in the central nervous system (significant voxels are highlighted according to suprathreshold t -values). Parameter estimates were extracted from the peak voxel (right; grey bar: pain-related BOLD response in the placebo group, white bar: pain-related BOLD responses in the control group). (B) Placebo-dependent activation: Under the illusion of having received a sedative treatment, enhanced BOLD responses in the rostral portion of the anterior cingulate cortex (rACC) were reported during unpleasant picture presentation (significant voxels are highlighted according to suprathreshold t -values). In return, unpleasantness ratings decreased under placebo (not shown here). (C) Decreased binding of a radio-labeled D2 dopamine receptor antagonist due to elevated endogenous dopamine levels in the striatum of PD patients after placebo treatment (right) compared to baseline (left). [Adapted from (64, 70, 83)]

3. Aim of this research project

This research project was designed to elucidate the neurobiological effects of placebo treatments on human fear and anxiety under controlled laboratory conditions. In three consecutive studies (Study 1-3), temporary states of fear and anxiety were induced and an inactive medication coupled with a verbally suggested expectation of anxiolysis was administered. No prior conditioning procedure was applied, so that mere treatment expectations could be made responsible for the observed placebo effects. Subjective fear ratings, SC-, pupillometry-, EEG- and fMRI recordings were used to assess activity on different levels of neural processing.

Phasic fear was induced over trials of 5 s through the anticipation of a previously experienced painful electrocutaneous stimulus signaled by a threat cue. Several threat (T) and no-threat (NT) cues (where no pain was to be expected) were presented in unpredictable order within experimental runs of 2-3 min to create a threatening context inducing tonically increased levels of autonomic arousal as in sustained states of anxiety. Participants received an inactive medication that was labeled and introduced as a potent anxiolytic drug in placebo runs (P) and as an inactive control treatment in No-Placebo runs (NP). A real anxiolytic medication was never applied.

In Study 1, the influence of the placebo treatment on phasic fear was measured by cue-related SC responses (SCR) and subjective fear ratings. To examine tonic levels of autonomic arousal in P- vs. NP runs, a novel approach separating tonic SC changes from phasic SCRs was applied. In Study 2, electroencephalograms were additionally recorded and placebo-dependent modulations of cue-induced ERPs were examined. The analysis focused on P300 and LPP components as markers of attentional processes in response to highly salient and emotional cues. To further test whether the placebo treatment is capable of inducing tonic cue-independent changes in oscillatory brain activity, EEG-spectra from the inter-trial intervals (ITI) were analyzed. In Study 3, fMRI images were acquired to localize the neural targets of the anxiolytic placebo treatment, thus examining placebo-induced decreases of phasic and tonic BOLD activity in threat responsive cortical and subcortical regions, including major SN key structures such as the dACC, the ai and the amygdala. In order to test for functional commonalities across regulatory sources mediating placebo analgesia and placebo anxiolysis, further analyses focused on placebo-induced BOLD responses in the rACC (a likely candidate for a common regulatory source). In addition to standard cue-related fMRI analyses, the placebo-induced effect on FC within and between

major ICNs was analyzed, making this the first study linking a placebo effect to shifts in global network activity.

4. Materials and Methods

4.1. Study participants

All participants were healthy, right-handed and had no prior experience with psychopharmacological medications in a therapeutic context. In the first behavioral study (Study 1), 30 volunteers (mean age 25.7 years, age range 20-45 years, 14 female) were enrolled. 29 additional volunteers (mean age 26 years, age range 20-34 years, 14 female) participated in the subsequent EEG study (Study 2) and 23 volunteers (mean age 24.6 years, age range 20-31 years, 13 female) in the final fMRI study (Study 3). State and trait anxiety scores were assessed before the experiments using the State-Trait Anxiety Inventory (84). Participants' trait anxiety scores ranged from 27 to 55 (mean±standard deviation 38.1±6.1) in Study 1, from 20 to 53 (37.7±8.2) in Study 2 and from 29 to 58 (38.4±7.2) in Study 3. State anxiety before the experiment ranged from 23 to 51 (33.6±6.4) in Study 1, from 25 to 63 (35.1±7.8) in Study 2 and from 25 to 59 (36.7±8.3) in Study 3. Prior to the experiment, participants rated the expected efficacy of the treatment. Participants who did not expect a beneficial effect were excluded. This procedure reduced sample sizes to N=28 in Study 1 and to N=27 in Study 2. In Study 3, the sample size remained N=23.

Of these, N=26 (Study 1), N=23 (Study 2) and N=18 (Study 3) participants could be analyzed for effects on SC, N=24 (Study 2) for effects on the EEG, N=20 (Study 3) for effects on the fMRI and N=16 (Study 3) for effects on pupil size. The Ethics Committee of the State Medical Board in Hamburg (Study 1 + 2) and Rheinland-Pfalz (Study 3), Germany, approved the studies and all participants gave written informed consent. The consent form included information about the experimental procedures, but did not include statements suggesting that participants would be deceived and that the purpose of the study was to investigate placebo anxiolysis. Participants were informed about these important aspects only during debriefing.

4.2. Experimental procedure

In Studies 1 and 2, the volunteers were informed that they would be participating in a clinical study examining the physiological effects of Lorazepam, a potent anxiolytic drug administered as a nasal spray. Lorazepam is in fact not available as nasal spray and was never administered in the experiments. To further induce positive treatment expectations, each participant received a fictive information brochure describing the effects and potential

side-effects of Lorazepam (see Appendix: Information brochure Study 1+2). Each participant received two differentially labeled nasal sprays that both contained normal saline. The placebo spray was labeled as a real drug and was marked with the uppercase letter “L”, whereas the control spray was labeled as normal saline with the uppercase letter “N” (NaCl). Participants were told that the perceived effects of the Lorazepam spray would appear after approximately 30 seconds and last for 2 to 3 min. Participants then rated their treatment expectations on a visual analog scale (VAS) ranging from 0 (no expectation) to 100 (very high expectations). The experiment itself consisted of 6 runs under placebo (P runs) and 6 control runs (no-placebo, NP runs) in pseudo-randomized order. Each run began with the instruction to apply the corresponding spray once into the indicated nostril. Instructions were presented for 45 s and were followed by 6 to 7 threat (T) and 5 no-threat (NT) trials. In T trials, participants knew from prior instruction that they might receive a painful electric stimulus with a probability of 25% at any time during the 5 seconds in which a red square was present on the screen. One or two of the T trials in each run were paired with a painful stimulus and were later excluded from the analysis. In NT trials, a green square was presented for 5 s and participants knew they would not be stimulated. Trials were separated by a 5 to 8 s presentation of a fixation cross. A treatment-induced reduction in fear of the painful electrocutaneous stimuli was explicitly suggested by the experimenter. Throughout the P runs, an L was additionally presented on the screen to remind participants of the applied treatment, while an N was presented in NP runs. At the end of each run, participants rated their average level of fear for both the T and NT trials on a VAS ranging from 0 (no fear/tension) to 100 (high fear/tension). The average duration of a single run was 2.3 min. After six runs, the participants paused for 3 minutes (Figure 6).

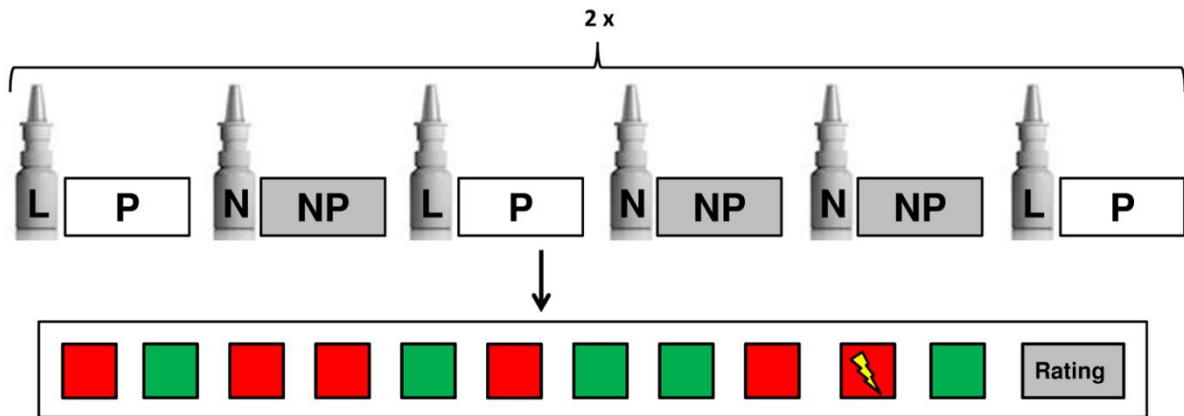


Figure 6: Study design (Studies 1+2)

An experiment comprised 6 runs in which participants were under the verbally induced illusion of having received an anxiolytic pharmacological treatment (placebo, P runs), and 6 runs without placebo (no-placebo, NP runs). Each run began with the application of one of two nasal sprays labeled either “L” (for Lorazepam, in P runs) or “N” (for NaCl, in NP runs). Each run consisted of 11 to 12 trials in the threat (T, signaled by a red square) or no-threat condition (NT, green square), each with a duration of 5 s. During the T trials, participants knew they could receive a painful electric shock (bolt symbol) with a probability of 25%. It was reasoned, that the T trials induce a phasic fear reaction compared to NT trials, whereas the temporally unpredictable occurrence of T trials within runs created an uncertain, threatening context that induces sustained anxiety. At the end of each run, participants were asked to rate their fear of the red and green squares.

Some procedural changes were applied in Study 3 in order to create a study design more suitable for fMRI. Volunteers were informed that they would be participating in a clinical study examining the effects of laughing gas on the CNS. The information brochure from Study 1 and 2 was adjusted accordingly (see Appendix: Information brochure Study 3) and participants were told that the perceived effects of laughing gas last for 2 to 3 min. The experiment itself consisted of 6 P- and 6 NP runs in pseudo-randomized order. Each participant expected to receive laughing gas in P runs and air in NP runs. At the beginning of each run, instructions informed participants what kind of treatment will be applied, followed by a 30 s inhalation phase, during which mint-scented air was administered in both P- and NP runs. The inhalation phase was followed by 4 or 5 threat (T) and 3 no-threat (NT) trials as indicated by different geometrical figures presented on the screen (square and circle). In the T trials, participants knew that they might receive a painful electric stimulus with a probability of 33% at any time within the 5 s of cue presentation. One or two of the T trials per run were paired with a painful stimulus and were later excluded from the analysis. In NT trials, participants knew they would not be stimulated during the 5 seconds of cue presentation. Trials were separated by a 5 to 11 s long presentation of a fixation cross (inter-trial interval = ITI). Throughout P runs, ‘LG’ (Lachgas = laughing gas in German) was additionally presented on the screen to remind participants of the applied treatment, whereas ‘LU’ (Luft = air in

German) was presented in NP runs. At the end of each run, participants rated their average level of fear for both T and NT trials on a VAS ranging from 0 (no fear/tension) to 100 (high fear/tension). The average duration of a single run was 2.3 min. After four runs, participants paused for 3 minutes (Figure 7).

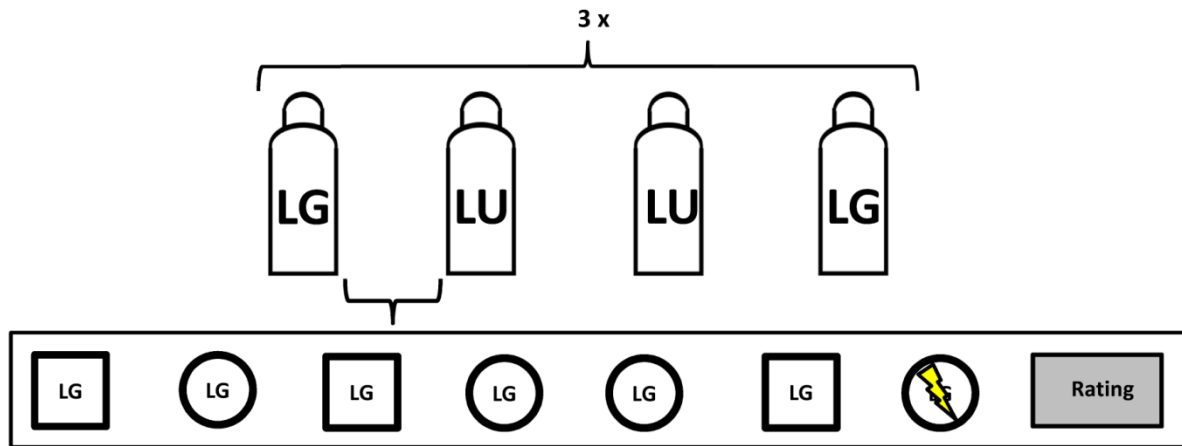


Figure 7: fMRI study design (Study 3)

An experiment comprised 6 P and 6 NP runs, during which participants expected to receive either laughing gas (LG) or air (LU), respectively. In fact, air was applied in all runs. Within each run, 7 to 8 T or NT trials were presented (here signaled by circles and squares, respectively), each with a duration of 5 s. During the T trials, participants expected to receive a painful electric shock (bolt symbol) with a probability of 33%. At the end of each run, participants were asked to rate their fear of circles and squares.

4.3. Electric stimulation

Painful electric stimuli consisted of trains of three square wave pulses of 2 ms each, separated by 50 ms intervals. Pain stimuli were generated by a DS7A electric stimulator (Digitimer Ltd., Welwyn Garden City, UK) and delivered on the right dorsal hand through a surface electrode. In a prior calibration procedure, participants were asked to rate increasing stimulus intensities on a scale from 0 (no pain) to 10 (strong pain). An intensity corresponding to a pain level of 7 was used in the experiment.

4.4. Skin conductance measurement

4.4.1. Skin conductance recordings

SC time courses were measured in Studies 1-3 by applying a small electric voltage (0.5 V) between two palmar electrodes at the thenar and hypothenar eminence with an MP150 SC unit (Biopac Systems Inc., USA) in Studies 1 and 3, and a CED2502-SA SC unit (Cambridge

Electronic Design, Cambridge, UK) in Study 2. Acknowledge 4.2 software (Biopac Systems Inc., USA) was used in Studies 1 and 3, and Spike 2 software (CED) was employed in Study 2. Data were down-sampled to 100 samples per second (sps) and denoised by applying a Butterworth low-pass filter with a cut-off frequency of 20 Hz and additional Gaussian smoothing.

4.4.2. Analysis of skin conductance responses and levels

SC varies as a function of sweat secretion from eccrine glands as controlled by the sympathetic branch of the ANS. The SC signal thus increases in states of emotional arousal with related sympathetic activity (22, 85). SC signals can generally be described as consisting of two separable components: a slowly varying component (the SC level, SCL) and a rapidly varying component (the phasic SC responses, SCRs). The SCL reflects a tonic or background state of sympathetic activity (85, 86), whereas SCRs are immediate sympathetic responses to discrete stimuli such as threat cues (45, 85, 87). In order to distinguish phasic fear-related responses induced by cue onset from sustained anxiety-related tonic arousal levels within a run, SC time courses were decomposed into a slowly varying tonic component SC_{tonic} and a rapidly changing phasic component SC_{phasic} using a deconvolution method implemented in the Matlab toolbox Ledalab V344 (87). The applied method first deconvolves the SC time course with an appropriate impulse response function (IRF) representing the standard SCR shape. This yields an estimate of the underlying function triggering phasic SCRs ($Driver_{\text{SC}}$). Inter-impulse sections in $Driver_{\text{SC}}$, where no SCRs are generated, are then used to estimate a tonic driver function ($Driver_{\text{tonic}}$) by an interpolation procedure. $Driver_{\text{tonic}}$ is finally convolved with the IRF and represents a suitable measure of the underlying SCL (SC_{tonic}) exempt from rapidly changing SCRs. Subtracting SC_{tonic} from SC allows for an estimate of the phasic activity (SC_{phasic}), which in turn does not contain any slow SC variations. An example for a decomposed time course is shown in Figure 8.

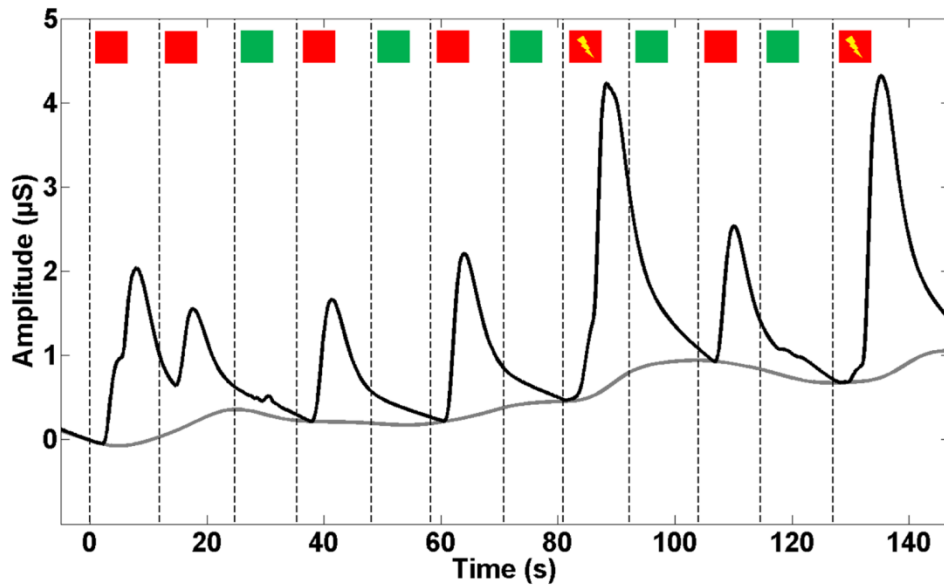


Figure 8: Example of a decomposed skin conductance (SC) time course

The SC time course and the underlying tonic component (SC_{tonic}) are represented by black and grey lines, respectively. The phasic component (SC_{phasic}) can be obtained by subtracting SC_{tonic} (grey line) from SC (black line). Dashed lines indicate trial onsets of T- (red squares) and NT trials (green squares). Painful electric stimuli (bolt symbol) were applied in trials 8 and 12.

SCL was defined as the average SC_{tonic} ranging from the onset of the first cue in a run to the onset of the rating phase minus the average SC_{tonic} in a 1 s time window prior to the first cue. Values were z-transformed and averaged for each participant. SCRs were manually scored from SC_{phasic} by using a custom-made computer program. SCR amplitudes in microsiemens (μS) were scored as the first response occurring from 0.9 to 4 s after cue onset with a minimal response amplitude of $0.02 \mu\text{S}$. Smaller SCRs were zeroed. Values were logarithmically transformed and log values were range corrected ($\log(1+\text{SCR})/\text{max}$) to account for intra- and inter-individual variability (88). A complete lack of threat-induced SCRs, excessive baseline activity and a technical problem involving one participant led to the exclusion of two participants in Study 1, four participants in Study 2 and five participants in Study 3. Finally, SC data from 26 participants in Study 1, 23 participants in Study 2 and 18 participants in Study 3 were analyzed.

4.5. Pupillometry

4.5.1. Pupil size recordings

Pupil size was measured monocularly in Study 3 using an MRI-compatible camera (MR Cam Model 12M; MRC Systems, Germany). iViewX 2.8 software (Sensomotoric Instruments,

Germany) was used for recordings (Figure 9). Data were down-sampled to 60 sps and missing values (mainly due to eye-blinks) were linearly interpolated from neighboring values. The data were then denoised by applying a Butterworth low-pass filter with a cut-off frequency of 4 Hz.

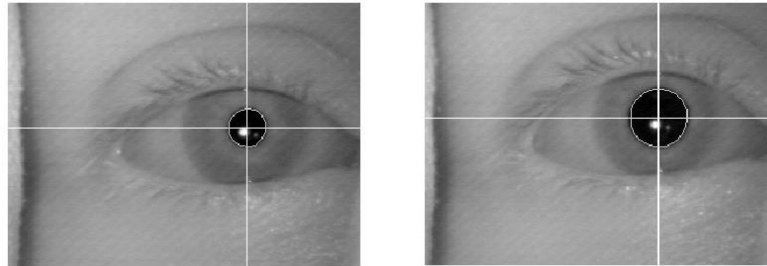


Figure 9: Pupillometry

Pupil size was recorded with an MRI-compatible camera. Constricted pupil (left), dilated pupil (right).

4.5.2. Analysis of pupil dilation

Pupil size is regulated by two competing muscle groups. Radial dilator muscles increase and sphincter muscles decrease the pupil diameter. The sphincter muscle has a parasympathetic innervation and the dilator a sympathetic innervation. Accordingly, the pupil size increases with sympathetic activity in response to emotionally arousing stimuli (89). Data epochs ranging from 1000 ms before to 5000 ms after cue onset were extracted for further analyses. Data were baseline-corrected to the average of 1000 ms to 0 ms prior to cue onset, and samples from 1000 ms to 5000 ms after cue onset were averaged for statistical analyses.

4.6. Statistical analysis of behavioral data

Statistical analyses of behavioral data were performed by repeated-measures analysis of variance (ANOVA) using the free software environment R (Version 3.0.0). Main and interaction effects on cue-related responses were further defined by the following contrasts:

Main effect of threat:	$[T/P+T/NP] - [NT/P+NT/NP] = T-NT$
Main effect of placebo:	$[T/P+NT/P] - [T/NP+NT/NP] = P-NP$
Threat by placebo interaction:	$[T/P-NT/P] - [T/NP-NT/NP] = \Delta T_P - \Delta T_{NP}$

“P” and “NP” indicated whether a T or NT trial occurred in P or NP runs. Significant effects (α -threshold = 0.05) were further characterized by one-tailed Student’s *t*-tests. Subdivision

into high (HR) and low (LR) placebo responders was performed by median split on the main effect of placebo contrast in fear ratings.

4.7. EEG

4.7.1. EEG recordings and preprocessing

Electroencephalograms were only recorded in Study 2. Recordings took place in a sound-attenuated and electrically shielded room. Participants were seated in a slightly reclined chair in front of a 19" computer monitor and were asked to keep their eyes open. The distance between the participant's eyes and the monitor was approximately 1 m. Data were collected at a rate of 1000 sps with 66 active electrodes mounted on an elastic cap (ActiCaps, Brain Products, Munich, Germany) using the Brain Vision Recorder software Version 1.10 (Brain Products, Munich, Germany). Electrodes were arranged according to a modified 10/10 system without electrodes at the positions FPz, F9, F10, T9, T10, CP3, CP4, P9, P10, PO7, PO8 and with additional electrodes at positions PO9 and PO10 (see Appendix Figure A1). Eye movements were recorded through four EOG channels (positioned at the outer canthi bilaterally and infra- and supraorbitally on the right). An electrode at the FCz position was used as the reference and the electrode at position AFz served as ground. Impedances were always kept below 5k Ω . Data were preprocessed and further analyzed by using the Matlab toolbox fieldtrip (Version 20131120; (90)). Continuous data sets were band-pass filtered for frequency analyses with cut-off frequencies of 0.1 and 40 Hz and low-pass filtered with a cut-off frequency of 40 Hz for ERP-analyses. Every trial was subdivided into pre- and post-cue onset epochs ranging from 3500 ms to 0 ms prior to trial onset (used as the inter-trial interval, ITI) and from 500 ms prior to trial onset to 1500 ms after trial onset, respectively. Data were down-sampled to 250 sps, re-referenced to the common average, and an independent component analysis (ICA) was applied to remove eye-blinks and horizontal eye-movements from epochs. Data were finally baseline-corrected to an average of 3500 ms to 3000 ms prior to trial onset for pre-cue onset epochs (ITIs) and to an average of 500 ms to 0 ms prior to trial onset for post-cue onset epochs. Trials that continued to contain residual artifacts were excluded from further analyses. ERP analyses were performed on post-cue onset epochs and frequency power analyses were performed on pre-cue onset epochs. Three participants were excluded from further EEG analyses due to excessive artifacts. EEG data from 24 participants were subsequently analyzed.

4.7.2. ERP analysis

ERPs of interest were predefined based on a pilot study (N=20, 3 participants were excluded), in which 60 T and 60 NT trials were presented without any placebo manipulation. Three time windows and corresponding electrode sets showing pronounced deflections under threat (T-NT) were selected (P100, P300, LPP) for Study 2.

Mean potentials within predefined time windows were averaged across trials and statistically analyzed. Therefore, *t*-contrasts for each electrode were defined as described in the statistical analysis of behavioral data. In order to account for the multiple comparison problem, nonparametric cluster-based permutation tests (91) were used on corresponding *t*-statistics for either the whole sample (two-tailed one-sample *t*-tests) or for the comparison of HRs and LRs (two-tailed two-sample *t*-tests). Electrodes with *p*-values < 0.05 were considered as candidate members of a cluster. Cluster-level statistics were calculated by taking the sum of the *t*-values within every cluster. The number of randomizations was set to 5000 and cluster *p*-values smaller than a critical alpha-level of $\alpha=0.05$ indicated significant effects.

4.7.3. EEG frequency analysis

EEG power spectra of ITI recordings were analyzed to explore whether the placebo treatment affects tonic cue-unrelated oscillatory activity. For this purpose, baseline-corrected segments of 3000 to 0 ms prior to trial onset were extracted from pre-cue onset epochs (see 4.7.1), Hanning-windowed and Fast Fourier transformed (FFT, 1 Hz resolution). Power spectra were averaged across P and NP runs and subdivided into multiple classical frequency bands: delta=1-3 Hz, theta=4-7 Hz, alpha=8-12 Hz, beta1=13-20 Hz, and beta2=21-30 Hz. Differences between P and NP runs were assessed by two-tailed *t*-tests, and cluster-based analyses on all electrodes were used to correct for multiple comparisons as described in 4.7.2.

4.8. fMRI

4.8.1. fMRI data recordings

MR data were obtained with a 3 Tesla MR scanner (MAGNETOM trio; Siemens, Germany) by using a 32-channel head coil. For fMRI, 38 continuous axial slices (3 mm thick) were acquired by using a T2*-sensitive gradient echo-planar imaging (EPI) sequence [repetition time: 2.5 s; echo time (TE): 30 ms; field of view (FOV): 208x208 mm; 2x2 mm in-plane

resolution]. The position of the slice package (image) was individually adjusted for whole-brain image acquisition. 3x400 images (fMRI time series) were acquired, each including data from four experimental runs. At the end of the experiment, a high-resolution T1-weighted structural image (1x1x1mm) was further acquired.

4.8.2. fMRI data preprocessing

To account for T1 equilibrium effects, the first five images of each time series were discarded, resulting in 3x395 fMRI images. fMRI data were preprocessed by a standard procedure and further analyzed using the Matlab toolbox SPM8 (Wellcome Trust Centre for Neuroimaging, UK). Preprocessing of the fMRI data first involved realignment and unwarping to correct for movements and nonlinear distortions due to inhomogeneities in the magnetic field, respectively. fMRI data were then coregistered with corresponding T1-weighted structural images and normalized to a standard template from the Montreal Neurological Institute (MNI) to allow for group comparisons. fMRI data were finally spatially smoothed with a 6-mm full-width-at-half-maximum (FWHM) isotropic Gaussian kernel. Excessive head movement led to the exclusion of 3 participants. fMRI data from 20 participants were analyzed.

4.8.3. Standard fMRI data analysis

Preprocessed single-subject fMRI data were concatenated to time series of 1185 images. Analyses of the concatenated time series were performed voxel-wise by a general linear model (GLM) approach implemented in the Matlab toolbox SPM8. In matrix notation, the GLM can be defined as $Y = X\beta + \epsilon$. Here, Y is a column vector representing the time series of $J = 1185$ image intensity values of a single voxel. X is a $J \times L$ matrix (design matrix) consisting of L concatenated column vectors (regressors) designed to explain signal variations in Y induced by the experimental procedure. Each trial type (NT/NP, NT/P, T/NP, T/P) was modeled as a $J \times 1$ “boxcar regressor” with value 1 during trials and 0 otherwise, indicating whether a trial type is turned on or off at the given time point of image acquisition j (unit=images). Boxcar regressors indicating P- and NP runs were also included and all regressors were convolved with a canonical hemodynamic response function (HRF) to model the shape of the expected BOLD signal induced by experimental trials and runs (Figure 10). Trials including electric shocks, electric shock events, ratings and inhalation phases as well as the three scan blocks were modeled in the same way and added as nuisance regressors. In the GLM, β is a column vector of L parameters to be estimated, with β_l corresponding to the l^{th} regressor. ϵ represents a column vector of residual errors. Parameter estimation was

performed by fitting values $\tilde{Y} = X\tilde{\beta}$ to the actual values Y . Optimal parameter estimates $\tilde{\beta}$ were calculated by using the method of ordinary least squares (OLS) in order to minimize the term $\epsilon\epsilon^T$. OLS estimates $\tilde{\beta}$ are denoted as $\hat{\beta}$, where $\hat{\beta}_l$ can be interpreted as the size of the estimated BOLD signal change explained by the l^{th} regressor. $\hat{\beta}_l$ values are referred to in the text as “parameter estimates” and were calculated for each single voxel, resulting finally in L $\hat{\beta}$ -images (brain maps), available for each participant (first-level analysis).

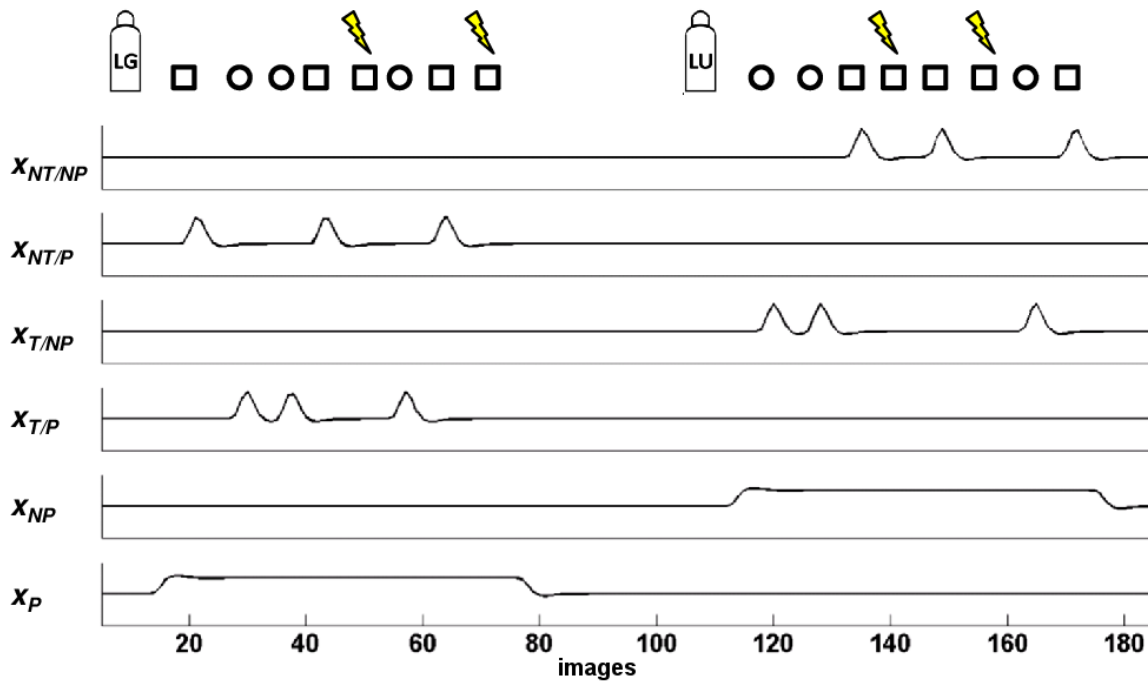


Figure 10: Regressors of the GLM design matrix

$X_{NT/NP}$, $X_{NT/P}$, $X_{T/NP}$, $X_{T/P}$, X_{NP} , X_P represent the expected shape of BOLD signals induced by experimental trials and runs. Only the first 185 values, each corresponding to a time point j of image acquisition, are plotted. Note that trials including electrocutaneous stimuli were modeled as additional nuisance regressors (not shown here).

Group statistics were performed by first contrasting the $\hat{\beta}$ -images in each participant and then performing group-level t -tests on each voxel, resulting in group-level t -images (t -maps) for the following contrasts (second-level analysis, see also 4.6).

Main effect of threat: $[T/P+T/NP] - [NT/P+NT/NP] = T-NT$
 Main effect of placebo: $[T/P+NT/P] - [T/NP+NT/NP] = P-NP$
 Threat by placebo interaction: $[T/NP-NT/NP] - [T/P-NT/P] = \Delta T_{NP} - \Delta T_P$

SPM calculates one-tailed t -tests, meaning that above contrasts only test for one direction of the effect ($T-NT = T > NT$, $P-NP = P > NP$, $\Delta T_{NP} - \Delta T_P = \Delta T_{NP} > \Delta T_P$). Inverse contrasts are thus reported separately as $NT-T$, $NP-P$ and $\Delta T_P - \Delta T_{NP}$. Results are reported at $p < 0.05$ corrected

with familywise error corrections (FWE) for multiple voxel comparisons (92). The statistical analysis of fMRI data is summarized and illustrated in Figure 11. For visualization of effects in *t*-maps the threshold is set to $p < 0.001$, uncorrected. Single voxel analyses on extracted parameter estimates were performed by repeated measures ANOVAs and one-tailed post hoc *t*-test.

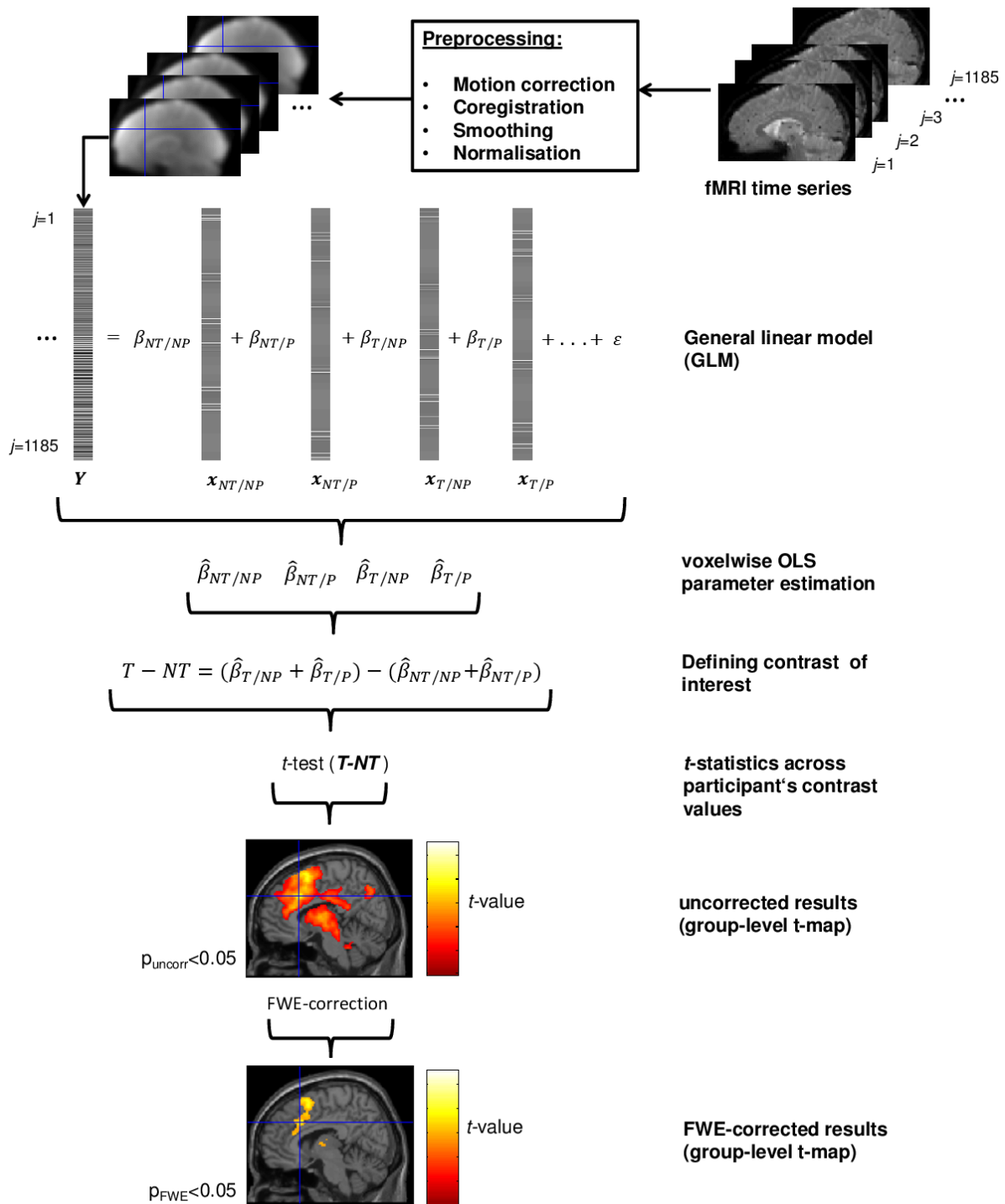


Figure 11: Standard fMRI data analysis

Raw fMRI time series are preprocessed and further analyzed by a general linear model (GLM) approach. GLM parameters ($\hat{\beta}$) are estimated voxel-wise in each participant, representing BOLD signal changes induced by different experimental conditions. Contrasts of interest are calculated on the basis of $\hat{\beta}$ -values (here exemplified by a main effect of threat T-NT) and tested on a group level. t -values are thresholded to correct for multiple comparisons (FWE correction) and thus suprathreshold voxels are finally reported as statistically significant effects.

4.8.4. Functional connectivity analyses

Functional connectivity (FC) represents a measure of joint activity of distinct brain regions. A psychophysiological interaction (PPI) describes changes in FC depending on different experimental conditions (Figure 12).

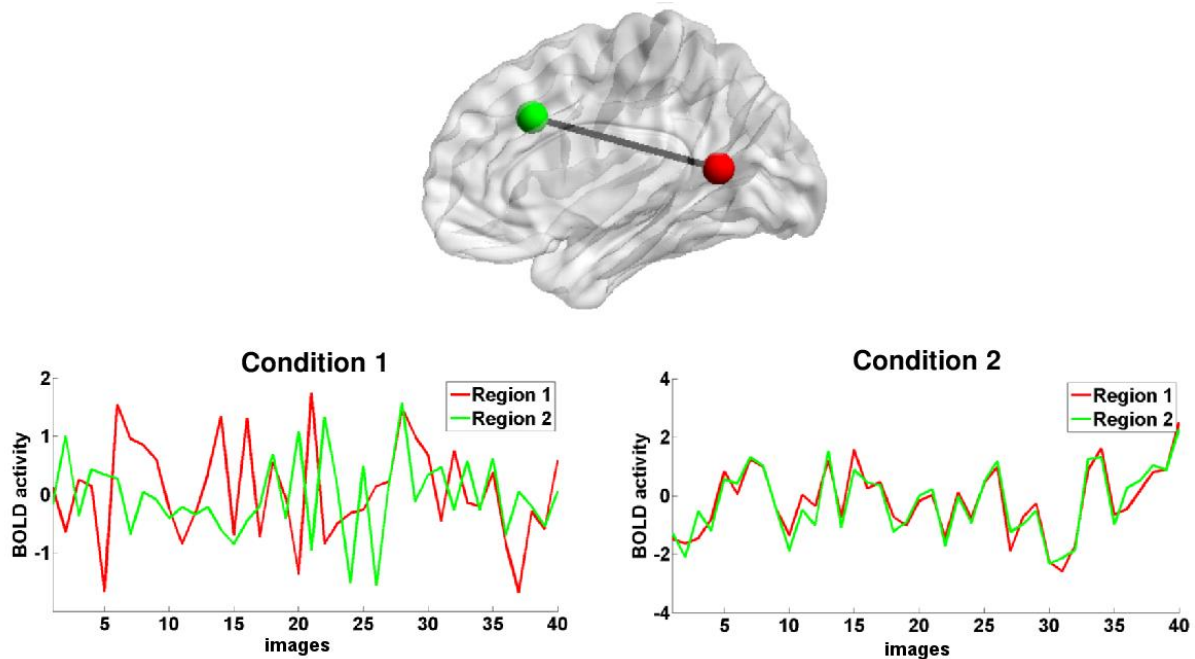


Figure 12: Psychophysiological interaction (PPI)

Functional connectivity (FC) between Region 1 and 2 (simulated data) differs depending on the experimental condition, with stronger FC in condition 2 compared to condition 1.

PPI analyses were performed by using SPM 8. To analyze changes in FC in P vs. NP runs, a GLM design matrix was defined including a physiological, a psychological, a PPI and further nuisance regressors. The physiological regressor reflected characteristic BOLD signal changes in a predefined seed region throughout the experimental procedure and was extracted as the 1st eigenvariate of BOLD signal time courses in a sphere (radius: 6mm) around a predefined seed voxel. The psychological regressor defined the differential effect between P and NP runs with values 1=P run, -1=NP run, otherwise 0. To obtain the PPI regressor, the physiological variable was deconvolved with the HRF, multiplied element-wise with the psychological regressor and again HRF-convolved. Parameter estimates were calculated voxel-wise. For each voxel B, the PPI parameter estimate $\beta_{A \rightarrow B}$ yields the placebo-dependent change in FC between B and the predefined seed region A. PPI analyses were performed with major SN and DMN nodes (see also 5.3.2.1) as seed regions, thus allowing for FC changes to be monitored for each pair of nodes within and between the two networks. It should be noted that PPI analyses are asymmetric and thus $\beta_{A \rightarrow B} \neq \beta_{B \rightarrow A}$.

Both directions were considered for group-level analyses. Overall coupling within and between networks was calculated by averaging corresponding parameter estimates for each participant. Unless otherwise stated, averaged parameter estimates were tested with two-tailed one sample t -tests ($\alpha=0.05$). Results were visualized with BrainNet Viewer (93). Edges were drawn between nodes in network plots when either $\beta_{A \rightarrow B}$ or $\beta_{B \rightarrow A}$ yielded significant results (two-tailed one sample t -test, $\alpha=0.05$).

5. Results

5.1. Study 1

5.1.1. Behavioral results

Fear ratings and SC were acquired in Study 1. SC time courses were decomposed into phasic (SC_{phasic}) and tonic components (SC_{tonic}), reflecting cue-related SCRs and cue-unrelated SCLs as measures of phasic and tonic sympathetic arousal, respectively. An example of a decomposed SC time course is shown in Figure 9.

Fear ratings (Figure 13A) taken at the end of each run revealed a successful induction of phasic fear by the threat predicting cues (red squares in Figure 9) (main effect of threat, T-NT: $F_{1,27}=355.2$, $p<0.001$). The expectation of anxiolysis by the nasal spray produced both a main effect of placebo (P-NP: $F_{1,27}=15.9$, $p<0.001$) and a threat by placebo interaction ($F_{1,27}=15.36$, $p<0.001$). This pattern was qualified by a pronounced placebo-induced decrease in perceived fear in T trials (T/P-T/NP: $t_{27}=-4.04$, $p<0.001$, one-tailed post-hoc t -test), which, however, was also accompanied by a significant (albeit less pronounced) decrease in NT trials (NT/P-NT/NP: $t_{27}=-2.7$, $p=0.006$). Fear ratings were generally low in NT trials, leaving the possibility of a floor effect that might have masked placebo-related reductions in those trials, thus potentially producing an artificial interaction. It thus remains unclear whether the anxiolytic placebo acted mainly by attenuating a cue-unspecific state of aversion or arousal (in both T and NT trials), or also by genuinely affecting threat cue-specific phasic fear (in T trials only).

In line with fear ratings, phasic SCRs (Figure 13B) to the threat and no-threat cues again showed main effects of threat (T-NT: $F_{1,25}=163.8$, $p<0.001$) and placebo (P-NP: $F_{1,25}=5.34$, $p=0.0294$), but only a non-significant, though trend-like interaction ($F_{1,25}=3.96$, $p=0.058$), again leaving uncertainty as to the genuine effects of placebo treatment on threat cue-specific responses. Clearly supporting a cue-unspecific placebo action, tonic SCLs (Figure 13C) throughout experimental runs were also reduced after application of the placebo spray (P runs) relative to the control spray (NP runs) ($t_{25}=-2.55$, $p=0.017$, two-tailed t -test).

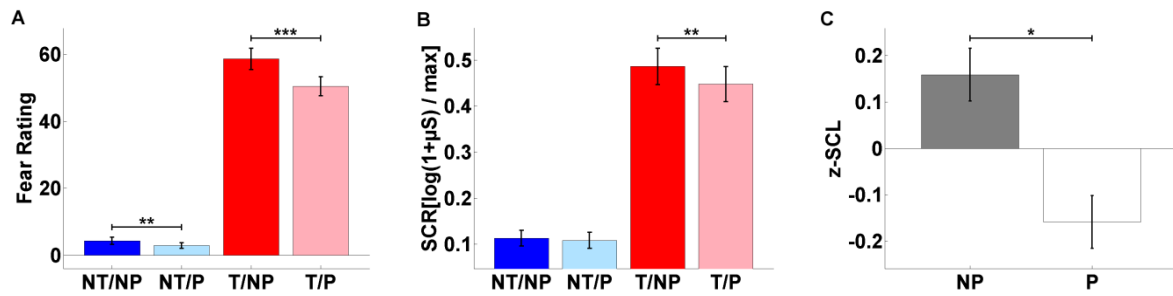


Figure 13: Behavioral results (Study 1)

Fear ratings (A) and skin conductance responses (SCRs; B) to the cues revealed main effects of placebo (P-NP), indicating a cue-unspecific placebo effect. Tonic skin conductance levels (SCL) measured throughout experimental runs (C) showed reduced arousal under placebo. NT, no-threat; T, threat; NP, no-placebo; P, placebo. *, $p < 0.05$; **, $p < 0.01$; ***, $p < 0.001$. Error bars indicate standard error of the mean (SEM).

Hence, participants appeared to be tonically less aroused and reactive to any salient event in the experiment (i.e., less vigilant) when under the illusion of having received an active anxiolytic treatment, suggesting the placebo reduced sustained states of anxiety. Effects on phasic fear were less clear. These results furthermore indicate that mere treatment expectation can reduce ANS activity and, thus, the placebo manipulation has a true psychobiological effect (i.e., not only represented by subjective ratings), as required in the definition of placebo effects.

5.2. Study 2

5.2.1. EEG Pilot study

To transfer a study design inducing states of anticipatory fear and anxiety to the EEG laboratory and furthermore to predefine electrodes of interest showing pronounced threat-related ERPs, a pilot study (N=23) was conducted, in which 60 T and 60 NT trials were presented without any placebo manipulation. Fear ratings and SCRs, indicating significant threat-related effects (Fear Ratings: $t_{22}= 11.54$; $p<0.001$; SCRs: $t_{22}= 8.85$, $p<0.001$), are shown in Figure 14.

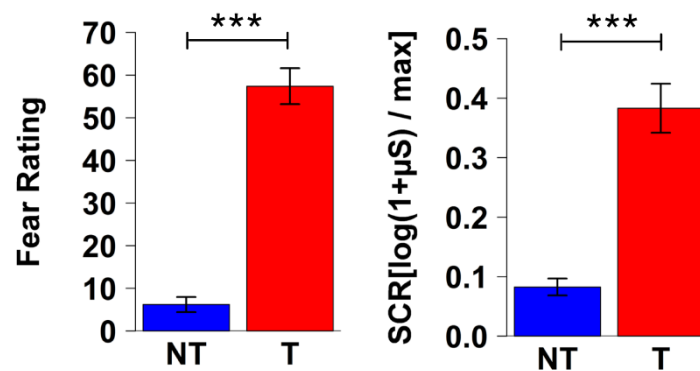


Figure 14: Behavioral results (EEG Pilot study)

Threat compared to no-threat cues significantly increased skin conductance responses (SCRs) and fear ratings. NT, no-threat; T, threat; *, $p<0.05$; **, $p<0.01$; ***, $p<0.001$. Error bars indicate standard error of the mean (SEM).

Three participants were excluded from further EEG analyses due to excessive artifacts (N=20). Midline electrodes showing pronounced threat-related effects were used to define ERP time windows of interest. Selected ERPs were termed as in the literature, so that e.g. P100 describes a positive potential deflection approximately 100 ms after cue onset. Three time windows and corresponding electrode sets showing pronounced deflections under threat were visually selected (T-NT, Figure 15): P100 (electrodes: POz, PO3-4, PO9-10, Oz, O1-2; time window: 100-140 ms), P300 and LPP (late positive potential) [electrodes: CPz, CP1-2, CP5-6, TP7-10, Pz, P1-8, POz, PO3-4, PO9-10, Oz, O1-2; time windows: 280-400 ms and 400-700 ms, respectively]. Each averaged selection revealed a strong main effect of threat (P100: $t_{19}=4.54$, $p<0.001$; P300: $t_{19}=5.28$, $p<0.001$; LPP: $t_{19}=8.5$, $p<0.001$). The ERP definitions were comparable to other studies on P100 (94), P300, LPP (32, 95), although time windows might differ slightly depending on the exact type of cue.

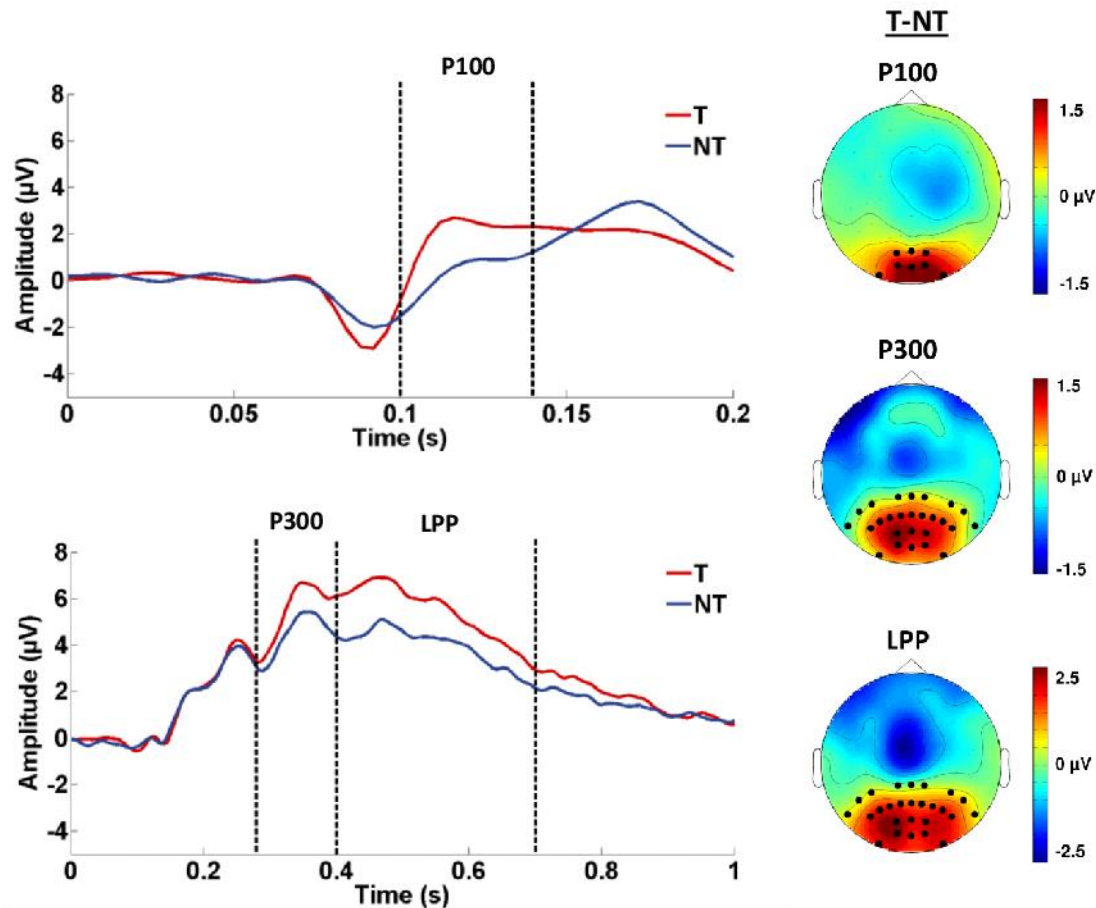


Figure 15: ERP definition (EEG Pilot Study)

Time windows of interest were defined on the basis of EEG signal changes in midline electrodes Oz (left, top) and Pz (left, bottom). Three time windows and corresponding electrodes of interest (right, black dots in the topographic maps) showing pronounced threat-related potentials (T-NT) were predefined in a pilot study: P100 (100-140 ms), P300 (280-400 ms), LPP (400-700 ms).

5.2.2. Behavioral Results

The experimental procedure of Study 1 was applied again with adapted behavioral measures (Fear ratings, SCR, SCL). Cue-unspecific placebo effects presumably indicating reduced vigilance were also evident in the EEG study, whereas again only limited support was found for genuine effects on threat cue-specific responses. As in Study 1, both fear ratings (Figure 16A) and SCRs (Figure 16B) showed main effects of threat (T-NT; ratings: $F_{1,26}=259.1$, $p<0.001$; SCRs: $F_{1,22}=153.9$, $p<0.001$) and placebo (P-NP; ratings: $F_{1,26}=18.98$, $p<0.001$; SCRs: $F_{1,22}=8.21$, $p=0.009$), with an interaction appearing only in fear ratings ($F_{1,26}=19.4$, $p<0.001$), but not in SCRs ($F_{1,22}=0.87$, $p=0.362$). In addition, tonic SCLs (Figure 16C) were again globally reduced by the placebo (P-NP: $t_{22}=-3.85$, $p<0.001$, two-tailed).

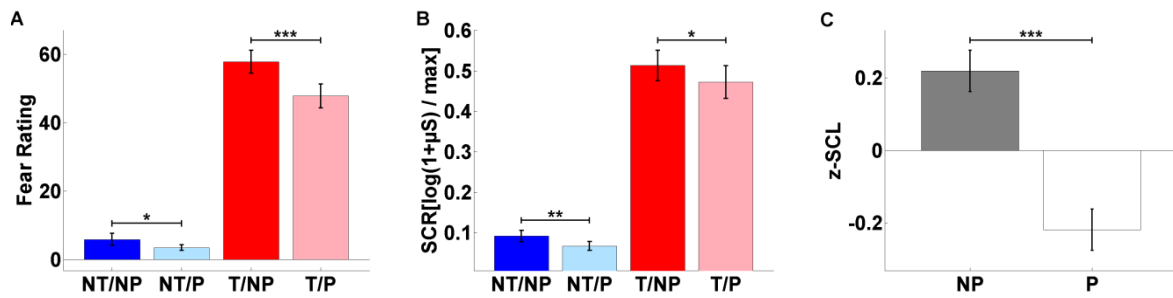


Figure 16: Behavioral results (Study 2)

As in Study 1, fear ratings (A) and SCRs (B) to the cues revealed main effects of placebo (P-NP), indicating a cue-unspecific placebo effect. Tonic SCLs (C) again showed reduced arousal under placebo. NT, no-threat; T, threat; NP, no-placebo; P, placebo. *, $p < 0.05$; **, $p < 0.01$; ***, $p < 0.001$. Error bars indicate standard error of the mean (SEM).

5.2.3. ERP results

Placebo-induced modulations of CNS-related cue responses were analyzed by means of predefined ERPs (see 5.2.1). Cluster-based permutation tests revealed significant main effects of threat (T-NT) for all predefined ERPs: P100 ($p = 0.004$), P300 ($p = 0.004$; Figure 17B) and LPP ($p < 0.001$; Figure 17B).

There was no modulation of the P100 component by the placebo. P300 and LPP amplitudes were further analyzed as threat-responsive EEG markers of externally directed attentional processes. The P300 component showed main effects of placebo (P-NP), both when analyzing the electrode exhibiting the strongest threat main effect (electrode P4: $F_{1,23} = 7.04$, $p = 0.014$; Figure 17A) as well as when performing a cluster-based permutation test within the pre-specified electrode set ($p = 0.002$; Figure 17B). However, no threat by placebo interaction could be identified with either approach. Like the P300 component, the LPP component also showed a placebo main effect in the cluster-based analysis ($p = 0.012$; Figure 17B) and, as with all other components, a lack of interaction. The absence of detectable threat cue-specific placebo effects in ERPs mirrors the behavioral results, with the observation of placebo main effects again indicating that the placebo manipulation acted globally on cue reactivity.

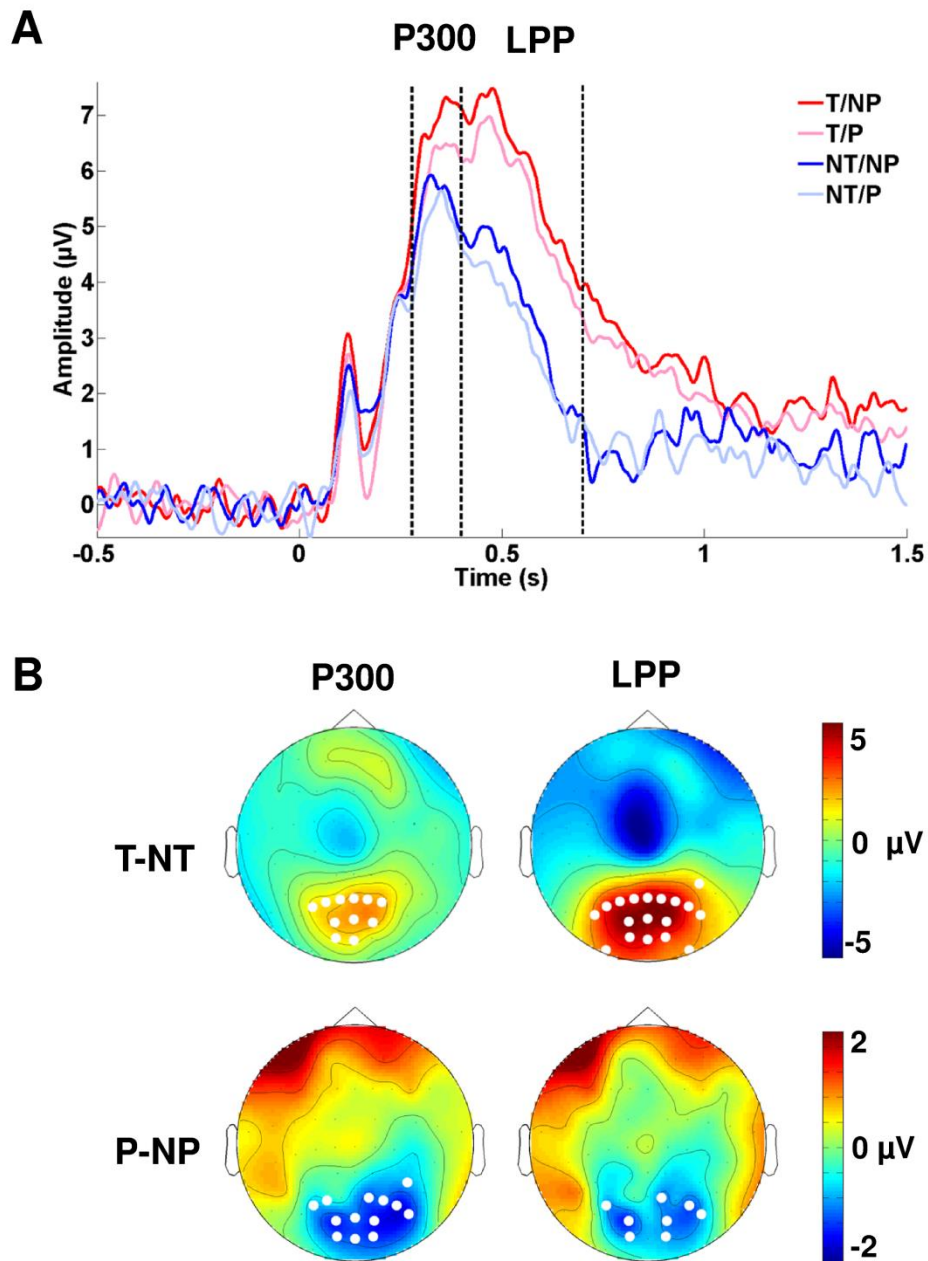


Figure 17: Event-related potentials (ERPs) (Study 2)

(A) Average activation time courses of electrode P4 time-locked to cue onset (0 s). Significant main effects of threat (T-NT, red-blue curves) and placebo (P-NP, light-dark curves) were found for the P300 and for the LPP components. (B) Topographic voltage difference maps for the threat and placebo main effects (T-NT: voltage increases, red; P-NP: voltage reductions, blue) in P300 and LPP. White dots indicate electrodes of significant clusters ($p < 0.05$).

Further highlighting a consistent effect of the placebo treatment on unspecific cue reactivity across both behavioral and neural measures, the P300 placebo main effect in the most threat-responsive electrode (P4) was predicted by participants' pre-experimental treatment

expectation ratings ($R=-0.56$, $p_{\text{Pear}}=0.005$; Figure 18A), meaning an inverse relationship existed between expected treatment efficacy and reactivity to salient cues. The P300 effect also correlated significantly with the main effect of placebo in fear ratings ($R= 0.445$, $p_{\text{Pear}}=0.029$; Figure 18B). This result remained valid when reducing the effect of strong fear rating outliers by robust regression (96) ($p_{\text{rob}}=0.037$). To further illustrate this result, average time courses of electrode P4 are shown for high and low placebo responders in Figure 19. A placebo-dependent reduction of both components was only observed in high (HR) but not in low responders (LR; see also 4.6).

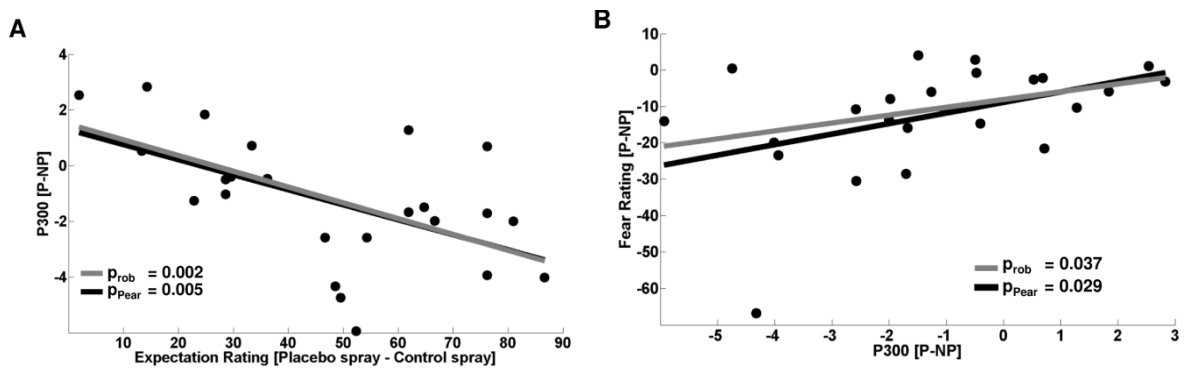


Figure 18: Brain-behavior correlations (Study 2)

The reduction of P300 amplitudes under placebo in electrode P4 was predicted by pre-experimental treatment expectations (A) and also correlated with the placebo main effects in fear ratings across participants (B). p_{Pear} , p-value of Pearson's correlation; p_{rob} , p-value of robust correlation.

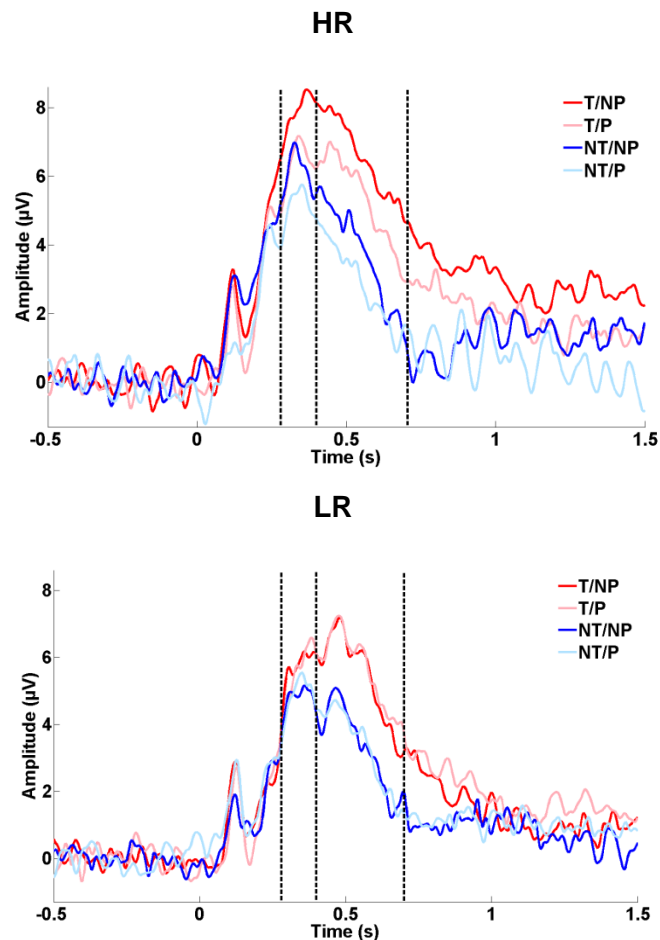


Figure 19: P300 and LPP in high (HR) and low (LR) placebo responders (Study 2)

Only high but not low placebo responders showed reduced P300 (280-400 ms) and LPP (400-700 ms) amplitudes in P vs. NP runs.

5.2.4. EEG oscillatory activity

The P300, like the subsequent LPP, is considered a marker for the allocation of attentional resources toward salient external stimuli (32, 33). To test if decreased external attention in P vs. NP runs was accompanied by increased measures of internalized attention, EEG power spectra of the ITIs were analyzed based on several studies showing increased frontal theta (4-7 Hz) and alpha (10-12 Hz) power during internally as opposed to externally directed attention (35, 38).

Figure 20 shows mean power spectra collapsed across conditions (average power during ITIs of P and NP runs) for midline electrodes Fz, Cz and Pz. Alpha and theta power distributions were characterized by parietal and frontal midline topologies, respectively, thus indicating separable underlying neural oscillators. Cluster-based analyses on all electrodes revealed an increase exclusively in alpha and theta power under placebo (alpha: $p=0.041$;

theta: $p=0.006$) that was driven solely by HRs (alpha: $p=0.011$; theta: $p<0.001$), thus leading to a significant difference between HRs and LRs (alpha: $p=0.014$; theta: $p=0.007$) (Figure 21). Significant placebo-dependent theta and alpha power increases and differential effects between HRs and LRs were mainly observed in frontal electrodes. Spectral power analyses thus supported the hypothesized shift from externally to internally directed attention as a potential cognitive mechanism underlying placebo anxiolysis.

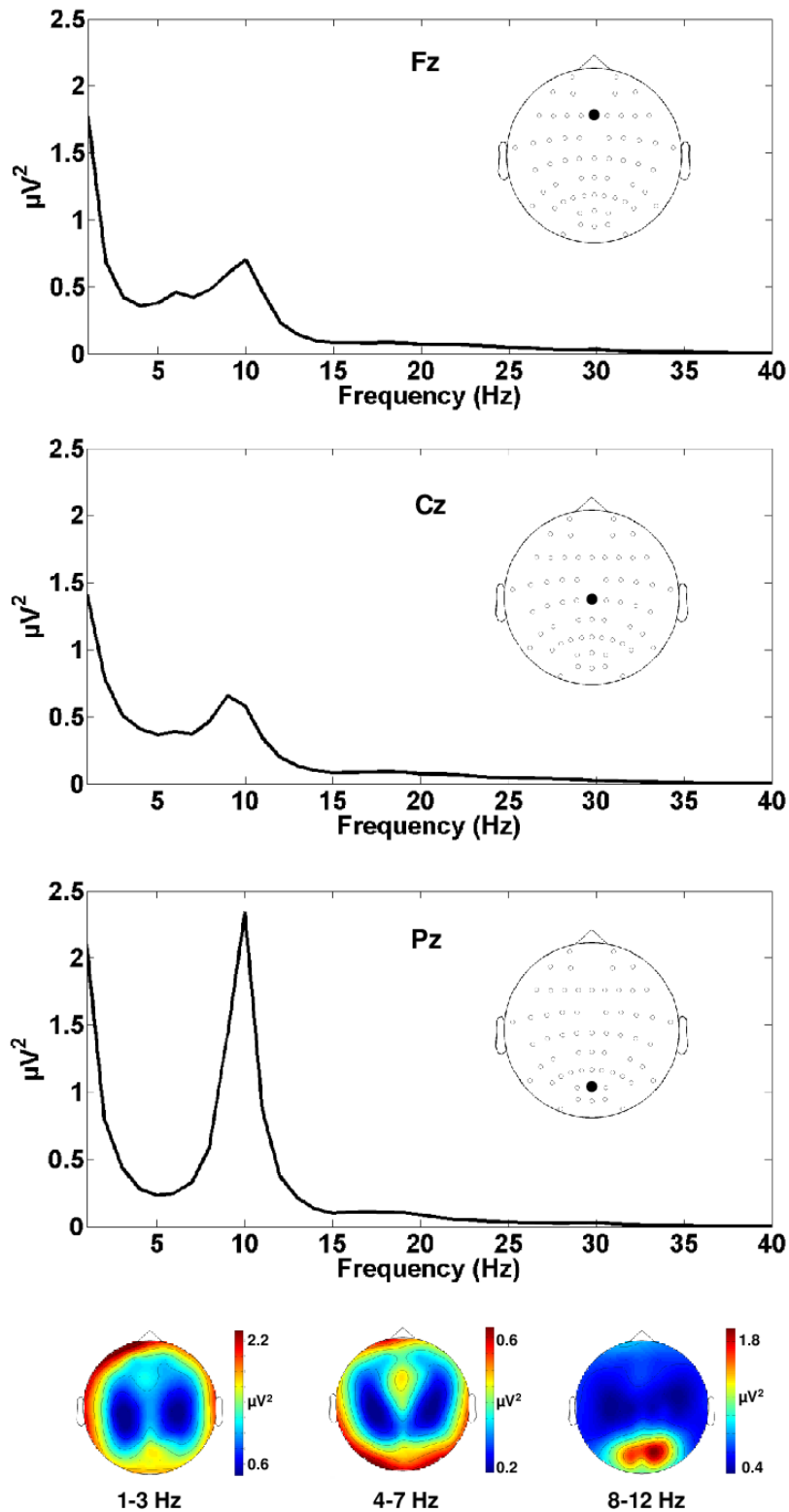


Figure 20: ITI power spectra (Study 2)

ITI power spectra collapsed across P and NP runs of electrodes Fz, Cz and Pz as well as power distributions for three classical frequency bands: delta (1-3 Hz), theta (4-7 Hz) and alpha (8-12 Hz).

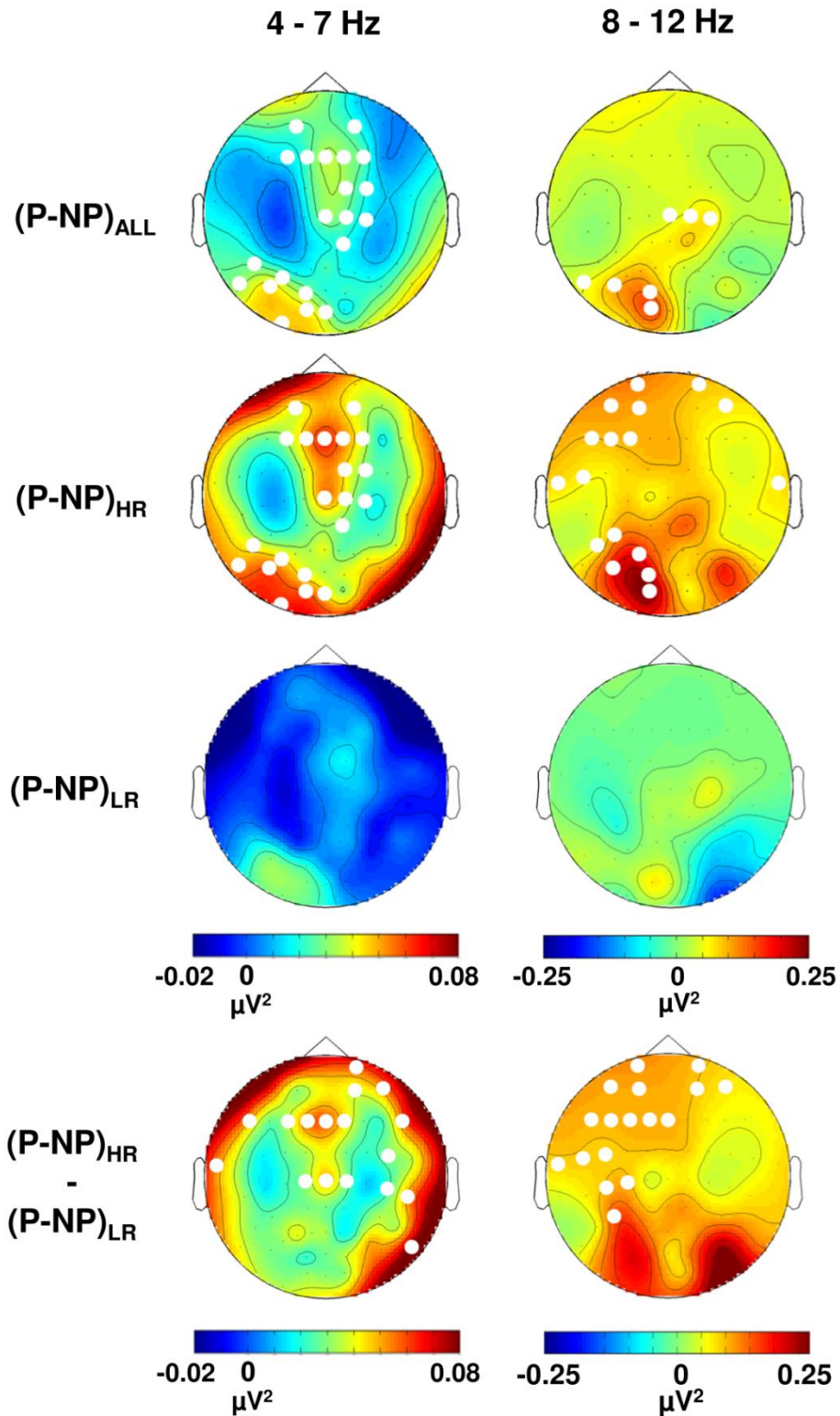


Figure 21: ITI theta (4-7 Hz) and alpha (8-12 Hz) activity (Study 2)

Theta and alpha power were significantly increased during ITIs in P compared to NP runs [(P-NP)_{ALL}] for the total sample. Only high [(P-NP)_{HR}] but not low responders [(P-NP)_{LR}] showed increased theta and alpha activity in placebo runs, leading to a significant difference between HRs and LRs [(P-NP)_{HR}-(P-NP)_{LR}]. White dots indicate electrodes of significant clusters ($p < 0.05$).

5.3. Study 3

5.3.1. Behavioral Results

Behavioral results mirrored those reported in Studies 1 and 2, thus further indicating reduced cue-unspecific reactivity and lowered tonic arousal levels. Both fear ratings (Figure 22A) and SCRs (Figure 22B) showed main effects of threat (T-NT; ratings: $F_{1,22}=123.65$, $p<0.001$; SCRs: $F_{1,17}=123.83$, $p<0.001$) and placebo (P-NP; ratings: $F_{1,22}=19.99$, $p<0.001$; SCRs: $F_{1,17}=4.86$, $p<0.042$), with an interaction again only appearing in fear ratings ($F_{1,22}=15.9$, $p=0.001$), but not in SCRs ($F_{1,17}=1.49$, $p=0.239$). Tonic SCLs (Figure 22C) were globally reduced by the placebo (P-NP: $t_{17}=9.615$, $p<0.001$, two-tailed).

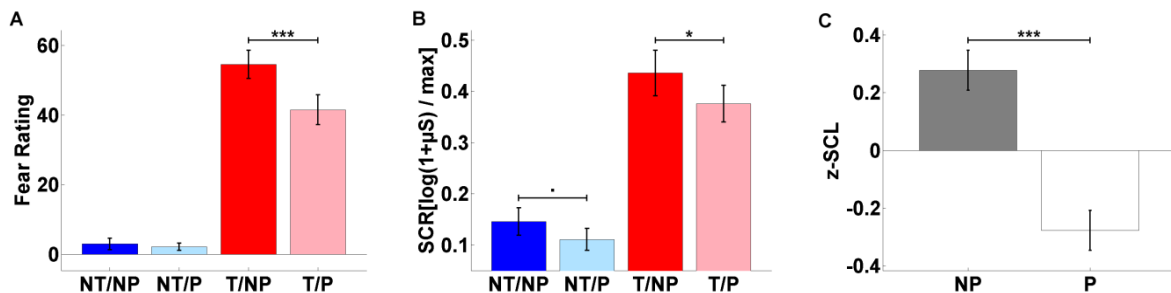


Figure 22: Behavioral results (Study 3)

As in Studies 1 and 2, a cue-unspecific placebo-effect was observed in fear ratings (A, P-NP) and SCRs (B, P-NP). Lowered arousal levels were again indicated by reduced tonic SCLs under placebo (C). NT, no-threat; T, threat; NP, no-placebo; P, placebo. *, $p<0.05$; **, $p<0.01$; ***, $p<0.001$. Error bars indicate standard error of the mean (SEM).

Pupil size was recorded as an additional measure of autonomically controlled cue reactivity. Time courses revealed sustained pupil dilation and constriction to threat and no-threat cues, respectively (Figure 23; T-NT: $F_{1,15}=22.49$, $p<0.001$). Both pupil dilation and constriction were significantly inhibited under placebo (T/NP-T/P: $t_{15}=2.48$, $p=0.013$, NT/NP-NT/P: $t_{15}=-2.25$, $p=0.02$, one-tailed), as also indicated by a threat by placebo interaction ($F_{1,15}=8.07$, $p=0.012$, Figure 23B). Pupil dilation and constriction are controlled by the sympathetic and parasympathetic portions of the ANS, respectively. The observed interaction thus further supports the concept of a globally reduced reactivity to external cues resulting from both sympathetic and parasympathetic responses.

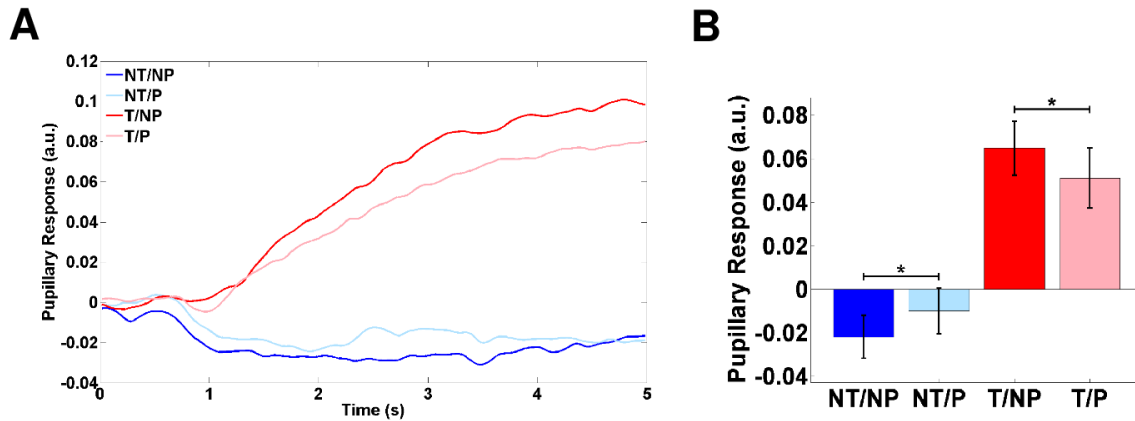


Figure 23: Pupillometry results (Study 3)

Averaged pupil responses revealed dilation and constriction in response to threat- and no-threat cues, respectively (A). Both pupil dilation and constriction were reduced under placebo (B). *, $p < 0.05$; **, $p < 0.01$; ***, $p < 0.001$. Error bars indicate standard error of the mean (SEM).

5.3.2. fMRI analysis

5.3.2.1. Cue-related BOLD responses

In a standard FWE-corrected whole brain analysis, stronger BOLD responses to threat predicting cues were observed in SN-related areas including the bilateral aI, dACC and thalamus, thus confirming the functional role of the SN in threat detection (T-NT, Figure 24A, Table 1). Threat-induced deactivations were observed in DMN-related areas including the vmPFC, retrosplenial cortex (rspC) and inferior parietal lobule (iPL) (NT-T, Figure 24B, Table 1). A main effect of placebo was found bilaterally in central thalamic regions and a threat cue-specific placebo effect was observed in the right insula (Figure 25, Table 1). No placebo-dependent modulation of DMN-related regions could be identified.

So far, in EEG or behavioral data, no pronounced effects specifically on phasic fear (as indicated by a threat cue-specific interaction) were observed. However, based on the fMRI results, a potential placebo effect on phasic fear cannot be entirely excluded.

Table 1: Standard FWE-corrected whole brain analyses

L: left, R: right, al = anterior insula, dACC: dorsal anterior cingulate cortex, dlPFC: dorsolateral prefrontal cortex, dmPFC: dorsomedial prefrontal cortex, FG: fusiform gyrus, FIO: frontal inferior operculum, fsG: frontal superior gyrus, HT: hypothalamus, iPL: inferior parietal lobule, I: insula, LG: lingual gyrus, MFG: middle frontal gyrus, MTG: middle temporal gyrus, PHG: parahippocampal gyrus, pre/postCG: pre-/postcentral gyrus, piPL: posterior inferior parietal lobule, rspC: retrosplenial cortex, SMA: supplementary motor area, Thal: thalamus, TPJ: temperoparietal junction, vmPFC: ventromedial prefrontal cortex, vlPFC: ventrolateral prefrontal cortex, VS: ventral striatum. Coordinates are denoted by x, y, z in mm (MNI-space).

Threat-induced activation (T-NT)				
Label	x y z [MNI]	cluster size [voxels]	t-value	p_{FWE}
R al	36 24 2	1447	11.12	<0.001
L al	-40 20 -4	842	10.86	<0.001
R TPJ	54 -42 36	616	9.13	<0.001
R SMA (extending to dmPFC and dACC)	12 14 60	948	9.05	<0.001
R dACC	8 22 34		7.58	<0.001
L TPJ	-62 -42 28	194	7.91	<0.001
R vlPFC	30 50 16	204	7.52	<0.001
L Thal extending to L VS	-14 -14 8	187	7.3	<0.001
R VS extending to R Thal	14 0 10	254	6.95	<0.001
L VS	-24 6 -2	64	6.54	0.001
L vlPFC	-30 48 20	47	6.48	0.002
R preCG	46 4 48	29	6.26	0.003
R Precuneus	14 -64 36	12	6.16	0.005
L Cerebellum	-34 -58 -26	28	6.16	0.005
	-42 -56 -32	4	5.81	0.015
L FIO	-60 8 8	14	5.71	0.021
R iPL	54 -46 52	5	5.67	0.023
L dACC	-4 8 40	2	5.52	0.038
Threat-induced deactivation (NT-T)				
L PHG	-22 -20 -16	152	9.79	<0.001
R PHG	22 -20 -16	100	8.23	<0.001
L FG	-32 -36 -14	99	7.8	<0.001
L MTG	-62 -8 -14	60	7.59	<0.001
HT	0 4 -10	26	7.2	<0.001
L rspC	-6 -58 12	130	7.16	<0.001
L piPL	-50 -72 26	100	7.14	<0.001
R rspC	6 -52 12	93	6.94	<0.001
vmPFC	0 44 -14	174	6.94	<0.001
R MTG	64 -4 -16	26	6.57	0.001
R piPL	50 -68 30	42	6.31	0.003
R postCG	44 -26 62	16	6.18	0.004
continued on next page				

R preCG	6 -24 66	30	6.05	0.007
L PHG	-16 -34 -6	4	5.94	0.01
R PHG	26 -40 -8	3	5.7	0.021
L vmPFC	-8 26 -16	4	5.68	0.022
L LG	-10 -40 -2	2	5.57	0.031
R postCG	64 -8 30	1	5.44	0.048
L fsG	-18 38 40	1	5.44	0.048
Cue-unspecific placebo effect (NP-P)				
L Thal	-14 -14 6	3	5.8	0.015
R Thal	20 -14 14	1	5.46	0.045
Threat cue-specific placebo effect ($\Delta T_{NP} - \Delta T_P$)				
R I	48 10 0	5	5.78	0.016

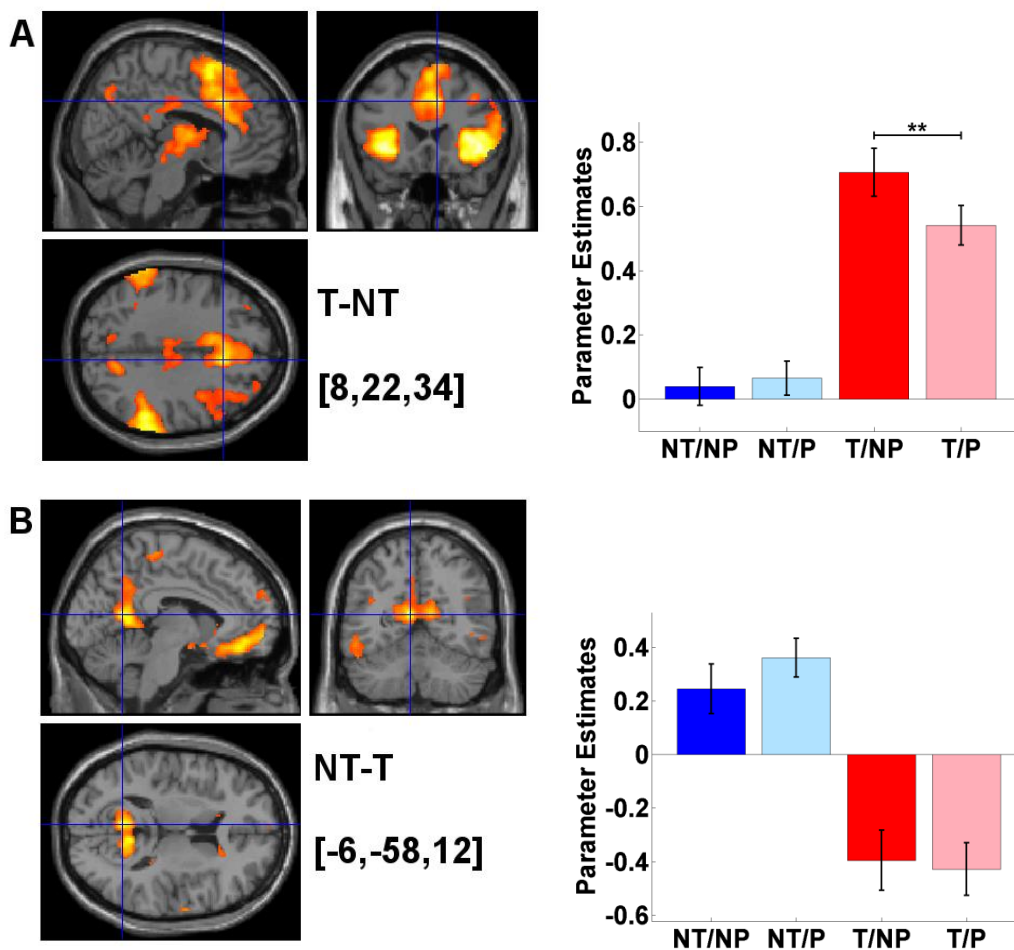


Figure 24: fMRI main effects of threat (Study 3)

Crosshairs and MNI-coordinates (mm) indicate voxels exhibiting maximal main effects of threat in representative clusters (cluster peak voxels). Parameter estimates were extracted from cluster peak voxels and are shown as bar graphs. Key regions of the SN including the dorsal anterior cingulate cortex ([8,22,34]) were activated (A), while classical DMN regions such as the retrosplenial cortex ([-6,-58,12]) were deactivated in response to threat predicting cues (B). Placebo effects were observed in SN-, but not in DMN-related structures (see bar graphs). The visualization threshold for all images was set to $p < 0.001$ uncorrected. *, $p < 0.05$; **, $p < 0.01$; ***, $p < 0.001$. Error bars indicate standard error of the mean (SEM).

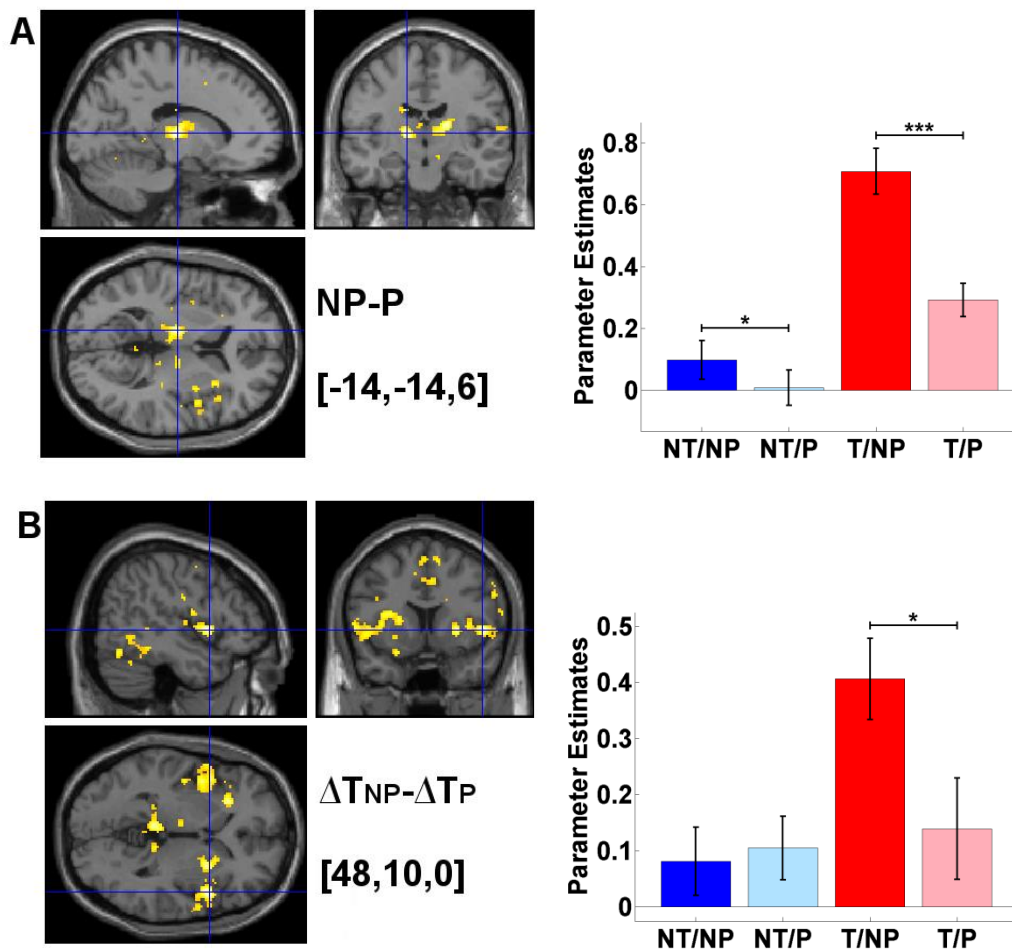


Figure 25: fMRI placebo effects in SN-related regions (Study 3)

Crosshairs and MNI-coordinates (mm) indicate voxels exhibiting maximal effects (peak voxels). Parameter estimates were extracted from peak voxels and are shown as bar graphs. Cue-unspecific (A) and threat cue-specific placebo effects (B) were identified in the thalamus and the insula, respectively. The visualization threshold for all images was set to $p < 0.001$ uncorrected. *, $p < 0.05$; **, $p < 0.01$; ***, $p < 0.001$. Error bars indicate standard error of the mean (SEM).

No significant threat-related amygdala activation was observed, even in a region of interest (ROI) analysis restricted to a predefined bilateral amygdala mask (see Appendix Figure A2). However, ROI-specific analyses revealed a significant threat cue-specific attenuation of the bilateral amygdala under placebo (R Amy: peak voxel=[24,2,-12], cluster size=7, $p_{FWE}=0.03$; L Amy: peak voxel=[-28,4,-18], cluster size=30, $p_{FWE}=0.04$; Figure 26). The absence of a main effect of threat in the amygdala might be explained by a decay in threat-responsivity, as reported in several studies on instructed and conditioned fear (97, 98). To test this hypothesis, a GLM was constructed to estimate BOLD signal changes in blocks of three trials (1-3, 4-6, 7-9, 10-12, 13-15 and 16-18). Parameter estimates of the $\Delta T_{NP} - \Delta T_P$ peak voxel [-28,4,-18] were extracted and are shown in Figure 27. Threat-related BOLD responses in NP runs were significantly higher in early (1-9) compared to late trials (10-18) ([T/NP-

NT/NP]₁₋₉>[T/NP-NT/NP]₁₀₋₁₈: $t_{19}=1.86$, $p<0.04$, one-tailed), indicating that the overall interaction was driven mainly by early threat-related amygdala activation in the NP runs, which was completely inhibited under placebo treatment ([TP>NTP]₁₋₉: $t_{19}=0.29$, $p=0.776$, one-tailed).

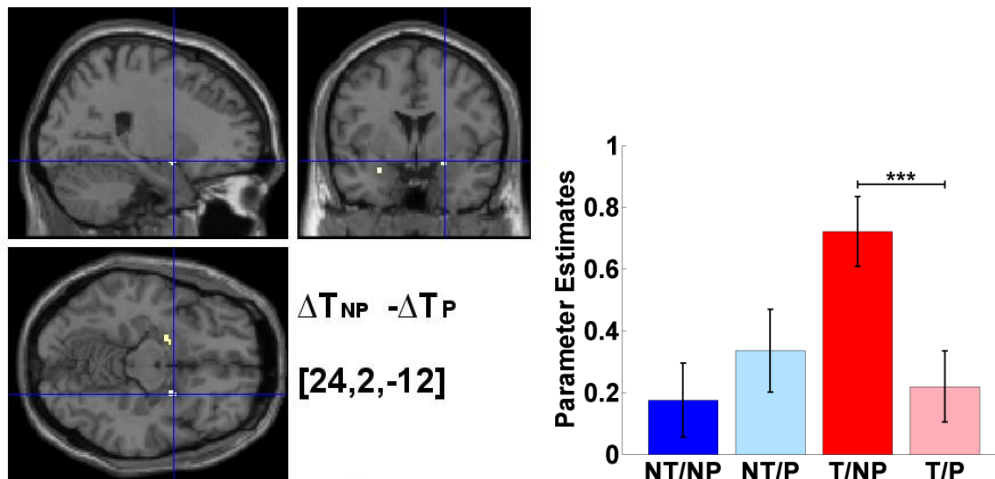


Figure 26: Amygdala ROI analysis (Study 3)

A threat cue-specific placebo effect was observed in the bilateral amygdala. (peak voxel in MNI-space (mm): [24,2,-12], see crosshair). Parameter estimates were extracted from the peak voxel and are shown as bar graph. The visualization threshold was set to $p<0.001$ uncorrected. *, $p<0.05$; **, $p<0.01$; ***, $p<0.001$. Error bars indicate standard error of the mean (SEM).

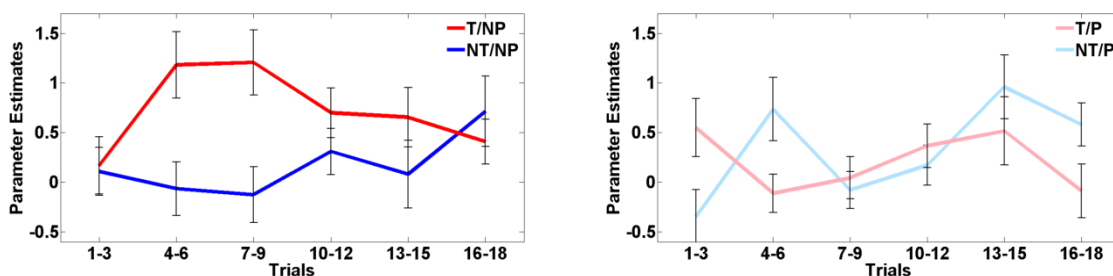


Figure 27: Time course of amygdala activation in blocks of three trials (Study 3)

Time courses were extracted from the $\Delta T_{NP}-\Delta T_P$ peak voxel. In NP runs, threat-related activation decayed in the second half of the experiment (left). Threat-related amygdala responses were completely attenuated under placebo (right). Error bars indicate standard error of the mean (SEM).

So far, the fMRI results have focussed exclusively on the placebo-dependent attenuations of BOLD responses in SN regions. To further investigate potential regulatory sources showing enhanced activity under placebo, a ROI analysis restricted to voxels of the anterior portion of the cingulate cortex was performed (ACC, see Appendix Figure A3). A cue-unspecific BOLD activation (P-NP), but no threat cue-specific effect was observed in the rostral part of the

ACC ([-14,48,8], $p_{FWE}=0.046$, Figure 28), which had been previously identified a likely candidate for mediating placebo effects in different clinical conditions including placebo analgesia (64, 99). Uncorrected whole brain analyses furthermore revealed that no other brain region showed stronger placebo-dependent activations than the rACC (see SPM glass brain in Figure 29). The P-NP contrast correlated significantly with the inverse NP-P contrast observed in the thalamus ($R= 0.595$, $p_{Pear}=0.006$, $p_{rob}=0.007$; Figure 29), suggesting that placebo-dependent rACC activation is coupled with thalamic deactivation. It should be mentioned that the rACC activation observed in this study greatly resembles findings from Petrovic et al. (2007), who applied a placebo to reduce negative emotions induced by aversive pictures ([-12,48,12], Figure 6B). In this way, previously published data supports the claim that neural substrates activated under placebo in pain processing and other negative emotional states are also involved in placebo anxiolysis, thus strengthening the hypothesis of a common neural mechanism responsible for placebo effects across different conditions. Interestingly, reduced BOLD responses in central thalamic regions have also been reported in studies on placebo analgesia. Considering the role of central thalamic regions in regulating levels of arousal and attentional resources (100), both, placebo analgesia and placebo anxiolysis might be based on dampened cue processing due to a thalamic deactivation. If however, the rACC controls thalamic deactivation cannot be answered here since causal inference from fMRI data is only possible to a very limited extent.

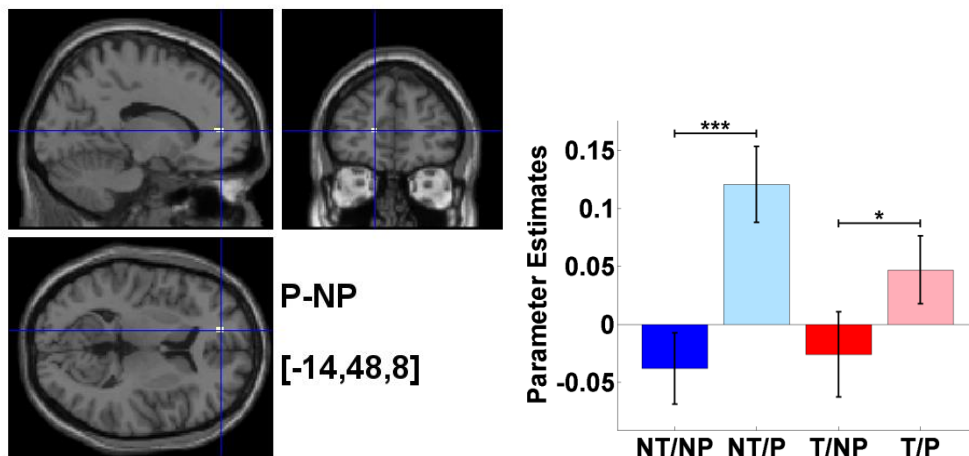


Figure 28: rACC activation under placebo (Study 3)

A cue-unspecific placebo effect (P-NP) was observed in the rACC. (peak voxel in MNI-space (mm): [-14,48,8], see crosshair). Parameter estimates were extracted from the peak voxel and are shown as bar graph. The visualization threshold was set to $p<0.001$ uncorrected. *, $p<0.05$; **, $p<0.01$; ***, $p<0.001$. Error bars indicate standard error of the mean (SEM).

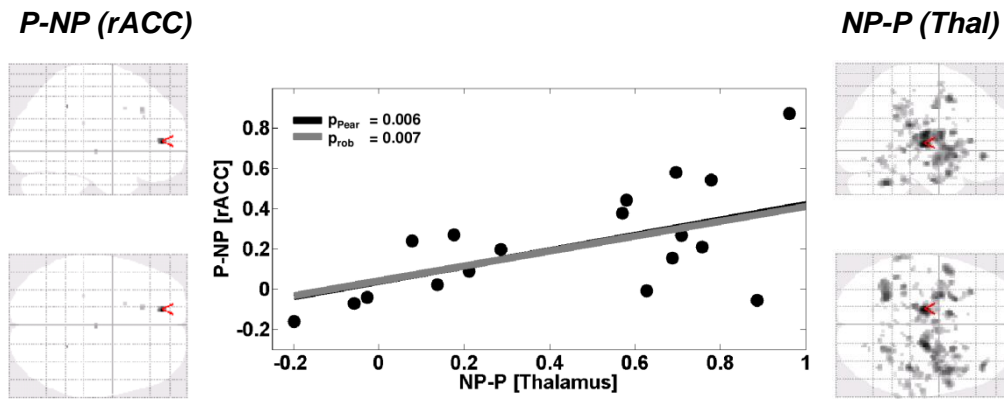


Figure 29: rACC activation vs. thalamus deactivation (Study 3)

Cue-unspecific placebo-dependent activation (P-NP) and deactivation (NP-P) was strongest in the rACC (left) and the thalamus (Thal, right), respectively. Thalamic deactivation predicted rACC activation (middle) under placebo. p_{Pear} , p-value of Pearson's correlation; p_{rob} , p-value of robust correlation.

To furthermore focus specifically on placebo effects in SN key structures (in the following referred to as SN nodes), parameter estimates of 8 cortical and 4 subcortical T-NT cluster peak voxels from a whole brain analysis with $\alpha_{\text{FWE}}=0.01$ and a minimal cluster size of ≥ 10 were extracted (listed in Table 2). As of yet, no literature exists addressing large-scale network activity during instructed fear tasks, making it necessary to first characterize the extracted nodes as true SN nodes. Therefore, cluster peak voxels were examined to determine whether these in fact matched SN regions reported in the literature. Three sets of coordinates reported as SN, DMN or CEN peak voxels by Seeley et al. (48) (CEN, SN) and Andrews-Hanna et al. (101) (DMN) (see Appendix: Table A1-3) were used as reference nodes. Nearest neighbours (NN) in each of the 3 reference networks were calculated by means of Euclidean distances for all cortical T-NT peak voxels. All cortical T-NT peak voxels had closest NNs in the reference SN, indicating that threat-related activation during instructed fear was mainly restricted to the SN. Subcortical voxels were not included in the mapping procedure due to the close proximity of the subcortical CEN- and SN regions as reported in Seeley et al. (48), thus implying a significant potential for mismatches. As expected for network-like activation, threat-related cortical and subcortical BOLD responses showed a high degree of internodal coupling as assessed by Pearson's correlations of T-NT contrast values (Figure 30, middle panel).

Threat-related BOLD responses were attenuated in all SN nodes under placebo (including unassigned subcortical nodes) (T/NP>T/P, Table 2, Figure 30A-D). However, overall BOLD response patterns varied, ranging from clear main effects of placebo (L Thal: $F_{1,19}=37.97$, $p<0.001$) to pronounced threat cue-specific interactions (L al: $F_{1,19}=19.78$, $p<0.001$). The thalamus and the insula have both been associated with the SN, but however, if considered

individually, both regions have been shown to subserve different functions in processing salient stimuli (48, 49). The central thalamus is involved in regulating levels of arousal and allocating higher cortical resources, whereas the insula (together with the dACC and the amygdala) plays a more important role in threat appraisal (47, 98). Thus, heterogeneous placebo effects within SN nodes might indicate some degree of functional segregation between the nodes and was also reflected by means of a 12(region) x 2(threat) x 2(placebo) ANOVA showing both a significant main effect of placebo ($F_{1,19}=15.44$, $p=0.001$) as well as a threat by placebo interaction ($F_{1,19}=15.66$, $p=0.001$). However, as stated above, the observed threat cue-specific effects might also be interpreted as evidence for a generalization of the placebo effect to both sustained states of anxiety and phasic fear.

Network specific analyses were also performed for threat-deactivated NT-T cluster peak voxels ($\alpha_{FWE}=0.01$, cluster size ≥ 10). All cortical NT-T peak voxels had closest NNs in the reference DMN. Threat-related deactivations were coupled across DMN nodes, indicating a concerted network-like (negative) response in T trials (Figure 31, middle panel). However, no placebo-dependent effects were identified in DMN nodes as revealed by single voxel analyses (Figure 31A-D) and a 12x2x2 ANOVA (main effect of placebo: $F_{1,19}=0.05$, $p=0.82$; threat by placebo interaction: $F_{1,19}=1.96$, $p=0.178$).

Table 2: Placebo effects in SN nodes

Placebo effects in SN nodes as revealed by 2x2 ANOVAs and posthoc *t*-tests (one-tailed) on individual parameter estimates (see Table 1 for abbreviations; *, $p<0.05$; **, $p<0.01$; ***, $p<0.001$). Coordinates are denoted by x, y, z in mm (MNI-space).

Label	x y z [MNI]	Main effect of placebo	Threat by placebo interaction	T/NP>T/P
L VS	-14 0 16	$F_{1,19}=10.28$ **	$F_{1,19}=6.12$ *	$t_{19}=4.75$ ***
R dACC	8 22 34	$F_{1,19}=6.08$ *	$F_{1,19}=3.02$.	$t_{19}=3.16$ **
R VS	14 0 10	$F_{1,19}=3.2$.	$F_{1,19}=2.25$	$t_{19}=2.47$ *
L al	-40 20 -4	$F_{1,19}=4.38$ *	$F_{1,19}=19.78$ ***	$t_{19}=4.09$ ***
L TPJ	-62 -42 28	$F_{1,19}=0.38$	$F_{1,19}=6.65$ *	$t_{19}=2.46$ *
R al	36 24 2	$F_{1,19}=12.08$ **	$F_{1,19}=9.82$ **	$t_{19}=4.15$ ***
L VS	-24 6 -2	$F_{1,19}=2.59$	$F_{1,19}=8.97$ **	$t_{19}=2.9$ **
R vIPFC	30 50 16	$F_{1,19}=3.85$.	$F_{1,19}=12.68$ **	$t_{19}=2.79$ ***
L vIPFC	-30 48 20	$F_{1,19}=0.26$	$F_{1,19}=10.9$ **	$t_{19}=2.24$ *
R SMA	12 14 60	$F_{1,19}=0.18$	$F_{1,19}=10.24$ **	$t_{19}=2.0$ *
R TPJ	54 -42 36	$F_{1,19}=3.69$.	$F_{1,19}=0.85$	$t_{19}=1.94$ *
L Thal	-14 -14 8	$F_{1,19}=37.97$ ***	$F_{1,19}=7.35$ **	$t_{19}=4.93$ ***

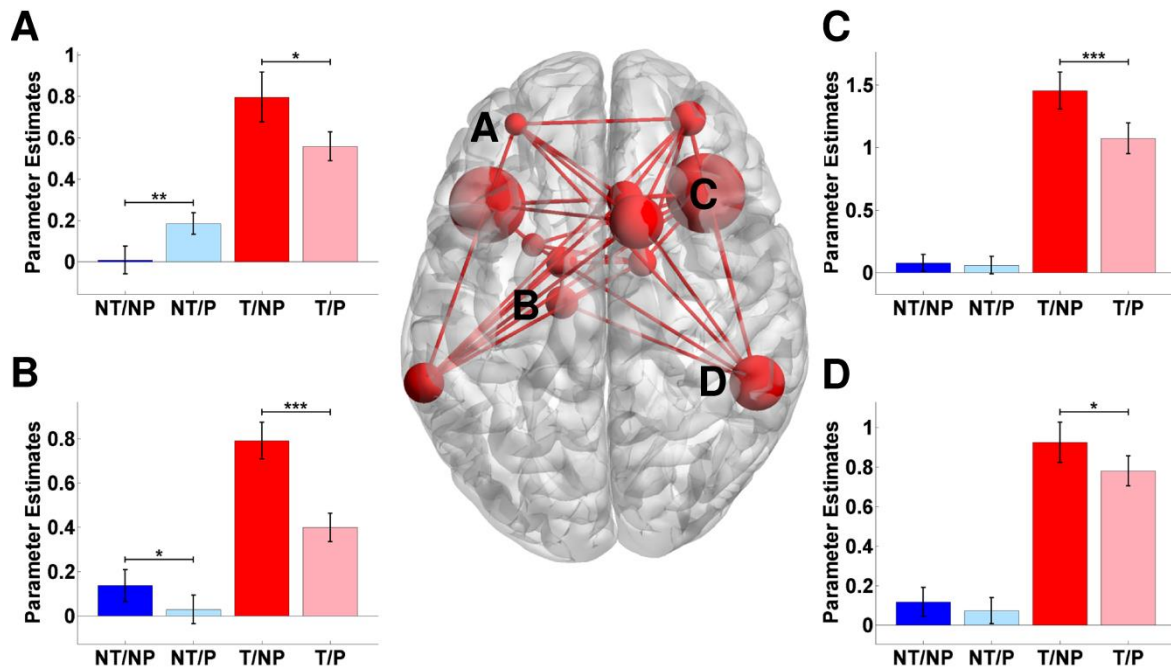


Figure 30: Threat-activated SN nodes and placebo-induced effects (Study 3)

In the middle panel, SN node sizes correspond to main effect of threat (T-NT) *t*-values and pairwise edges indicate significant internodal coupling as assessed by Pearson's correlations of T-NT contrast values. Threat-responsivity was coupled across SN nodes, indicating a concerted network-like response to threat-related stimuli. Varying placebo-related effects were observed in SN nodes (main effect of placebo / threat by placebo interaction), with an attenuation of threat-related BOLD responses observed in all regions (T/NP>T/P). Extracted parameter estimates are shown as bar graphs for 4 example regions: L vIPFC (A), L Thal (B), R al (C), R TPJ (D). For abbreviations see Table 1. *, $p < 0.05$; **, $p < 0.01$; ***, $p < 0.001$. Error bars indicate standard error of the mean (SEM).

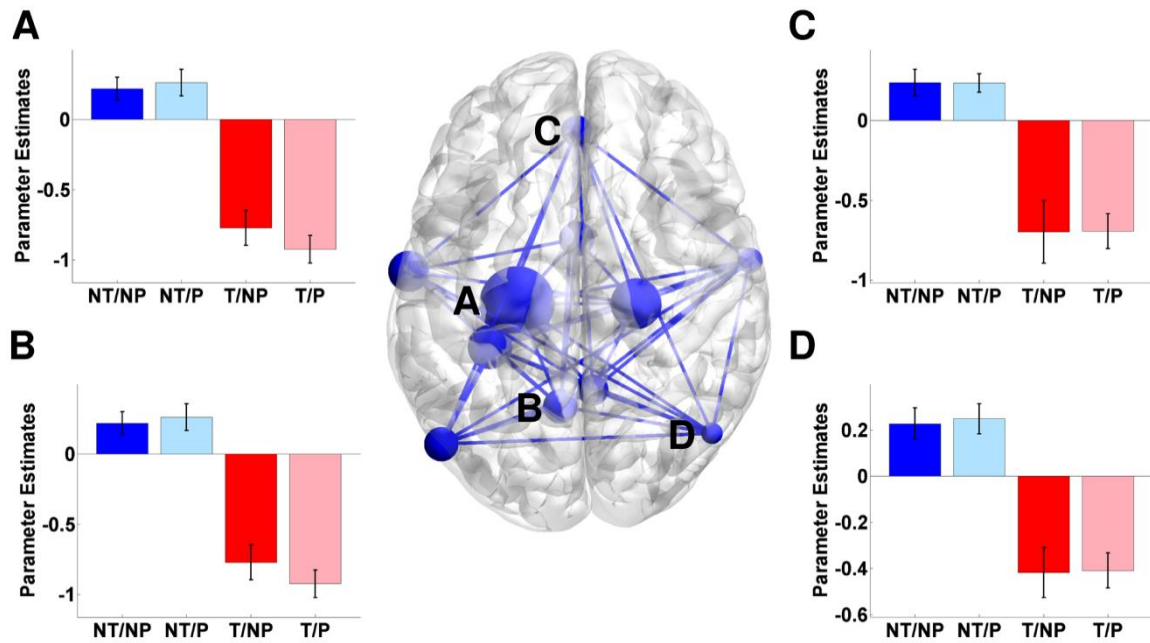


Figure 31: Threat-deactivated DMN nodes (Study 3)

In the middle panel, DMN node sizes correspond to NT-T t -values and pairwise edges indicate significant internodal coupling as assessed by Pearson's correlations of NT-T contrast values. Negative threat-responsivity was coupled across DMN nodes, indicating a concerted network-like response to threat-related stimuli. No placebo-dependent modulation was observed in any of the extracted DMN nodes. Extracted parameter estimates are shown as bar graphs for 4 example regions: L PHG (A), L rspC (B), vmPFC (C), R piPL (D). For abbreviations see Table 1. *, $p < 0.05$; **, $p < 0.01$; ***, $p < 0.001$. Error bars indicate standard error of the mean (SEM).

5.3.2.2. Tonic cue unrelated BOLD signal changes

Tonic BOLD responses in P vs. NP runs were analyzed separately from phasic cue-related BOLD signal changes (see 4.8.3), but did not reveal any significant effects. The lack of tonic placebo effects in experimental runs might be due to the long duration of the individual runs (2-3 mins), allowing for the slow fluctuations in the BOLD signal to compromise the mean activation over the course of a run.

5.3.2.3. Functional connectivity (FC) in large-scale neural networks

Intrinsic SN FC has been shown to increase when anticipating and detecting potential threats (49), as opposed to DMN FC, which increases in states of internally directed attention at rest (55, 101). Based on the EEG results showing enhanced markers (frontal alpha and theta power during ITIs) of sustained internalized attention in P vs. NP runs, the anxiolytic placebo effect was examined for corresponding changes in FC within and between large-scale neural networks. For this purpose, the placebo-dependent change in FC within and between the cortical SN and DMN nodes was assessed by PPI analyses. For each participant, DMN/SN node selection was optimized by choosing voxels exhibiting maximal T-NT (SN) and NT-T

(DMN) effects in a 6mm sphere around the peak voxel reported in group-level analyses ($\alpha_{FWE}=0.01$, minimal cluster size ≥ 10 , see 5.3.2.1).

Overall, average FC in P vs. NP runs was significantly increased within DMN, but not in SN nodes (DMN: $t_{19}=3.43$, $p=0.003$; SN: $t_{19}=1.32$, $p=0.201$). Furthermore, inter-network coupling between DMN and SN nodes (SN-DMN) was also found to be enhanced ($t_{19}=3.22$, $p=0.005$). Figure 32 illustrates the placebo-dependent changes in FC within and between the two networks. To further examine whether the observed changes were more pronounced in HRs than in LR, overall connectivity was tested separately for both groups. Between network coupling (SN-DMN) was significantly higher in HRs than LR ($t_{18}=1.98$, $p=0.032$, one-tailed), with a significant effect found only in HRs ($t_9=3.42$, $p=0.008$), but not in LR ($t_9=1.21$, $p=0.256$). Similarly, intrinsic DMN FC was higher in HRs ($t_9=4.32$, $p=0.002$) than in LR ($t_9=1.06$, $p=0.318$), again with a significant difference between the groups ($t_{18}=2.28$, $p=0.012$, one-tailed) (Figure 33).

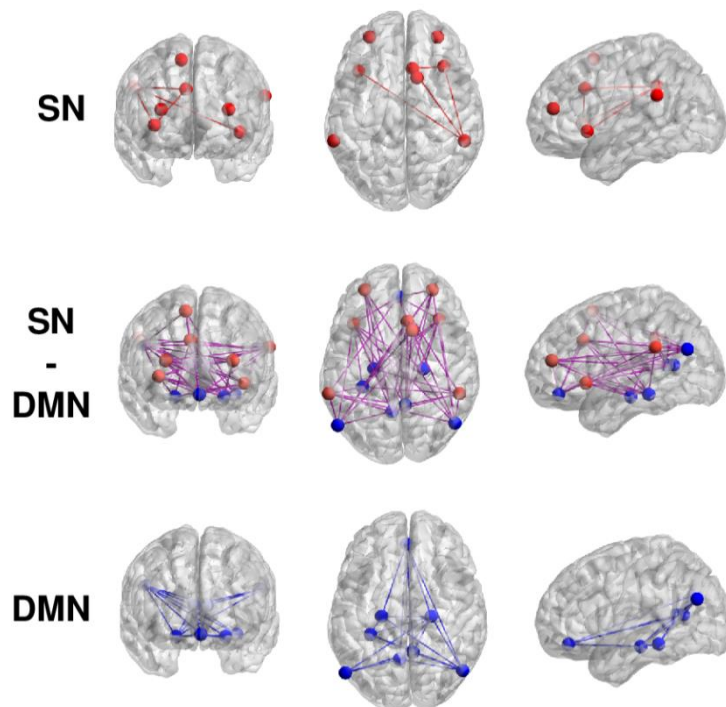


Figure 32: Placebo-dependent SN, SN-DMN and DMN FC (Study 3)

Placebo-dependent changes in FC were observed in the DMN (bottom) but not in the SN (top). FC between both networks was significantly strengthened under placebo (middle). Lines indicate significant increases in FC ($\alpha=0.05$).

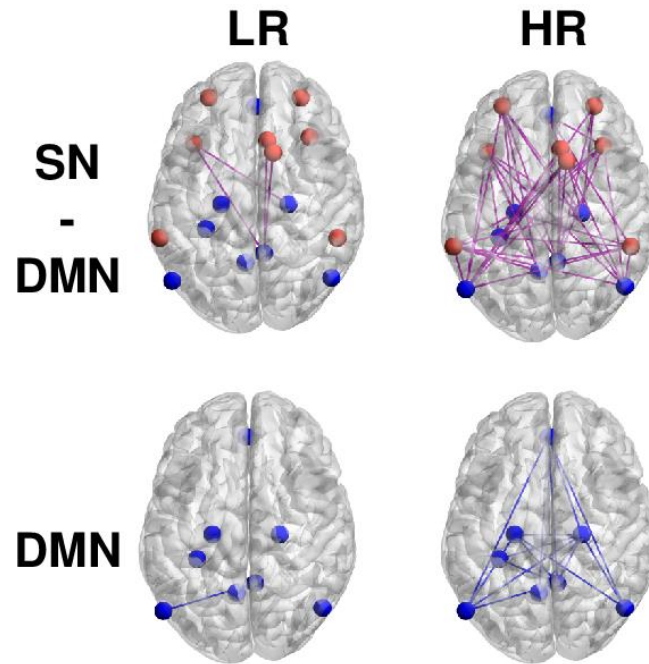


Figure 33: Placebo-dependent FC in HRs vs. LR (Study 3)

Significant placebo-dependent changes in intrinsic DMN and SN-DMN FC were only observed in HRs. Lines indicate significant increases in FC ($\alpha=0.05$).

Significant FC changes might be due to a change from low or no coupling during NP to positive coupling during P runs. However, furthermore a change from negative to positive or negative to low or no coupling might have driven enhanced inter- and intra-network FC during P runs. To identify the underlying direction of coupling changes, BOLD signal time courses from representative SN and DMN regions of single participants were extracted. In Figure 34, each dot indicates BOLD activity at a certain time point during P (black dots) and NP (red dots) runs in the dACC (x-axis) and the vmPFC (y-axis) representing SN-DMN FC (top) and in the vmPFC (x-axis) and rspC (y-axis) representing intrinsic DMN FC (bottom). Red and black lines represent linear fits to the data, with the slope indicating FC strength, i.e. positive slopes indicate positive coupling between regions. The observed pattern indicates low positive SN-DMN FC during NP runs, which was enhanced under placebo (top). Strong positive intrinsic DMN FC during NP runs was found to be further strengthened under placebo (bottom). Similar patterns were observed in a majority of participants.

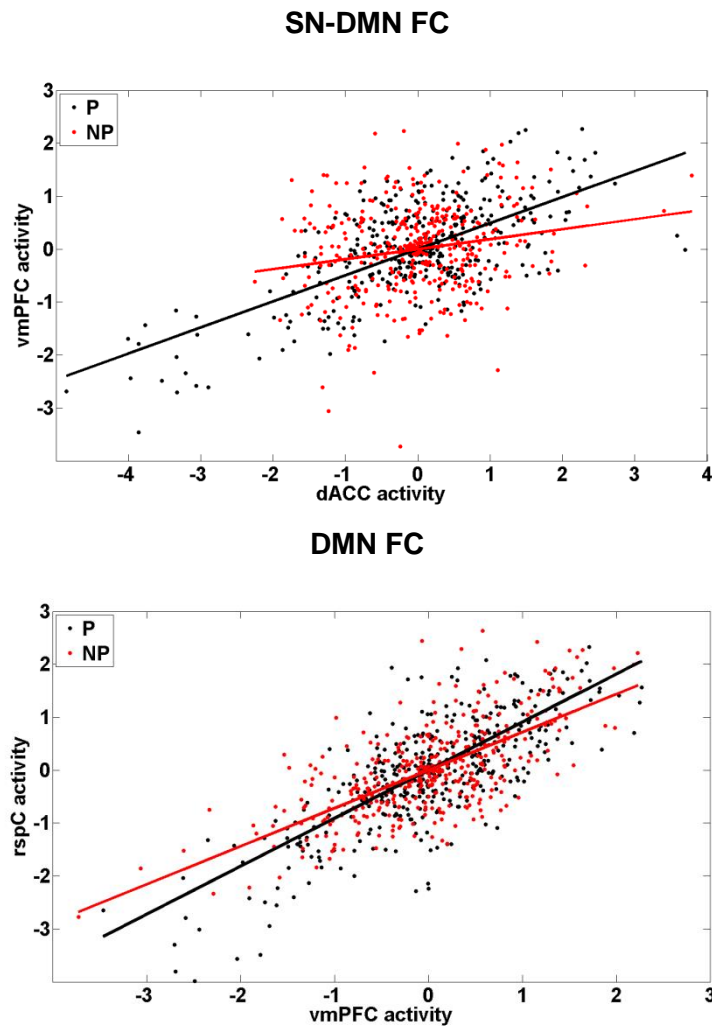


Figure 34: Placebo-dependent increases in inter- and intra-network FC for a single participant

SN-DMN FC is represented by dACC-vmPFC coupling (top) and intrinsic DMN FC by vmPFC-rspC coupling (bottom). Each dot represents BOLD activity in two regions and the slope of linear fits (lines) indicates FC strength. In both cases enhanced FC is observed during placebo runs (black lines) vs. No-placebo runs (red lines).

In summary, the placebo treatment increased intrinsic DMN coupling, thereby supporting the hypothesis of increased internally focused attention under placebo. Inter-network FC between SN and DMN nodes was furthermore increased under placebo. Both effects were significantly stronger in high vs. low responders, indicating a close relationship between FC changes in large-scale neural networks and behavioral effects. However, future studies are required to further determine the functional role of SN-DMN FC and its relationship to the observed attenuation of BOLD responses in the SN.

FC analyses revealed strong inter-network coupling between SN and DMN nodes in P vs. NP runs. To test if SN BOLD activity was furthermore coupled to non-DMN regions, an intermediate conjunction analysis was performed. Therefore, eight PPI whole-brain analyses,

each testing for significant placebo-dependent FC changes with one of the SN seed voxels, were combined into a single conjunction analysis. In intermediate conjunction analyses a parameter k is defined to calculate the probability, if less than or equal to k seed voxels show significant FC changes in P vs. NP runs. If thus, for a given voxel, the null hypothesis is rejected with $k=3$, significant FC changes occur with at least 4 of the 8 seed voxels (50%). Glass brain plots in Figure 35 indicate significant placebo-dependent FC changes of SN nodes mainly with DMN nodes. The effect is clearly observable if k is gradually increased, thereby showing that significant effects are successively restricted to DMN nodes. The analysis reveals that 75% of the SN nodes ($k=5$) show significant placebo-dependent FC changes mainly with major DMN regions (Table 3). Classical DMN nodes, as reported in the literature, comprise the vmPFC (including the rACC, see also Figure 3), rspC and inferior parietal portions. In fact, all classical DMN regions exhibited stronger coupling to 75% of the SN nodes (Table 3). This means that in single SN regions placebo-dependent FC changes might be observable with non-DMN nodes, but however when considering whole network interaction, the effect is mainly restricted to DMN nodes.

Seven of the eight SN seed voxels (Figure 35, $k=6$) showed enhanced coupling to the rACC ($[-8,52,0]$) under placebo, which together with the observed cue-unspecific increase of rACC BOLD responses (P-NP peak voxel: $[-14,48,8]$) suggests a pivotal role for the rACC in mediating the anxiolytic placebo effect. However, as already stated, future studies analyzing the relationship between cue-related BOLD responses and FC changes in large-scale neural networks are required to further link both effects.

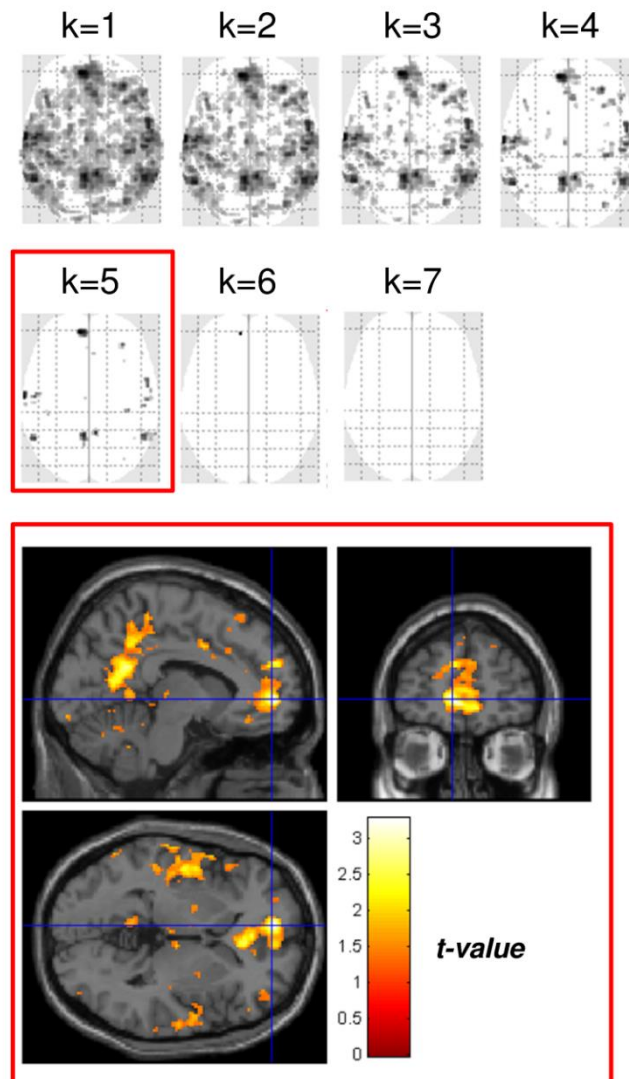


Figure 35: Intermediate conjunction analysis of SN PPIs

8 PPI whole brain analyses with SN nodes as seed voxels were combined into a single conjunction analysis. At least 6 of 8 SN nodes ($k=5$) showed stronger FC under placebo mainly with major DMN nodes. 7 of 8 SN nodes ($k=6$) showed stronger FC under placebo with the rACC. Results for $k=5$ are depicted as t -map (red box). Crosshairs indicate the peak voxel for $k=5$ in the rACC. The visualization threshold for the t -map was set to $p < 0.001$ uncorrected.

Table 3: Intermediate conjunction analysis of SN PPIs

Intermediate conjunction analysis combining 8 PPI whole brain analyses with SN nodes as seed voxels and k=5. L: left, R: right, O = Operculum, piPL: posterior inferior parietal lobule, pMTG: posterior middle temporal gyrus, rACC: rostral anterior cingulate cortex, rspC: retrosplenial cortex, TP = temporal pole. Coordinates are denoted by x, y, z in mm (MNI-space).

Intermediate conjunction analysis (k=5) of SN PPI results				
Label	x y z [MNI]	cluster size [voxels]	t-value	p_{FWE}
L rACC	-8 52 0	45	6.21	<0.001
L MTG	-64 -12 -4	13	5.99	<0.001
L rspC	-6 -52 22	56	5.95	<0.001
R rspC	6 -48 18	19	5.84	<0.001
L piPL	-54 -54 16	17	5.81	0.001
R piPL/pMTG	54 -52 26	19	5.71	0.001
L O	-54 -12 12	12	5.64	0.001
R TP	58 4 -28	14	5.57	0.002
R MTG	56 -16 48	13	5.49	0.003
R O	38 -26 20	10	5.39	0.006
L piPL/pMTG	56 -50 12	15	5.35	0.007

6. Discussion

6.1. Summary of results

This research project was designed to elucidate the neurobiological effects of placebo treatments on human fear and anxiety under controlled laboratory conditions. In three consecutive studies, temporary states of fear and anxiety were induced and an inactive medication coupled with a verbally suggested expectation of anxiolysis was administered. Different levels of neural processing were assessed by peripheral measures of autonomic activity (SCR, SCL and pupil size), EEG and fMRI recordings as well as subjective ratings in order to quantify the anxiolytic placebo effect and to investigate its underlying mechanisms. The main results are summarized in the following and discussed in more detail in 6.2-6.8. A psychobiological model of placebo anxiolysis is finally proposed in 6.9.

Main results:

- Verbally suggested treatment expectation induced placebo anxiolysis
- Autonomic cue reactivity and arousal were attenuated under placebo
- EEG markers of externally directed attention decreased under placebo
- EEG markers of internally directed attention increased under placebo
- BOLD responses in the SN were attenuated under placebo
- Placebo-dependent rACC activity indicated a common neural substrate for different placebo effects
- DMN and SN-DMN functional connectivity (FC) increased under placebo

6.2. Verbally suggested treatment expectation induced placebo anxiolysis

A placebo effect can be induced by verbally suggested treatment expectation, classical conditioning or a combination of both. In placebo analgesia, each of these factors has been shown to generate placebo effects independently; however, treatment expectation alone is known to induce only weak analgesic effects (102, 103). To further boost the participant's expectations, a conditioning procedure is usually performed in which the intensity of the painful stimulation is surreptitiously lowered for the placebo but not for the control treatment. The placebo treatment is thus repeatedly associated with an analgesic effect in the conditioning phase, while in a later test phase, the intensity remains identical for both

treatments. However, a mechanistic interpretation of the data can be complicated, assuming that both the effects of classical conditioning as well as expectation are represented by different neural substrates.

For quite some time, it was assumed that conditioned placebo effects in the context of pain and emotions are mainly induced by boosted expectations and do not result from classical conditioning directly. This was first suggested by Montgomery et al. (1997), who found that conditioned analgesic placebo effects can be completely eliminated if verbal information about the placebo manipulation is provided (65). However, Jensen et al. (2012, 2014) could show that learned analgesic placebo effects do not necessarily require conscious expectations. Therefore, the authors used CS cues presented outside of conscious awareness, which in a post-conditioning test phase induced placebo responses (67, 68). In a recent study, Schafer et al. (2015) furthermore reported analgesic placebo effects after a long conditioning procedure (4 days), though study participants were made aware of receiving a placebo in the test phase (66). Thus, there is growing evidence that classical conditioning has a direct effect on the placebo response and should not be considered exclusively as a reinforcement of the participant's treatment expectation.

The placebo manipulation performed in the context of this study was based solely on verbally suggested treatment expectation and induced notable effects in three consecutive studies. It can only be speculated as to why placebo anxiolysis but not placebo analgesia can induce strong effects based solely on treatment expectation without prior conditioning. One possible explanation might be that particularly anxiety and the placebo-related expectation of relief represent tonic emotional states which are counteracted over the course of minutes, whereas pain sensation is often limited to only a few seconds (74, 79, 103). It might thus be the time window, allowing for mutual interferences between aversive and beneficial states, which has a crucial impact on the magnitude of the placebo effect.

6.3. Autonomic cue reactivity and arousal were attenuated under placebo

Subjective ratings, pupillary responses and SCRs indicated a robust placebo-dependent unspecific attenuation of participant's reactivity to external cues, rather than a threat cue specific effect. Unlike SC, which is solely controlled by sympathetic activity, pupil size changes as a function of sympathetic (dilation) and parasympathetic (constriction) activity. In Study 3, the placebo treatment inhibited both sympathetic pupil dilation and parasympathetic pupil constriction in threat and no-threat trials, respectively. Thus, reduced sympathetic responses were reflected by both the SCRs and pupillary responses, but however only the latter also revealed a placebo-dependent modulation of parasympathetic activity. Inhibited

cue-unspecific autonomic (sympathetic + parasympathetic) responses indicated a persistent placebo effect throughout the experimental runs, a result which was further supported by SCL analyses showing that tonic sympathetic arousal levels decreased correspondingly.

In psychology, unspecifically enhanced cue reactivity is also referred to as hypervigilance (104), which, together with increased sympathetic arousal levels, represents a key symptom of anxiety (105). It can thus be stated that the placebo treatment had a persistent effect throughout the experimental runs on symptoms induced by sustained states of anxiety as opposed to phasic fear. There is some evidence that the placebo treatment in fact mimics true anxiolytic drug effects. Baas et al. (106), for example, could show that the benzodiazepine alprazolam does not affect startle responses to explicit threat cues (inducing phasic fear), but instead affects anxiety-like states induced by threatening environmental contexts. However, the masking of a threat cue-specific effect due to reduced cue reactivity in threat and no-threat trials cannot entirely be ruled out. Therefore, study designs separating phasic fear from sustained anxiety are required to further clarify this point.

6.4. Externally directed attention decreased under placebo

The great potential of EEG lies in the fact that well-described electrophysiological markers of various cognitive processes can be easily measured in a simple experimental setup. In Study 2, EEGs were recorded to explore the cognitive mechanisms of placebo anxiolysis. ERP analyses revealed a cue-unspecific reduction of P300 and LPP amplitudes, which have both been considered measures of allocation of attention and working memory resources towards salient external stimuli (32, 33).

The P300 has been described in the literature as a positive deflection located over parietal sites ~300ms following salient visual or auditory stimuli. It has been most extensively studied in oddball paradigms, i.e. infrequent target stimuli are presented in a background of frequent control stimuli (33), making the targets salient. The P300 amplitude can be modulated by various stimulus attributes such as the probability of occurrence, task-relevance (29) and emotional valence (32). The neurophysiological basis of P300 amplitudes is still debated, but however lesion- and EEG-fMRI studies do suggest a widely distributed network of prefrontal and parietal regions as underlying neural generators (107–110). There is some evidence from monkey studies for a close relationship between P300 amplitudes and phasic noradrenergic activity in the Locus coeruleus (LC) (111–113), since both show higher responses to target compared to control stimuli, both can be triggered multimodally and furthermore both are modulated by stimulus probabilities (111). Interestingly, like the P300 amplitude, the SN is also activated in response to highly salient external cues (47, 49) and has been shown to depend on noradrenergic activity (49). It can thus be speculated, that in

phases of acute stress, P300 amplitudes, phasic noradrenergic LC activity and SN BOLD responses represent different aspects of the same underlying neural system. This is furthermore supported by studies, showing that some SN nodes, including the right TPJ, strongly contribute to P300 potentials (110) and are closely associated with attention allocation in response to salient environmental cues (111). In response to emotional stimuli (32, 114), the P300 is often followed by a sustained late positive potential (LPP), as reported in studies on aversive picture processing (32, 114), symptom provocation in phobics (31, 95) and threat of shock (115, 116). In the current project, threat-induced P300 and LPP amplitudes were characterized by similar topologies and were similarly modulated by the placebo treatment. Thus, the possibility that both ERPs are part of the same functional process and that the observed LPPs should be interpreted as elongated P300 potentials cannot be ruled out.

P300/LPP amplitudes in response to both threat and no-threat cues were found to be diminished under placebo, indicating decreased externally directed attention, regardless of the cue-related emotional valence. Based on a resource allocation model developed by Kahnemann et al. (117), reduced P300 amplitudes might result from either lowered arousal levels or concurrent cognitive tasks blocking the limited amount of attentional capacities (33). One factor contributing to P300/LPP inhibition might thus be a lowered autonomic arousal level in P vs. NP runs, as evidenced by SCL analyses. However, as discussed further in the next section, spectral analyses of ITIs also lend support to the potential influence of concurrent cognitive processes requiring internally directed attention.

6.5. Internally directed attention increased under placebo

As shown in the previous section, EEG markers indicating externally focused attention were attenuated under placebo. The analysis of lower frequency oscillations during ITIs was employed to investigate whether internally focused attention was more pronounced in return. Frontal theta (4-7 Hz) and alpha (8-12 Hz) power were applied as suitable EEG markers of internalized attention (38). Both theta and alpha power were increased in P vs. NP runs.

Alpha waves were the first rhythmic activity described in EEG and are strongest in states of relaxed wakefulness and with eyes closed (118). Alpha power decreases during stimulus processing, which first led to the hypothesis that alpha waves reflect idling rhythms during resting states (119). However, research over the last three decades has found evidence for an additional, more specific function of alpha oscillations. Klimesch et al. (2007) suggested that alpha activity can inhibit non-task relevant cortical areas during tasks requiring internally focussed attention. Therefore, rather than being a mere secondary consequence of placebo-induced relaxation, sustained alpha increases might also actively contribute to the anxiolytic

effect. Frontal theta oscillations are less pronounced in the electroencephalogram and were first described in the 1950s during problem solving tasks (120). Numerous studies later supported the close relationship between mental activity and frontal theta oscillations based on a wide range of cognitive tasks (36, 121). Both frequency bands have been shown to increase in different experimental tasks, which, however, are mainly characterized by an attentional shift towards internally directed states.

It can be hypothesized that focussed internalized attention in this study led to reduced responsiveness for arousing external cues in placebo anxiolysis. Interestingly, such behaviour is also supported by various meditation strategies, and in fact it has been repeatedly shown that frontal alpha and theta amplitudes are increased during meditation (38, 39, 122). Assuming limited processing capacities of the human brain (33, 117), a key mechanism behind placebo anxiolysis might thus be an increase in internally and in return a decrease in externally directed attention, with the latter being reflected by lowered P300/LPP amplitudes and reduced ANS responses to external cues. Whether placebo anxiolysis, like meditation, is actively controlled by the participant, however, is a difficult question to answer.

6.6. SN activity was attenuated under placebo

The neural target regions of the anxiolytic placebo treatment were investigated by fMRI. Multiple cortical and subcortical SN regions including dACC, bilateral insula and thalamus exhibited strong threat-related activation, whereas classical DMN regions including vmPFC and rspC were deactivated. Threat-induced BOLD activation and deactivation correlated across SN and DMN nodes, respectively, indicating a concerted network response to threat-related cues. The placebo treatment had no effect on threat-induced DMN deactivation, but robustly inhibited BOLD responses in the SN.

In accordance with behavioral and ERP outcomes, some SN portions exhibited cue-unspecific placebo effects, but however others showed clear threat cue-specific interactions. This heterogeneity across placebo effects in different SN nodes might be explained by a functional segregation between the nodes and thus varying placebo responsivities. In fact, the SN can be decomposed into different functional subunits associated with arousal regulation (thalamus) (100), attentional reorienting (right TPJ) (111) and threat appraisal (dACC, al, amygdala) (47, 98).

EEG (Study 2) and behavioural data (Study 1-3) indicated a sustained placebo effect on externalized attention (P300/LPP) and arousal (SCL) throughout experimental runs. In line with this, a strong cue-unspecific effect was observed bilaterally in central thalamic regions and a trend-like cue-unspecific effect in the right TPJ. Thalamic deactivation furthermore correlated significantly with BOLD responses in the rACC, a potential regulatory source of

the placebo effect. However, if central thalamic portions are primarily affected under placebo cannot be stated here, mainly due to a limited temporal resolution allowing only a very limited causal inference from fMRI data.

As expected, threat-cue specific effects were mainly observed in regions associated with threat-specific processing, such as the aI, dACC and the amygdala. The latter is part of the SN and crucially involved in detecting and assessing threatening environmental stimuli (43, 98, 123). It is well known that amygdala responses habituate easily, which might be the reason why fMRI studies, particularly on instructed fear, do not consistently report significant threat-related amygdala activation. Accordingly, only early threat-related BOLD responses were observed in a time-resolved GLM analysis. There was, however, a robust threat cue-specific inhibition under placebo. The observed placebo-dependent effects on amygdala activation are consistent with placebo studies on aversive picture processing (64, 124) and social phobia (125), making the region another common target for placebo treatments administered to downregulate negative emotional states.

Phasic noradrenergic activity in response to salient external cues is thought to induce global SN activation as well as P300 potentials in the EEG measurement. A direct comparison of ERPs and BOLD responses may thus be considered a tempting approach. However, it should be noted that P300/LPP amplitudes were restricted to time windows ranging from 240-700ms, whereas fMRI results reflect hemodynamic changes induced within 5 s periods of cue presentation. A direct comparison would thus be highly speculative and can only be reliably performed when combining both EEG and fMRI recordings in future experimental setups.

6.7. Placebo effects in different conditions activate common neural substrates

The analysis of placebo-dependent BOLD signal increases was restricted to the ACC, primarily in line with studies showing placebo-dependent activations in its rostral portion (rACC) for example during pain anticipation (126), pain administration (74, 79, 99) and aversive picture processing (64). In this project, a placebo-dependent cue-unspecific BOLD activation was observed in the rACC, in close proximity to regions in which placebo activations were reported by Petrovic et al. 2005 (see 2.7). No other brain region exhibited such strong cue-unspecific activation under placebo. These results suggest some basic functional commonalities across placebo effects in different conditions including placebo anxiolysis.

The rACC is an opioid-receptor rich region (127) and its activation has been most consistently shown in studies on placebo analgesia. Eippert et al. (2009), for example,

observed placebo-dependent rACC activation during painful stimulation and in return a deactivation in pain-sensitive areas including the thalamus, insula and dACC. Neural effects were accompanied by decreased subjective pain ratings under placebo. A μ -opioid receptor blocker attenuated placebo effects in both directions (rACC activation + deactivation of pain-sensitive areas), thus indicating that endogenous opioids induced opposing effects depending on the neural substrate. The inhibition of placebo-induced decreases in BOLD responses in pain-sensitive areas was most pronounced in the thalamus, thus indicating a strong modulation by endogenous opioids. This finding is well in line with animal studies, showing that thalamic neurons are inhibited by μ -opioid peptides (128).

In the current project, cue-unspecific BOLD activation and deactivation were also most pronounced in the rACC and the thalamus, respectively, and both effects were significantly correlated. As already described for placebo analgesia, these findings strongly suggest the influence of endogenous opioids on cue processing under placebo analgesia. However, final evidence from pharmacological studies is required to confirm an influence of endogenous opioids on placebo analgesia.

6.8. DMN and SN-DMN functional connectivity increased under placebo

Previous results have clearly indicated that sustained states of internally as opposed to externally directed attention are strengthened under placebo, an effect that should also be reflected in corresponding connectivity changes in the SN and the DMN. The DMN is the most researched ICN and exhibits strong intrinsic coupling in resting states as well as deactivation in most stimulus-driven tasks (54, 55, 101). Since resting states are characterized by internally directed attention and self-referential thoughts (unperturbed by all salient external cues), it was hypothesized that placebo-dependent behavioral changes are accompanied by a shift in large scale network activity towards enhanced intrinsic DMN FC.

The DMN showed enhanced intrinsic FC under placebo and the effect was only observed in high and not in low placebo responders. Thus, as was already seen to be the case for EEG measures of sustained internally (theta, alpha) and cue-related externally (P300/LPP) directed attention, a strong association could again be shown between observed behavioral (fear ratings) and neural effects. However, it remains an open question how theta and alpha oscillations are related to changes in intrinsic DMN connectivity. Intrinsic coupling in the SN did not change under placebo. Instead, the SN showed increased inter-network connectivity to the DMN, which was again closely associated with behavioral measures. Interestingly, some studies related inter-network coupling between the DMN and the SN to the ability of

exhibiting task-related cognitive control (129), which has been discussed as a key component for mediating analgesic placebo effects (130, 131).

There is thus broad evidence from EEG and fMRI data for an increase in internally as opposed to externally focused attention under placebo, which can be considered a potential key mechanism of placebo anxiolysis. However, in order to link cue-related BOLD responses and FC changes in large-scale neural networks, some open questions need to be clarified in future studies. First of all, it is yet unclear, if and how placebo-dependent decreases in SN BOLD responses are related to placebo-dependent increases in SN-DMN coupling. Secondly, it remains to be shown how enhanced placebo-dependent BOLD responses in the rACC are related to intrinsic DMN and SN-DMN FC, in particular since SN-DMN FC was most pronounced between the rACC and the SN. However, despite these open questions and in line with studies on placebo analgesia, a pivotal role of the rACC can be assumed for mediating anxiolytic placebo effects.

6.9. A psychobiological model of placebo anxiolysis

In this chapter, a psychobiological model is proposed, which can be considered a first attempt to explain the observed effects and serve as a starting point for future studies. The model is depicted in Figure 36. All abbreviations are explained in the following:

Triggered by the administration of the placebo treatment, sustained oscillatory activity changes were observed throughout experimental runs, which have been associated in the literature with states of internally focused attention. In Study 3, this hypothesis has been furthermore supported by a placebo-dependent increase in intrinsic DMN FC, which represents a neural correlate of internalized attention (IA). In return, placebo intake, lowered the reactivity of the SN and thus dampened cue processing as reflected by attenuated BOLD responses in the SN (Study 3) and consequently diminished autonomic (ANS) output (Study 1-3). The placebo effect on the SN is well in line with the observed attenuation of P300/LPP amplitudes, reflecting a reduced allocation of attentional resources for processing salient external cues. Based on the current results, it can be speculated (as proposed in the model by an inhibitory connection), that lowered SN reactivity is a direct consequence of increased DMN coupling, assuming a limited availability of processing capacities involved in internally as opposed to externally directed attention.

The SN comprises various structures, which can be considered different functional subunits. It is presumably the concerted interplay between units involved in attentional reorienting (AR; e.g. right TPJ), arousal regulation (A; thalamus) and threat appraisal (TA, e.g. dACC, al, amygdala), which characterizes the overall network behavior. If a particular subunit constitutes a primary target or if all SN nodes are equally affected under placebo, remains to

be shown. However, the central portion of the thalamus might be a candidate region for a primary placebo-dependent modulation, since central thalamic deactivation correlated with enhanced BOLD responses in the rACC, which constitutes a regulatory key region in various placebo effects and as part of the vmPFC, a key region of the DMN (see also Figure 3). Widespread thalamic connections with cortical regions might thus explain the overall attenuation of SN nodes (including the amygdala).

As stated above, this model can be regarded as a first attempt to elucidate the mechanisms underlying placebo anxiolysis. However, future studies, further unraveling the link between placebo-dependent increases in FC within and between large-scale neural networks and cue-related BOLD responses are required to further support or if necessary adjust the proposed model.

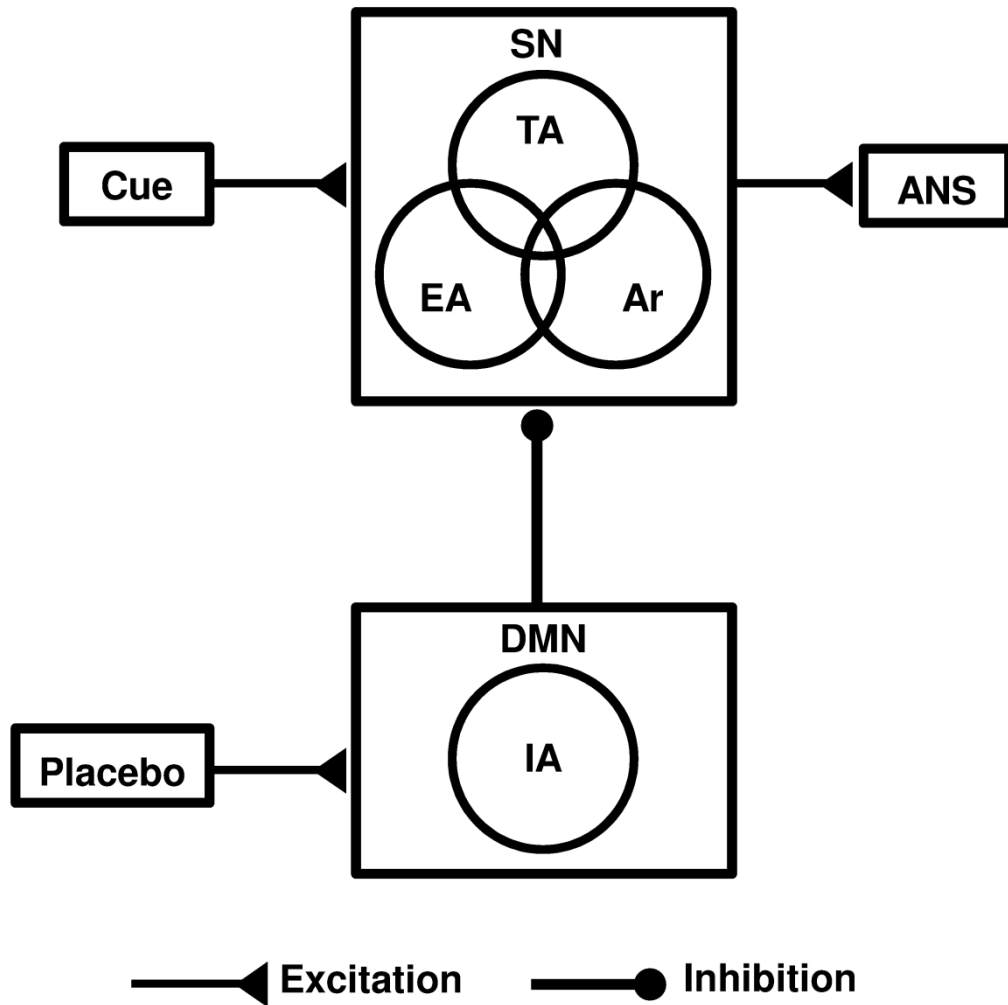


Figure 36: A psychobiological model of placebo anxiolysis

Excitatory connections (Excitation) indicate enhancing and inhibitory connections (Inhibition) attenuating effects. Internally directed attention, mediated by the default mode network (DMN), increases under placebo and in return inhibits cue-processing in the salience network (SN). The SN comprises interacting functional subunits, involved in arousal regulation (A), attentional reorienting (AR) and threat appraisal (TA). Cue-related responses in the autonomic nervous system (ANS) are reduced due to SN inhibition.

6.10. Outlook

In the current project the neural mechanisms of placebo anxiolysis were elucidated and finally a psychobiological model was proposed to establish a starting point for future studies. Some remaining unanswered questions are summarized in the following and should be addressed in future projects:

(a) Enhanced cue-related BOLD responses and increased placebo-dependent FC to almost all SN nodes were observed in the rACC under placebo. Furthermore, under placebo, all SN nodes were characterized by attenuated BOLD responses and the rACC/vmPFC exhibited enhanced coupling to major DMN regions. Future studies are essential to further clarify the link between cue-related BOLD responses and FC changes in large-scale neural networks.

(b) rACC activation and thalamus deactivation suggested an important role of endogenous opioids in mediating placebo anxiolysis. The administration of a μ -opioid receptor blocker could confirm this hypothesis and should, in the case of an opioid-dependent placebo effect, block the placebo response. Such results would further underscore the close link between placebo anxiolysis and placebo analgesia.

(c) EEG and fMRI data were acquired separately, with both techniques revealing neural correlates of internally and externally directed attention. In their interplay, both are hypothesized to strongly contribute to the observed placebo effects. However, it is not yet clear how EEG and fMRI signals are related to each other. For this reason, combined EEG-fMRI might help to relate both signals and thus clarify the relationship between threat-induced ERPs and BOLD responses in the SN and further between theta/alpha oscillations and connectivity changes within and between large-scale brain networks.

(d) Although phasic fear and sustained states of anxiety were both induced in a single study design, the placebo effect was found to mainly reduce the latter. In order to specifically analyze the effects of placebos on sustained anxiety, a study design is required that rules out temporary states of phasic fear. Sustained anxiety might, for example, be induced by threatening study participants with an electric shock over a 5 min time period, which in fact is never applied. The obtained data (EEG, fMRI, EEG-fMRI) would be highly suitable for analyzing stress- and placebo-related changes within and between large-scale brain networks and might also enable the analysis of ongoing activity in small nuclei such as the BNST or the LC.

Placebo anxiolysis is certainly of great interest in the field of placebo research, due to the far-reaching influence in clinical contexts. However, the anxiolytic effect induced by the placebo manipulation might also be a very promising avenue for the development of new therapeutic approaches in the treatment of anxiety disorders (ADs).

A current survey of a sample of 5318 adult participants in Germany revealed that 27.7% met the criteria for at least one mental disorder during the past 12 months. Among them, anxiety disorders were most frequently observed (15.3%) (134). In contrast, pharmaceutical

companies have increasingly withdrawn from psychopharmacological research, in no small part due to low drug compared to high placebo response rates (132). Accordingly, a current meta-analysis evaluated ten placebo-controlled double-blind studies on the efficacy of Paroxetine (a selective serotonin reuptake inhibitor [SSRI] and a common first line therapy in the treatment of ADs) in treating anxiety. Baseline severity of anxiety ranged from 18.7 to 26.0 on an anxiety rating scale from 0 to 56 and a mean statistically significant drug-placebo difference of only 2.31 ($p < 0.01$) was reported. The weighted mean change on the rating scale was 11.11 points for paroxetine but still 8.77 for placebo. In other words, the change in the placebo groups explained 79% of the mean change score in the paroxetine groups.

The overall retreat from psychopharmacological research is certainly an alarming signal considering the prevalence of mental disorders, in particular ADs. In this research project, inert treatments led to unexpectedly strong anxiolytic effects although the placebo treatment was introduced as a mild anxiolytic drug. There is therefore no reason to classify anxiolytic placebo effects as powerless marginal phenomena, as has been suggested by some authors (133). Instead, the stimulation of the neural correlates of placebo anxiolysis (without deceiving the patient) by using behavioral strategies, brain stimulation techniques (e.g. transcranial direct current stimulation [tDCS] or transcranial magnetic stimulation [TMS]), neurofeedback or even more targeted pharmacological interventions might represent a promising new avenue in the treatment of ADs.

7. List of abbreviations

AD	= anxiety disorder
al	= anterior insula
ANOVA	= analysis of variance
ANS	= autonomic nervous system
BNST	= bed nucleus of the stria terminalis
BOLD	= blood oxygen level dependency
CEN	= central executive network
CN _A	= central nucleus of the amygdala
CNS	= central nervous system
CR	= conditioned response
CS	= conditioned stimulus
dACC	= dorsal anterior cingulate cortex
DFG	= Deutsche Forschungsgemeinschaft (German Research Foundation)
dIPFC	= dorsolateral prefrontal cortex
dmPFC	= dorsomedial prefrontal cortex
DMN	= default mode network
EA	= external attention
EEG	= electroencephalography
ERP	= event-related potential
FFT	= fast Fourier transformation
FC	= functional connectivity
FG	= fusiform gyrus
FIO	= frontal inferior operculum
fMRI	= functional magnetic resonance imaging
FOV	= field of view
fsG	= frontal superior gyrus
FWE	= familywise error
FWHM	= full width at half maximum
GH	= growth hormone
GLM	= general linear model
HR	= high responders
HRF	= hemodynamic response function
HT	= hypothalamus
I	= insula

IA	= internal attention
ICA	= independent component analysis
ICN	= intrinsically coupled neural network
IF- γ	= interferon-gamma
IL-2	= interleukin-2
iPL	= inferior parietal lobule
IRF	= impulse response function
ITI	= inter-trial interval
L	= left
LG	= lingual gyrus
LPP	= late positive potential
LR	= low responders
MFG	= middle frontal gyrus
MNI	= Montreal Neurological Institute
MRI	= magnetic resonance imaging
MTG	= middle temporal gyrus
NP	= no placebo
NT	= no threat
O	= operculum
OLS	= ordinary least squares
P	= placebo
PAG	= periaqueductal grey
PD	= Parkinson's disease
PET	= positron emission tomography
PHG	= parahippocampal gyrus
pIPL	= posterior inferior parietal lobule
Plac	= Placebo
pMTG	= posterior middle temporal gyrus
pre/postCG	= pre-/postcentral gyrus
p_{rob}	= p-value of robust correlation
p_{Pear}	= p-value of Pearson's correlation
PTSD	= post-traumatic stress disorder
R	= right
RAC	= [^{11}C]raclopride
rACC	= rostral anterior cingulate cortex
rspC	= retrosplenial cortex
RVM	= rostral ventromedial medulla

SC	= skin conductance
SCR	= skin conductance response
SCL	= skin conductance level
SEM	= standard error of the mean
SMA	= supplementary motor area
SN	= salience network
SPM	= statistical parametric mapping
sps	= samples per second
T	= threat
TA	= threat appraisal
TE	= echo time
Thal	= thalamus
TP	= temporal pole
TPJ	= temporoparietal junction
US	= unconditioned stimulus
VAS	= visual analogue scale
vmPFC	= ventromedial prefrontal cortex
vlPFC	= ventrolateral prefrontal cortex
VS	= ventral striatum

8. References

1. Shapiro AK, Shapiro E (2010) *The Powerful Placebo: From Ancient Priest to Modern Physician* (JHU Press).
2. Benedetti F (2008) *Placebo Effects: Understanding the mechanisms in health and disease* (Oxford University Press, U.S.A., Oxford). 1st Ed.
3. Colloca L, Klinger R, Flor H, Bingel U (2013) Placebo analgesia: Psychological and neurobiological mechanisms. *PAIN* 154(4):511–514.
4. Benedetti F, et al. (2004) Placebo-responsive Parkinson patients show decreased activity in single neurons of subthalamic nucleus. *Nat Neurosci* 7(6):587–588.
5. Schmidt L, Braun EK, Wager TD, Shohamy D (2014) Mind matters: placebo enhances reward learning in Parkinson's disease. *Nat Neurosci* 17(12):1793–1797.
6. Leuchter AF, Cook IA, Witte EA, Morgan M, Abrams M (2002) Changes in brain function of depressed subjects during treatment with placebo. *Am J Psychiatry* 159(1):122–129.
7. Benedetti F, et al. (2003) Open versus hidden medical treatments: The patient's knowledge about a therapy affects the therapy outcome. *Prev Treat* 6(1). doi:10.1037/1522-3736.6.1.61a.
8. Stein DJ, Baldwin DS, Dolberg OT, Despiegel N, Bandelow B (2006) Which factors predict placebo response in anxiety disorders and major depression? An analysis of placebo-controlled studies of escitalopram. *J Clin Psychiatry* 67(11):1741–1746.
9. Sugarman MA, Loree AM, Baltés BB, Grekin ER, Kirsch I (2014) The Efficacy of Paroxetine and Placebo in Treating Anxiety and Depression: A Meta-Analysis of Change on the Hamilton Rating Scales. *PLoS ONE* 9(8):e106337.
10. Nitzan U, Lichtenberg P (2004) Questionnaire survey on use of placebo. *BMJ* 329(7472):944–946.
11. Sherman R, Hickner J (2008) Academic Physicians Use Placebos in Clinical Practice and Believe in the Mind–Body Connection. *J Gen Intern Med* 23(1):7–10.

12. Grillon C (2008) Models and mechanisms of anxiety: evidence from startle studies. *Psychopharmacology (Berl)* 199(3):421–437.
13. Davis M, Walker DL, Miles L, Grillon C (2010) Phasic vs sustained fear in rats and humans: role of the extended amygdala in fear vs anxiety. *Neuropsychopharmacol Off Publ Am Coll Neuropsychopharmacol* 35(1):105–135.
14. DSM-5 (2013) *Diagnostic and Statistical Manual of Mental Disorders, 5th Edition: DSM-5* (American Psychiatric Publishing, Washington, DC). 5 edition.
15. LeDoux JE, Iwata J, Cicchetti P, Reis DJ (1988) Different projections of the central amygdaloid nucleus mediate autonomic and behavioral correlates of conditioned fear. *J Neurosci Off J Soc Neurosci* 8(7):2517–2529.
16. Tovote P, et al. (2005) Dissociation of temporal dynamics of heart rate and blood pressure responses elicited by conditioned fear but not acoustic startle. *Behav Neurosci* 119(1):55–65.
17. Davis M (1992) The Role of the Amygdala in Fear and Anxiety. *Annu Rev Neurosci* 15(1):353–375.
18. Walker DL, Davis M (1997) Anxiogenic effects of high illumination levels assessed with the acoustic startle response in rats. *Biol Psychiatry* 42(6):461–471.
19. Davis M, Walker DL, Miles L, Grillon C (2010) Phasic vs Sustained Fear in Rats and Humans: Role of the Extended Amygdala in Fear vs Anxiety. *Neuropsychopharmacology* 35(1):105–135.
20. Walker DL, Miles LA, Davis M (2009) Selective Participation of the Bed Nucleus of the Stria Terminalis and CRF in Sustained Anxiety-Like versus Phasic Fear-Like Responses. *Prog Neuropsychopharmacol Biol Psychiatry* 33(8):1291–1308.
21. Gross CT, Canteras NS (2012) The many paths to fear. *Nat Rev Neurosci* 13(9):651–658.
22. Schmidt RF, Thews G, Lang F (2000) *Physiologie des Menschen* (Springer). 28., korr. u. aktualisierte Aufl.
23. Logothetis NK, Wandell BA (2004) Interpreting the BOLD signal. *Annu Rev Physiol* 66:735–769.

24. Hillman EMC (2014) Coupling mechanism and significance of the BOLD signal: a status report. *Annu Rev Neurosci* 37:161–181.
25. Nunez PL, Srinivasan R (2006) *Electric fields of the brain: the neurophysics of EEG* (Oxford Univ. Press, Oxford). 2. ed.
26. Lopes da Silva F (2013) EEG and MEG: Relevance to Neuroscience. *Neuron* 80(5):1112–1128.
27. Luck SJ (2014) *An introduction to the event-related potential technique* (MIT Press, Cambridge, Mass.). 2. ed.
28. Gonsalvez CJ, Barry RJ, Rushby JA, Polich J (2007) Target-to-target interval, intensity, and P300 from an auditory single-stimulus task. *Psychophysiology* 44(2):245–250.
29. Pritchard WS (1981) Psychophysiology of P300. *Psychol Bull* 89(3):506–540.
30. Isreal JB, Wickens CD, Chesney GL, Donchin E (1980) The event-related brain potential as an index of display-monitoring workload. *Hum Factors* 22(2):211–224.
31. Scharmüller W, Leutgeb V, Schäfer A, Köchel A, Schienle A (2011) Source localization of late electrocortical positivity during symptom provocation in spider phobia: An sLORETA study. *Brain Res* 1397:10–18.
32. Hajcak G, MacNamara A, Olvet DM (2010) Event-Related Potentials, Emotion, and Emotion Regulation: An Integrative Review. *Dev Neuropsychol* 35(2):129–155.
33. Polich J (2007) Updating P300: An integrative theory of P3a and P3b. *Clin Neurophysiol* 118(10):2128–2148.
34. Varela F, Lachaux J-P, Rodriguez E, Martinerie J (2001) The brainweb: Phase synchronization and large-scale integration. *Nat Rev Neurosci* 2(4):229–239.
35. Cooper NR, Croft RJ, Dominey SJJ, Burgess AP, Gruzelier JH (2003) Paradox lost? Exploring the role of alpha oscillations during externally vs. internally directed attention and the implications for idling and inhibition hypotheses. *Int J Psychophysiol Off J Int Organ Psychophysiol* 47(1):65–74.
36. Hsieh L-T, Ranganath C (2014) Frontal midline theta oscillations during working memory maintenance and episodic encoding and retrieval. *NeuroImage* 85:721–729.

37. Klimesch W (1999) EEG alpha and theta oscillations reflect cognitive and memory performance: a review and analysis. *Brain Res Brain Res Rev* 29(2-3):169–195.
38. Aftanas LI, Golocheikine SA (2001) Human anterior and frontal midline theta and lower alpha reflect emotionally positive state and internalized attention: high-resolution EEG investigation of meditation. *Neurosci Lett* 310(1):57–60.
39. Aftanas LI, Golocheikine SA (2002) Non-linear dynamic complexity of the human EEG during meditation. *Neurosci Lett* 330(2):143–146.
40. Mulert C, Lemieux L (2009) *EEG - fMRI: Physiological Basis, Technique, and Applications* (Springer Science & Business Media).
41. Büchel C, Dolan RJ (2000) Classical fear conditioning in functional neuroimaging. *Curr Opin Neurobiol* 10(2):219–223.
42. Haaker J, et al. (2013) Single dose of L-dopa makes extinction memories context-independent and prevents the return of fear. *Proc Natl Acad Sci* 110(26):E2428–E2436.
43. LaBar KS, Gatenby JC, Gore JC, LeDoux JE, Phelps EA (1998) Human Amygdala Activation during Conditioned Fear Acquisition and Extinction: a Mixed-Trial fMRI Study. *Neuron* 20(5):937–945.
44. Alvarez RP, Chen G, Bodurka J, Kaplan R, Grillon C (2011) Phasic and sustained fear in humans elicits distinct patterns of brain activity. *NeuroImage* 55(1):389–400.
45. Büchel C, Morris J, Dolan RJ, Friston KJ (1998) Brain Systems Mediating Aversive Conditioning: an Event-Related fMRI Study. *Neuron* 20(5):947–957.
46. Butler T, et al. (2007) Human fear-related motor neurocircuitry. *Neuroscience* 150(1):1–7.
47. Mechias M-L, Etkin A, Kalisch R (2010) A meta-analysis of instructed fear studies: implications for conscious appraisal of threat. *NeuroImage* 49(2):1760–1768.
48. Seeley WW, et al. (2007) Dissociable Intrinsic Connectivity Networks for Salience Processing and Executive Control. *J Neurosci* 27(9):2349–2356.
49. Hermans EJ, et al. (2011) Stress-related noradrenergic activity prompts large-scale neural network reconfiguration. *Science* 334(6059):1151–1153.

50. McDonald AJ, Shammah-Lagnado SJ, Shi C, Davis M (1999) Cortical afferents to the extended amygdala. *Ann N Y Acad Sci* 877:309–338.
51. Shi CJ, Cassell MD (1998) Cortical, thalamic, and amygdaloid connections of the anterior and posterior insular cortices. *J Comp Neurol* 399(4):440–468.
52. Menon V (2011) Large-scale brain networks and psychopathology: a unifying triple network model. *Trends Cogn Sci* 15(10):483–506.
53. Harrison BJ, et al. (2008) Consistency and functional specialization in the default mode brain network. *Proc Natl Acad Sci U S A* 105(28):9781–9786.
54. Laird AR, et al. (2009) Investigating the functional heterogeneity of the default mode network using coordinate-based meta-analytic modeling. *J Neurosci Off J Soc Neurosci* 29(46):14496–14505.
55. Raichle ME, et al. (2001) A default mode of brain function. *Proc Natl Acad Sci U S A* 98(2):676–682.
56. Koechlin E, Summerfield C (2007) An information theoretical approach to prefrontal executive function. *Trends Cogn Sci* 11(6):229–235.
57. Straube T, Glauer M, Dilger S, Mentzel H-J, Miltner WHR (2006) Effects of cognitive-behavioral therapy on brain activation in specific phobia. *NeuroImage* 29(1):125–135.
58. Benedetti F, et al. (2003) Conscious Expectation and Unconscious Conditioning in Analgesic, Motor, and Hormonal Placebo/Nocebo Responses. *J Neurosci* 23(10):4315–4323.
59. Elsenbruch S, et al. (2012) Neural mechanisms mediating the effects of expectation in visceral placebo analgesia: an fMRI study in healthy placebo responders and nonresponders. *Pain* 153(2):382–390.
60. Bingel U, et al. (2011) The Effect of Treatment Expectation on Drug Efficacy: Imaging the Analgesic Benefit of the Opioid Remifentanyl. *Sci Transl Med* 3(70):70ra14–70ra14.
61. Leslie JC (1996) *Principles of Behavioral Analysis* (Psychology Press).
62. Pavlov (1927) PI (2010) Conditioned reflexes: An investigation of the physiological activity of the cerebral cortex. *Ann Neurosci* 17(3):136–141.

63. Goebel MU, et al. (2002) Behavioral conditioning of immunosuppression is possible in humans. *FASEB J Off Publ Fed Am Soc Exp Biol* 16(14):1869–1873.
64. Petrovic P, et al. (2005) Placebo in Emotional Processing— Induced Expectations of Anxiety Relief Activate a Generalized Modulatory Network. *Neuron* 46(6):957–969.
65. Montgomery GH, Kirsch I (1997) Classical conditioning and the placebo effect. *Pain* 72(1-2):107–113.
66. Schafer SM, Colloca L, Wager TD (2015) Conditioned placebo analgesia persists when subjects know they are receiving a placebo. *J Pain Off J Am Pain Soc* 16(5):412–420.
67. Jensen KB, et al. (2012) Nonconscious activation of placebo and nocebo pain responses. *Proc Natl Acad Sci* 109(39):15959–15964.
68. Jensen KB, et al. (2014) A Neural Mechanism for Nonconscious Activation of Conditioned Placebo and Nocebo Responses. *Cereb Cortex*:bhu275.
69. Kaptchuk TJ, et al. (2010) Placebos without Deception: A Randomized Controlled Trial in Irritable Bowel Syndrome. *PLoS ONE* 5(12):e15591.
70. de la Fuente-Fernandez R (2001) Expectation and Dopamine Release: Mechanism of the Placebo Effect in Parkinson's Disease. *Science* 293(5532):1164–1166.
71. Büchel C, Geuter S, Sprenger C, Eippert F (2014) Placebo analgesia: a predictive coding perspective. *Neuron* 81(6):1223–1239.
72. Levine J (1978) THE MECHANISM OF PLACEBO ANALGESIA. *The Lancet* 312(8091):654–657.
73. Amanzio M, Benedetti F (1999) Neuropharmacological Dissection of Placebo Analgesia: Expectation-Activated Opioid Systems versus Conditioning-Activated Specific Subsystems. *J Neurosci* 19(1):484–494.
74. Eippert F, et al. (2009) Activation of the Opioidergic Descending Pain Control System Underlies Placebo Analgesia. *Neuron* 63(4):533–543.
75. Wager TD, Atlas LY (2015) The neuroscience of placebo effects: connecting context, learning and health. *Nat Rev Neurosci* 16(7):403–418.

76. Apkarian AV, Bushnell MC, Treede R-D, Zubieta J-K (2005) Human brain mechanisms of pain perception and regulation in health and disease. *Eur J Pain Lond Engl* 9(4):463–484.
77. Watkins LR, Mayer DJ (1982) Organization of endogenous opiate and nonopiate pain control systems. *Science* 216(4551):1185–1192.
78. Price JL (1999) Prefrontal cortical networks related to visceral function and mood. *Ann N Y Acad Sci* 877:383–396.
79. Bingel U, Lorenz J, Schoell E, Weiller C, Büchel C (2006) Mechanisms of placebo analgesia: rACC recruitment of a subcortical antinociceptive network. *Pain* 120(1-2):8–15.
80. Zubieta J-K (2005) Placebo Effects Mediated by Endogenous Opioid Activity on - Opioid Receptors. *J Neurosci* 25(34):7754–7762.
81. Schultz W, Apicella P, Ljungberg T (1993) Responses of monkey dopamine neurons to reward and conditioned stimuli during successive steps of learning a delayed response task. *J Neurosci* 13(3):900–913.
82. O'Doherty JP, Dayan P, Friston K, Critchley H, Dolan RJ (2003) Temporal difference models and reward-related learning in the human brain. *Neuron* 38(2):329–337.
83. Eippert F, Finsterbusch J, Bingel U, Büchel C (2009) Direct evidence for spinal cord involvement in placebo analgesia. *Science* 326(5951):404.
84. Spielberger C (1985) Assessment of state and trait anxiety: Conceptual and methodological issues. *Southern Psychol* 2:6–16.
85. Boucsein W, et al. (2012) Publication recommendations for electrodermal measurements. *Psychophysiology* 49(8):1017–1034.
86. Zahn TP, Rapoport JL, Thompson CL (1981) Autonomic effects of dextroamphetamine in normal men: implications for hyperactivity and schizophrenia. *Psychiatry Res* 4(1):39–47.
87. Benedek M, Kaernbach C (2010) A continuous measure of phasic electrodermal activity. *J Neurosci Methods* 190(1):80–91.
88. Lykken DT, Venables PH (1971) Direct measurement of skin conductance: a proposal for standardization. *Psychophysiology* 8(5):656–672.

89. Granholm E, Steinhauer SR (2004) Pupillometric measures of cognitive and emotional processes. *Int J Psychophysiol Off J Int Organ Psychophysiol* 52(1):1–6.
90. Oostenveld R, Fries P, Maris E, Schoffelen J-M (2011) FieldTrip: Open source software for advanced analysis of MEG, EEG, and invasive electrophysiological data. *Comput Intell Neurosci* 2011:156869.
91. Maris E, Oostenveld R (2007) Nonparametric statistical testing of EEG- and MEG-data. *J Neurosci Methods* 164(1):177–190.
92. Nichols T, Hayasaka S (2003) Controlling the familywise error rate in functional neuroimaging: a comparative review. *Stat Methods Med Res* 12(5):419–446.
93. Xia M, Wang J, He Y (2013) BrainNet Viewer: a network visualization tool for human brain connectomics. *PloS One* 8(7):e68910.
94. Di Russo F, Martínez A, Sereno MI, Pitzalis S, Hillyard SA (2002) Cortical sources of the early components of the visual evoked potential. *Hum Brain Mapp* 15(2):95–111.
95. Scharmüller W, Leutgeb V, Schäfer A, Schienle A (2012) Investigating phobic specificity with standardized low resolution brain electromagnetic tomography (sLORETA). *Brain Res* 1477:74–82.
96. Huber PJ (1981) *Robust statistics* (Wiley, New York, NY).
97. Büchel C, Morris J, Dolan RJ, Friston KJ (1998) Brain Systems Mediating Aversive Conditioning: an Event-Related fMRI Study. *Neuron* 20(5):947–957.
98. Phelps EA, et al. (2001) Activation of the left amygdala to a cognitive representation of fear. *Nat Neurosci* 4(4):437–441.
99. Amanzio M, Benedetti F, Porro CA, Palermo S, Cauda F (2012) Activation likelihood estimation meta-analysis of brain correlates of placebo analgesia in human experimental pain. *Hum Brain Mapp* (3):734–752.
100. Coull JT, Frith CD, Dolan RJ, Frackowiak RS, Grasby PM (1997) The neural correlates of the noradrenergic modulation of human attention, arousal and learning. *Eur J Neurosci* 9(3):589–598.
101. Andrews-Hanna JR, Reidler JS, Sepulcre J, Poulin R, Buckner RL (2010) Functional-Anatomic Fractionation of the Brain's Default Network. *Neuron* 65(4):550–562.

102. Colloca L, Benedetti F (2006) How prior experience shapes placebo analgesia. *Pain* 124(1-2):126–133.
103. Klinger R, Soost S, Flor H, Worm M (2007) Classical conditioning and expectancy in placebo hypoalgesia: A randomized controlled study in patients with atopic dermatitis and persons with healthy skin. *Pain* 128(1-2):31–39.
104. Miller-Keane Encyclopedia & Dictionary of Medicine, Nursing & Allied Health -- Revised Reprint, 7e (2005) (Saunders). 7 edition.
105. Eysenck M (2014) *Anxiety and Cognition: A Unified Theory* (Psychology Press).
106. Baas JMP, et al. (2002) Benzodiazepines have no effect on fear-potentiated startle in humans. *Psychopharmacology (Berl)* 161(3):233–247.
107. Bledowski C, et al. (2004) Localizing P300 Generators in Visual Target and Distractor Processing: A Combined Event-Related Potential and Functional Magnetic Resonance Imaging Study. *J Neurosci* 24(42):9353–9360.
108. Soltani M, Knight RT (2000) Neural origins of the P300. *Crit Rev Neurobiol* 14(3-4):199–224.
109. Knight RT (1984) Decreased response to novel stimuli after prefrontal lesions in man. *Electroencephalogr Clin Neurophysiol* 59(1):9–20.
110. Knight RT, Scabini D, Woods DL, Clayworth CC (1989) Contributions of temporal-parietal junction to the human auditory P3. *Brain Res* 502(1):109–116.
111. Corbetta M, Patel G, Shulman GL (2008) The reorienting system of the human brain: from environment to theory of mind. *Neuron* 58(3):306–324.
112. Nieuwenhuis S, Aston-Jones G, Cohen JD (2005) Decision making, the P3, and the locus coeruleus-norepinephrine system. *Psychol Bull* 131(4):510–532.
113. Pineda JA, Foote SL, Neville HJ (1989) Effects of locus coeruleus lesions on auditory, long-latency, event-related potentials in monkey. *J Neurosci Off J Soc Neurosci* 9(1):81–93.
114. Liu Y, Huang H, McGinnis-Deweese M, Keil A, Ding M (2012) Neural Substrate of the Late Positive Potential in Emotional Processing. *J Neurosci* 32(42):14563–14572.

115. Baas JMP, Kenemans JL, Böcker KBE, Verbaten MN (2002) Threat-induced cortical processing and startle potentiation. *Neuroreport* 13(1):133–137.
116. Weymar M, Bradley MM, Hamm AO, Lang PJ (2013) When fear forms memories: Threat of shock and brain potentials during encoding and recognition. *Cortex* 49(3):819–826.
117. Kahneman D (1973) *Attention and effort* (Prentice-Hall, Englewood Cliffs, N.J).
118. Berger H (1991) *Das Elektrenkephalogramm des Menschen* ed Mühlau G (pmi-Verl, Frankfurt am Main). Kommentierter Reprint des Erstdr. aus dem Jahre 1938, Halle.
119. Pfurtscheller G, Stancák A, Neuper C (1996) Event-related synchronization (ERS) in the alpha band — an electrophysiological correlate of cortical idling: A review. *Int J Psychophysiol* 24(1-2):39–46.
120. Brazier M a. B, Casby JU (1952) Cross-correlation and autocorrelation studies of electroencephalographic potentials. *Electroencephalogr Clin Neurophysiol* 4(2):201–211.
121. Inanaga K (1998) Frontal midline theta rhythm and mental activity. *Psychiatry Clin Neurosci* 52(6):555–566.
122. Kubota Y, et al. (2001) Frontal midline theta rhythm is correlated with cardiac autonomic activities during the performance of an attention demanding meditation procedure. *Brain Res Cogn Brain Res* 11(2):281–287.
123. Ledoux J (1998) *The Emotional Brain: The Mysterious Underpinnings of Emotional Life* (Simon & Schuster, New York, NY). Touchstone.
124. Zhang W, Qin S, Guo J, Luo J (2011) A follow-up fMRI study of a transferable placebo anxiolytic effect. *Psychophysiology* 48(8):1119–1128.
125. Furmark T, et al. (2008) A Link between Serotonin-Related Gene Polymorphisms, Amygdala Activity, and Placebo-Induced Relief from Social Anxiety. *J Neurosci* 28(49):13066–13074.
126. Wager TD, et al. (2004) Placebo-induced changes in FMRI in the anticipation and experience of pain. *Science* 303(5661):1162–1167.
127. Vogt BA (2005) Pain and Emotion Interactions in Subregions of the Cingulate Gyrus. *Nat Rev Neurosci* 6(7):533–544.

128. Brunton J, Charpak S (1998) mu-Opioid peptides inhibit thalamic neurons. *J Neurosci Off J Soc Neurosci* 18(5):1671–1678.
129. Jilka SR, et al. (2014) Damage to the Salience Network and interactions with the Default Mode Network. *J Neurosci Off J Soc Neurosci* 34(33):10798–10807.
130. Krummenacher P, Candia V, Folkers G, Schedlowski M, Schönbachler G (2010) Prefrontal cortex modulates placebo analgesia. *PAIN* 148(3):368–374.
131. Benedetti F (2010) No prefrontal control, no placebo response. *Pain* 148(3):357–358.
132. Hürden in der Forschung: Gehen den Psychiatern bald die Pillen aus? Available at: http://www.aerztezeitung.de/medizin/krankheiten/neuro-psychiatrische_krankheiten/article/851843/huerden-forschung-gehen-psychiatern-bald-pillen.html [Accessed October 30, 2015].
133. Hróbjartsson A, Gøtzsche PC (2004) Is the placebo powerless? Update of a systematic review with 52 new randomized trials comparing placebo with no treatment. *J Intern Med* 256(2):91–100.
134. Jacobi F, et al. (2014) Twelve-month prevalence, comorbidity and correlates of mental disorders in Germany: the Mental Health Module of the German Health Interview and Examination Survey for Adults (DEGS1-MH). *Int. J. Methods Psychiatr. Res.* 23: 304–319.

9. Appendix

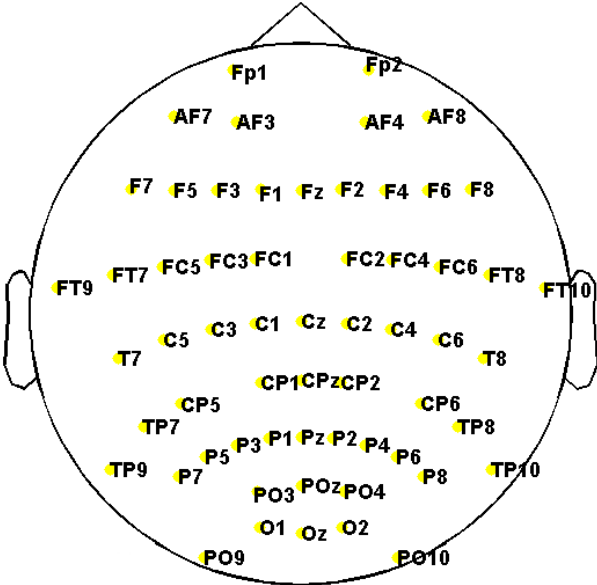


Figure A 1: EEG electrode set (Study 2)

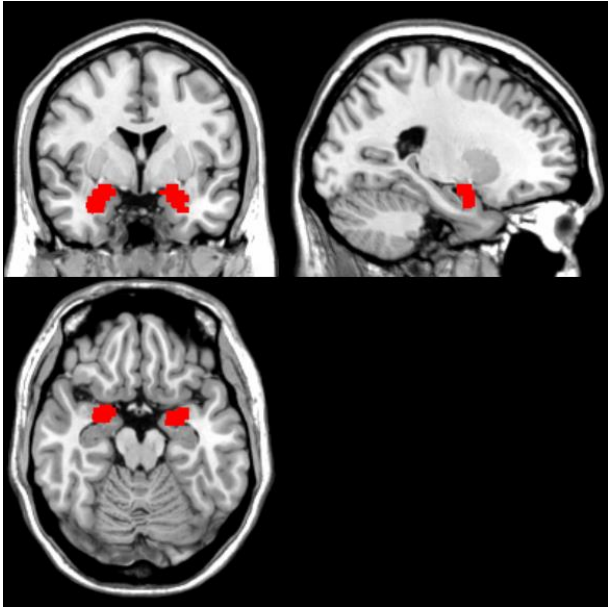


Figure A 2: Amygdala mask (Study 3)

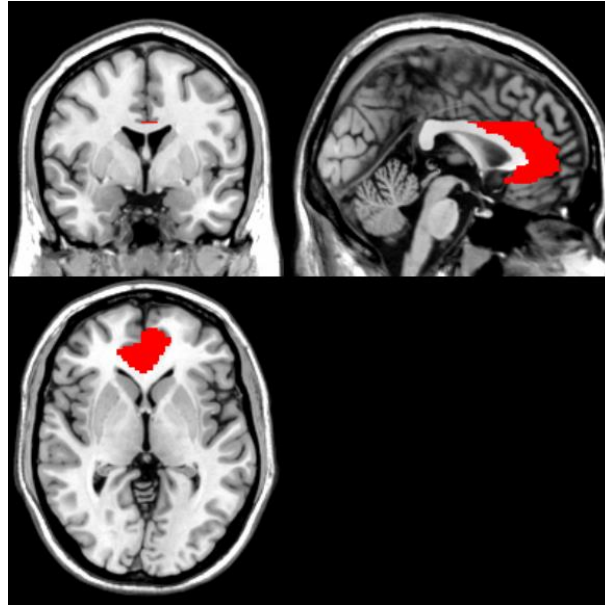


Figure A 3: ACC mask (Study 3)

Table A 1: Central executive network (CEN)

CEN as identified by Seeley et al. (2007). L: left, R: right. Coordinates are denoted by x, y, z in mm (MNI-space).

Label	x y z [MNI]
L orbital frontoinsula	-36 24 -10
R dorsolateral prefrontal cortex	46 46 14
L dorsolateral prefrontal cortex	-34 46 6
R ventrolateral prefrontal cortex	34 56 -6
L ventrolateral prefrontal cortex	-32 54 -4
R frontal operculum	56 14 14
R dorsolateral prefrontal cortex / frontal eye field	30 12 60
L dorsolateral prefrontal cortex / frontal eye field	-32 18 50
dorsomedial prefrontal cortex	0 36 46
R lateral parietal	38 -56 44
R inferior temporal	58 -54 -16
R dorsal caudate	12 14 4
L dorsal caudate	-16 -14 20
R ventromedial caudate	10 12 2
R anterior thalamus	10 2 8
L anterior thalamus	-8 -2 8

Table A 2: Salience network (SN)

SN as identified by Seeley et al. (2007). L: left, R: right, ACC. Coordinates are denoted by x, y, z in mm (MNI-space).

Label	x y z [MNI]
R orbital frontoinsula	42 10 -12
L orbital frontoinsula	-40 18 -12
R temporal lobe	52 20 -18
L temporal lobe	-52 16 -14
Paracingulate	0 44 28
R dorsal anterior cingulate cortex	6 22 30
L dorsal anterior cingulate cortex	-6 18 30
R supplementary motor area (SMA) /Pre-SMA	6 8 58
L supplementary motor area (SMA) /Pre-SMA	-4 14 48
R Superior temporal	64 -38 6
L Superior temporal	-62 -16 8
R parietal operculum	58 -40 30
L parietal operculum	-60 -40 40
Frontal pole	-24 56 10
R ventrolateral prefrontal cortex	42 46 0
R dorsolateral prefrontal cortex	30 48 22
L dorsolateral prefrontal cortex	-38 52 10
R ventral striato-pallidum	22 6 -2
L ventral striato-pallidum	-22 12 -6
R dorsomedial thalamus	12 -18 6
R hypothalamus	6 -16 -6
L hypothalamus	-10 -14 -8
R SLEA / paraolfactory	26 4 -20
L SLEA / paraolfactory	-28 4 -18
L periaqueductal grey	-4 -24 -2
R substantia nigra / ventral tegmental area	8 -8 -14
L substantia nigra / ventral tegmental area	-10 -14 -10

Table A 3: Default mode network (DMN)

DMN as identified by Andrews-Hanna et al. (2010). L: left, R: right. Only left-sided coordinates are reported. For the comparison of network topologies in the current study, mirrored right-sided coordinates were also considered. Coordinates are denoted by x, y, z in mm (MNI-space).

Label	x y z [MNI]
Anterior medial prefrontal cortex	-6 52 -2
Posterior cingulate cortex	-8 -56 26
Dorsal medial prefrontal cortex	0 52 26
Temporal parietal junction	-54 -54 28
Lateral temporal cortex	-60 -24 -18
Temporal pole	-50 14 -40
Ventral medial prefrontal cortex	0 26 -18
Posterior inferior parietal lobule	-44 -74 32
Retrosplenial cortex	-14 -52 8
Parahippocampal cortex	-28 -40 -12
Hippocampal formation	-22 -20 -26

Information brochure Study 1+2 (in German)

Aufklärungsbroschüre zur Einnahme eines anxiolytischen Präparats

1. Allgemeine Informationen zur Studienmedikation

1a. Lorazepam 25mg intranasal (Lorasan©)

In dieser Studie erhalten sie das niedrig dosierte Kurzzeit-Anxiolytikum („Angstlöser“) Lorasan©. Der darin enthaltene Wirkstoff Lorazepam wird bei diesem Präparat als Nasenspray verabreicht und ausschließlich über die Nasenschleimhaut (intranasal) aufgenommen.

Lorazepam ist ein Arzneistoff aus der Gruppe der Benzodiazepine, der wie alle Benzodiazepine eine anxiolytische (angstlösend) und muskelrelaxierende Wirkung besitzt. Deshalb wird es hauptsächlich als Beruhigungsmittel bei Angst und Panikstörungen eingesetzt. Bei der intranasalen Verabreichung wird eine geringe Menge des Wirkstoffs direkt über die Riechnerven (transneuraler Transport) oder über die perineurale Diffusion in die Gehirn-Rückenmarks-Flüssigkeit (Liquor cerebrospinalis) abgegeben. Der Vorteil hierbei ist eine zügig einsetzende Wirkung (nach ca 30 sec), weshalb die intranasale Gabe von Lorazepam sich auch bei der Behandlung von Panikattacken bewährt hat. Das Präparat kann in dieser Darreichungsform nicht über den Magen-Darm-Trakt (gastrointestinal) aufgenommen werden, weshalb ein verspätet einsetzender kumulativer Effekt auszuschließen ist.

Das einmalige Betätigen des Nasensprays führt zu einer Abgabe von ca 0,15 mg des Wirkstoffs, von denen ca 20% auf dem oben beschriebenen Weg direkt in das zentrale Nervensystem aufgenommen werden. Die verabreichte Menge ist vergleichsweise gering und wird z.B. bei der Behandlung einer akuten Panikattacke um das 30-fache gesteigert. Die geringe Menge und die kurze Halbwertszeit des Wirkstoffs bedingen ein rasches Nachlassen der Wirkung schon nach 2-3 Minuten. Dieses rasche Nachlassen der Wirkung und die zügig einsetzende Wirksamkeit machen die intranasale Gabe von Lorazepam zu einem geeigneten Vergleichsstandard bei der Analyse anxiolytischer Mechanismen.

1b. NaCl 0,9%

Um die Wirkung von Lorazepam in diesem Versuch zu erfassen, muss außerdem ein Grundzustand (Baseline), ohne den Einfluss des Wirkstoffs miterhoben werden. Hierfür ersetzen wir in der Hälfte der Versuchsdurchgänge den Wirkstoff durch eine wirkstofffreie, ebenfalls intranasal verabreichte Kochsalzlösung (NaCl 0,9%). Die Einnahme der Kochsalzlösung hat den Effekt, dass sich verbleibende Reste des Wirkstoffs von der Nasenschleimhaut lösen und somit unwirksam bleiben.

2. Nebenwirkungen und Gegenanzeigen der Studienmedikation

2a. Nebenwirkungen und Gegenanzeigen Lorazepam:

Zu den gelegentlichen (bei weniger als 1% aber mehr als 0,1% der Patienten) Nebenwirkungen zählen v.a. Sedierung, Müdigkeit, eingeschränkte Aufmerksamkeit / Konzentration und Benommenheit. Die meisten beschriebenen Nebenwirkungen von Lorazepam treten bei diesem Präparat aufgrund der geringen Dosierung nur selten (bei weniger als 0,01%, aber mehr als 0,001% der Patienten) oder in Einzelfällen (bei weniger als 0,001% der Patienten) auf. Selten können Muskelschwäche, Sehstörungen (Diplopie, verschwommenes Sehen), sowie Blutdruckabfall (Hypotonie) ausgelöst werden. Sehr selten beobachtete Nebenwirkungen sind allergische Hautreaktionen, paradoxe Reaktionen wie z. B. Angst, Erregungszustände und aggressives Verhalten, sowie Schlafstörungen.

Lorazepam darf nicht angewendet werden bei bekannter Überempfindlichkeit gegen Lorazepam oder andere Benzodiazepine oder gegen einen der sonstigen Bestandteile sowie bei Abhängigkeitsanamnese. In der Schwangerschaft sollte Lorazepam nicht angewendet werden, da keine ausreichenden Erfahrungen mit Lorazepam in der Geburtshilfe vorliegen.

2b. Nebenwirkungen und Gegenanzeigen NaCl 0,9%:

Es sind keine Nebenwirkungen oder Gegenanzeigen bekannt.

Ich bestätige durch meine Unterschrift, dass ich die Aufklärung verstanden habe und mich mit der Durchführung der vorgenannten Studie, einschließlich der Verabreichung eines anxiolytischen Medikaments, einverstanden erkläre.

Hamburg, den

Datum

Unterschrift

Name in Druckbuchstaben

Unterschrift des aufklärenden Untersuchers:

Hamburg, den

Information brochure Study 3 (in German)

Aufklärungsbroschüre zur Einnahme eines inhalativen Anxiolytikums

„Neurale Mechanismen der Anxiolyse“

Liebe Teilnehmerin, lieber Teilnehmer,

Ziel unserer Forschung ist es die Mechanismen der Angst und der Angstreduktion systemisch zu erfassen. Hierbei erforschen wir nicht nur die angstreduzierende Wirkung von nichtmedikamentösen kognitiven Strategien, sondern auch den systemischen Einfluss verschiedener angstreduzierender Medikamente (Anxiolytika).

In diesem Forschungsvorhaben wird Ihnen eine geringdosierte Menge eines angstreduzierenden Inhalats verabreicht, das Ihnen über einen Silikonschlauch in die Nase geleitet wird. Die Wirkung dieser Studienmedikation wird mit einer sog. Kontroll-Messung verglichen, in der Ihnen lediglich Luft zugeführt wird. Beide Inhalate werden mit einer geringen Menge eines ätherischen Öls versetzt. Dies fördert zum einen die Aufnahme des Wirkstoffs und zum anderen wird so möglichen Schleimhautreizungen vorgebeugt.

Allgemeine Informationen zur Studienmedikation

Distickstoffmonoxid N₂O (Lachgas)

Distickstoffmonoxid ist auch unter dem Trivialnamen Lachgas bekannt und wird in der medizinischen Praxis häufig als Inhalations-Narkosemittel bei kurzen mäßig schmerzhaften Eingriffen eingesetzt. Vor allem in der Zahnmedizin findet N₂O als Beruhigungsmittel ängstlicher Patienten häufig Anwendung. N₂O ist in geringer Konzentration geruchsneutral und wird über die Atmung von der Lunge aufgenommen. Nach kurzer Zeit (ca 30 Sekunden) gelangt der Wirkstoff in das zentrale Nervensystem und entfaltet dort seine anxiolytische (angstlösend) und muskelrelaxierende Wirkung. In dieser Studie wird eine vergleichbar

geringe Konzentration von 10% eingesetzt. Dies hat den Vorteil, dass die Wirkung nur über einen Zeitraum von 2 bis 3 Minuten anhält und der Wirkstoff so zeitlich sehr gezielt

eingesetzt werden kann. Der Wirkstoff wird vollständig über Haut und Lunge wieder ausgeschieden, so dass eine weitere Beobachtung des Probanden nach dem Experiment nicht erforderlich ist.

Risiken und Nebenwirkungen

N₂O gilt als nebenwirkungsarmes Sedierungsmittel (Beruhigungsmittel), so dass in der angewandten Konzentration kaum Nebenwirkungen zu erwarten sind. In gelegentlichen Fällen kann es zu einer länger anhaltenden Sedierung, Müdigkeit und zu eingeschränkter Aufmerksamkeit/Konzentration kommen. In seltenen Fällen wurden Übelkeit und paradoxe Reaktionen, wie Angst oder Erregungszustände beobachtet. N₂O darf nicht angewendet werden bei bekannter Überempfindlichkeit gegen N₂O sowie bei Abhängigkeitsanamnese. In der Schwangerschaft sollte N₂O nicht angewendet werden.

Ich bestätige durch meine Unterschrift, dass ich die Aufklärung zur Einnahme eines inhalativen Anxiolytikums gelesen und verstanden habe und dass ich mich mit der Verabreichung während des Experiments einverstanden erkläre.

Mainz, den

Datum

Unterschrift

Name in Druckbuchstaben

Unterschrift des aufklärenden Untersuchers:

Mainz, den

Declaration on oath

I hereby declare, on oath, that I have written the present dissertation by my own and have not used other than the acknowledged resources and aids.

Hamburg, 06.01.2016

Benjamin Meyer